Versican: regulation, purification, and biological properties of a candidate prognostic indicator for breast cancer

Supaporn Suwiwat (M.Sc)

For the Degree of Doctor of Philosophy

Dame Roma Mitchell Cancer Research Laboratories

Department of Medicine, Faculty of Health Sciences

The University of Adelaide and The Hanson Institute

December 2003

Table of contents

Summary

Versican, a large chondroitin sulfate proteoglycan, is a recognized modulator of attachment and motility for mesenchymal cells and their malignant derivatives, viz astrocytoma and melanoma. It is also a candidate prognostic marker for these cancers. Recent studies indicate that although versican is a product of stromal cells, elevated expression predicts relapse for men treated for early stage, organ-confined, prostate cancer. This suggested that elevated expression of versican in peritumoral stroma may also be a candidate prognostic marker for breast cancer.

The initial aim of this thesis was to investigate whether versican might predict relapse in women with node-negative breast cancer. Because versican binds to hyaluronan (HA) and tenascin in extracellular matrix (ECM), both of which have been implicated as predictors of outcome for breast cancer, the relative predictive power of these components was investigated. Chapter 2 employed image measurement of immunohistochemical staining, analyzed by Cox regression and Kaplan-Meier life table plots. The results indicated that whereas tumor size was predictive of both relapse and overall survival in this cohort, versican was predictive of relapse only, tenascin was predictive of overall survival only, and HA was predictive of neither.

Elevated expression of versican in stromal tissue of cancers which progress, suggests that aggressive tumors are able to modulate versican secretion by stromal fibroblasts. Chapter 3 investigated whether soluble mediators in conditioned medium (CM) from several breast cancer cell lines regulated versican secretion by mammary fibroblasts, derived from malignant and non-malignant breast tissue. Quantitative immunoblotting results indicated

that soluble cancer cell mediators were present in CM. Specific neutralizing antibodies identified PDGF and TGF-β1 as candidate mediators.

Chapter 4 investigated whether versican purified from culture medium of mammary fibroblasts regulated attachment of breast cancer cells to ECM components, fibronectin and laminin. Versican inhibited attachment of MCF-7 breast cancer cells to fibronectin-coated substrates, in an RGD-dependent manner. The inhibitory activity of versican for breast cancer cell attachment also depended on the presence of chondroitin sulfate side chains.

Motility of smooth muscle cells *in vitro* depends on the presence of a pericellular sheath of matrix consisting of HA cross-linked by versican. Chapter 5 investigated whether breast cancer cells assembled pericellular sheath using a particle exclusion assay. Under normal culture conditions breast cancer cell lines do not assemble a pericellular sheath, but do when supplied with HA and versican from mammary fibroblasts. Incorporation of mammary fibroblast culture medium containing HA and versican into collagen type I / fibronectin coatings of perforated membranes of Boyden Chambers, reduced cell transit time for MCF-7.

In summary, this study revealed new knowledge regarding the regulation and biological activity of versican, a candidate prognostic marker for node-negative breast cancer.

Declaration

This work contains no material which has been accepted for the award of any other degree or diploma in any University or other tertiary institution and, to the best of my knowledge and belief, contains no material previously published or written by another person, except where due reference has been made in the text.

I give my consent to this copy of my thesis, when deposited in the University library, being made available for loan and photocopying.

Supaporn Suwiwat

December, 2003

Acknowledgements

Throughout my study, there have been many persons who were willing to help me and gave me invaluable encouragement. I would like to extend my gratitude to the following persons for their contribution toward my educational endeavour.

Keiko Mayne, who kindly taught, advised and helped me for immunoblot and purification of versican . In moments of stress, her friendship always comforted me.

Anne Morrison and Lisa Jonavicius, who gave their generous assistance for cutting and staining (H&E) sections used for my immunohistochemical work.

Virginia Papangelis, for collecting fresh breast tissues used in tissue culture and cutting sections used in preliminary staining.

Jim Brennan, for his technical knowledge and assistance for immunohistochemical staining.

Andrew Sakko, who taught me for techniques for tissue culture and kindly gave me protocol of many techniques used in this thesis.

Raija Tammi, Markku Tammi, Paivi Auvinen, and Veli-Matti Kosma (University of Kuopio and Kuopio University Hospital, Kuopio, Finland), for their helping me with staining and evaluation of HA presented in chapter 2.

Richard LeBaron (University of Texas at San Antonio), for his donation of versican antibody used for my immunoblot and immunohistochemical work.

Eva A Turley (The University of Western Ontario, Canada), for her donation of RHAMM antibody used for immunohistochemical work.

Carmela Ricciardelli, my co-advisor, for her teaching me image analysis, helping with statistical analysis, guidance, and endless help.

David Horsfall, my supervisor, for his enthusiastic support, guidance, faith in my abilities through difficulties, and greatly appreciated editing of this thesis.

Royal Thai Government, for granting me scholarship.

Winyou Mitranun, head of Department of Pathology, Prince of Songkla University, for his generous support and granting me permission to take leave of absence from my work to study.

Finally, my beloved family and friends always stay with me by regular e-mail and encourage me to keep going through difficult situation.

Publications Arising From This Thesis

1. Ricciardelli C, Brooks JH, Suwiwat S, Sakko AJ, Mayne K, Raymond WA, Seshadri R, LeBaron RG & Horsfall DJ (2002). Regulation of stromal versican expression by breast cancer cells and importance to relapse-free survival in patients with node-negative primary breast cancer. Clin Cancer Res 8, 1054-1060.

2. Suwiwat S, , Tammi R, Tammi M, Auvinen P, Kosma VM, LeBaron RG, Raymond WA, Tilley WD, & Horsfall DJ (2004). Expression of extracellular matrix components versican, chondroitin sulfate, tenascin and hyaluronan, and their association with disease outcome in node-negative breast cancer. Clin Cancer Res, 10, 2491-2498.

3. Suwiwat S, Ricciardelli C, Mayne K, Tilley WD, & Horsfall DJ (2004). Modulation of breast cancer cell attachment to matrix by versican (in preparation).

4. Suwiwat S, Ricciardelli C, Tilley WD, & Horsfall DJ (2004). Breast cancer cell mediators regulating versican production by mammary fibroblasts (in preparation).

5. Suwiwat S, Ricciardelli C, Tilley WD, & Horsfall DJ (2004). Formation of hyaluronan-versican rich pericellular matrix by breast cancer cells (in preparation).

Abbreviations

ABC	avidin-biotin-peroxidase complex
bp	base pair (s)
bFGF	basic fibroblast growth factor
bHABC	biotinylated complex of bovine cartilage aggrecan HA-binding region and link proteinn
bHABP	biotinylated hyaluronic acid binding protein
BSA	bovine serum albumin
cDNA	complementary DNA
CMF-Hanks	calcium and magnesium-free Hanks solution
CS	chondroitin sulphate
C-0-S	unsulphate CS
C-4-S	CS sulphate in position 4
C-6-S	CS sulphate in position 6
CM	conditioned medium
DAB	3,3'-diaminobenzidene tetrahydrochloride
DEPC	diethyl pyrocarbonate
DMSO	dimethyl sulphoxide
DNA	deoxyribonucleic acid
Dnase 1	deoxyribonuclease 1
DS	dermatan sulphate
E_2	oestradiol
ECL	enhanced chemiluminescence
ECM	extracellular matrix
EDTA	ethylenediaminetetraacetic acid
EGF	epithelial growth factor
EGFR	epithelial growth factor receptor
ER	oestrogen receptor
FBS	foetal bovine serum
FN	fibronectin
GAG	glycosaminoglycan
GADPH	glyceraldehyde 3-phosphate dehydrogenase
h	hour (s)
HA	hyaluronan or hyaluronic acid
HABP	hyaluronic acid binding protein
HAS	hyaluronan synthase
HS	heparan sulphate
IαI	inter-α-inhibitor
IGF-1	insulin-like growth factor-1
IgG	immunoglbulin
IHABP	intracellular hyaluronic acid binding protein
ITS	insulin, transferrin and sodium selenite media supplement
Kda	kilo Dalton (s)
KS	keratan sulphate
M	molar (moles/litre)

MIOD	mean integrated optical density
M_r	relative molecular weight
mRNA	messenger RNA
MTT	3-[4,5-dimethylthiazol-2-y1]-2,5-diphenyltetrazolium bromide
OS	overall survival
PBS	phosphate buffered saline
PCR	polymerase chain reaction
PDGF	platelet-derived growth factor
PG	proteoglycan
PR	progesterone receptor
RGD	arginine-glycine-aspartate tripeptide sequence
RFS	relapse-free survival
RHAMM	receptor for hyaluronan mediated motility
RNA	ribonucleic acid
RNase	ribonuclease
rpm	revolutions per minute
RT	reverse transcriptase
SD	standard deviation
SDS	sodium dodecyl sulfate
TBS	Tris-buffered saline
TBS-T	Tris-buffered saline Tween 20
TEMED	tetramethylethylenediamine
TGF-β1	transforming growth factor-β1
TMB	3,3',5,5 tetramethyl benzidine
TN	tenascin
TSG-6	tumor-necrosis-factor-stimulated gene-6
UV	ultra violet
V	volt (s)
VIA	video image analysis
VEGF	vascular endothelial growth factor
vs	versus

Chapter 1 General Introduction

1.1 Background

1.1.1 Incidence of breast cancer

Breast cancer is one of the most common malignant tumors among women. The incidence and mortality rate of this disease is high in developed western countries. It has been reported that over 180,000 new cases in the USA are diagnosed annually (Polyak, 2001). In South Australia, breast cancer remains the leading cause of cancer incidence and cancer mortality in women (Epidemiology of Cancer in South Australia, 2001). With advances in diagnosis, treatment, and public health awareness, the mortality rate of breast cancer has begun to decline. Although breast cancer can be identified at an early stage prior to lymph node involvement, still about one third of patients will die of their disease (Bland et al., 1998).

1.1.2 Risk factors for breast cancer

Breast cancer is a complex and heterogeneous disease. The etiology of breast cancer is uncertain, with many risk factors being related:

Geographic variation. The rate of incidence and mortality of breast cancer varies between countries. The rate in North America and Northern Europe is significantly higher than in Asia and Africa (Kumar et al., 1997). Environmental factors rather than genetic determinants probably contribute to disease differences, because the risk of disease increases among immigrants moving from low incidence areas to high incidence areas (Buell, 1973).

Family history and genetics. Family history is associated with an increased risk of breast cancer, particularly when disease occurs in first-degree relatives at a young age. The risk is increased 1.5 to 2 times for women having one first-degree relative with breast cancer and

up to 4 to 6 times for those having two affected first-degree relatives (Harris et al., 1992). Familial breast cancer is due to inherited mutations of the tumor suppressor genes p53, BRCA-1 and BRCA-2. Li-Fraumeni syndrome, an autosomal dominant familial syndrome is due to germline mutation of the p53 gene. Sufferers of this syndrome develop a variety of cancers including breast cancer. The breast cancers usually occur in women before the age of 40 and often are bilateral (Malkin et al., 1990). BRCA-1 is a tumor suppressor gene located on chromosome 17q21 (Hall et al., 1990). Women carrying a mutation of BRCA-1 have a high lifetime risk of developing breast cancer (approximately 87%) and a 40-60% lifetime risk of ovarian cancer (Easton et al., 1995). BRCA2 is located on chromosome 13q12-13 (Wooster et al., 1994). The lifetime risk of breast cancer and ovarian cancer in women with mutations of BRCA2 is 85% and 10-20% respectively (Easton et al., 1995).

Hormonal status. Early onset of menstrual cycling, late menopause, delayed child-bearing, and nulliparity all prolong exposure to estrogens, which predisposes breast epithelium to proliferation rather than differentiation.

Preexisting proliferative breast disease. A proliferative epithelial lesion, eg atypical hyperplasia, within the breast results in a doubling of the risk of breast cancer compared with women without such lesions (London et al., 1992, Dupont et al., 1993).

The above risk factors are well-established, predisposing influences for breast cancer. In addition, there are many less-well established risk factors including estrogen replacement therapy (ERT), oral contraceptives, obesity, alcohol consumption, cigarette smoking, and high-fat diet (Harris et al., 1992).

1.1.3 Breast structure and histology

Mammary glands are highly modified apocrine sweat glands, and in the female undergo further development and function under hormonal influence (Yong and Heath, 2000). With

the onset of puberty, the breasts grow under the influence of pituitary and ovarian hormones. During menstrual cycling, the breasts undergo cyclical changes influenced by the ovarian hormones. At menopause, the waning of hormone stimulation induces progressive glandular atrophy and involution.

Structurally, the breast consists of three major components: the skin, the subcutaneous adipose tissue, and the functional glandular tissue that is composed of parenchyma and stroma. The glandular component of the adult breast comprises 15-25 lobes, separated from each other by dense connective tissue and surrounded with adipose tissue (Junqueira et al., 1995). Each lobe is subdivided into several lobules (Figure 1.1A). The lobules, the secretory unit, consist of a variable number of alveoli or glands (also referred to as acini or terminal ductules) embedded within loose connective tissue. The alveoli are lined by epithelial cells with myoepithelial cells overlaying the basement membrane (Figure 1.1B). The epithelial cells discharge milk and fluid into the lumen under appropriate hormonal influences. Within this branching duct system, the alveoli connect to intralobular ducts which drain into extralobular ducts. The extralobular ducts drain into interlobular ducts which empty into lactiferous ducts with a sinus opening on the surface of the nipple. The skin at the nipple, the areola, contains abundant sensory nerves, and sebaceous and apocrine glands. The epithelial lining of the mammary ducts demonstrates a gradual transition from a single layer of columnar or cuboidal cells in the terminal duct to double layers of cuboidal cells in the lactiferous sinus. The epithelial cells of the lactiferous sinus are replaced by stratified squamous epithelium at the external opening.

A

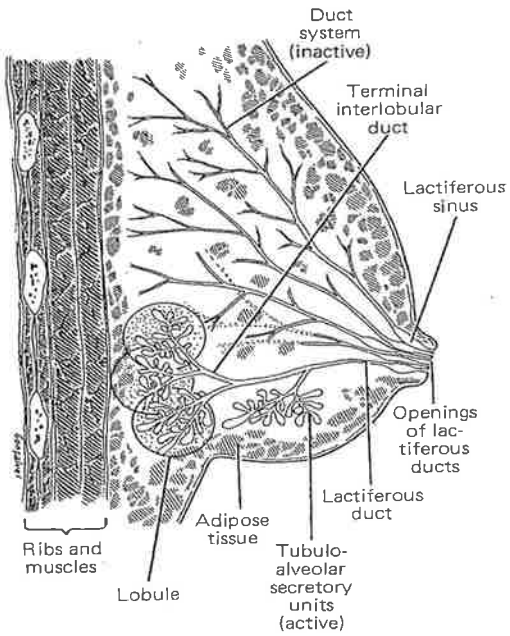

B

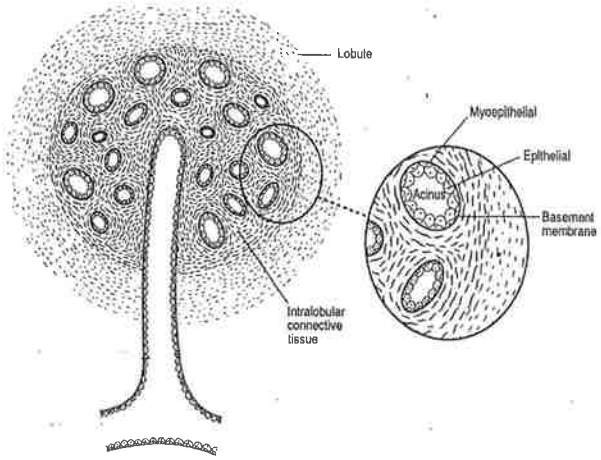

Figure 1.1 A. Schematic illustration of female breast shows that mammary gland is divided into several lobules. The terminal glands in lobules connect terminal interlobular ducts and lactiferous duct then open through nipple by lactiferous sinus. Figure derived from Junqueira et al. (1995).

B. The alveoli or acini in lobules are lined with single layer of epithelial cells and myoepithelial cells overlaying the basement membrane.

1.2 Pathogenesis and classification of breast cancer.

1.2.1 Pathogenesis

There are three factors influencing the development of breast cancer: genetic changes, hormonal influences, and environmental factors. Several studies support the concept that breast carcinogenesis is a multistep process (Dawson et al., 1996, Dupont et al., 1993, Page et al., 1985). Breast cancer is considered to arise from a benign lesion at the terminal duct lobular unit (TDLU), which progresses through epithelial hyperplasia without atypia to atypical hyperplasia, subsequently developing into *in situ* and invasive cancer (Figure 1.2). Similarly, atypical lobular hyperplasia (ALH) is considered to progress to lobular carcinoma *in situ* (LCIS) and then invasive breast carcinoma (IBC).

1.2.2 Classification

Most breast cancers arise from ductal epithelium, and the various histologic types are classified using the World Health Organization Classification:

A. Non invasive (in situ)

1. Intraductal carcinoma
2. Intraductal carcinoma with Paget's disease
3. Lobular carcinoma in situ

B. Invasive (infiltrating)

1a. Invasive ductal carcinoma not otherwise specified (NOS)

1b. Invasive ductal carcinoma with Paget's disease

2. Invasive lobular carcinoma
3. Medullary carcinoma
4. Colloid carcinoma (mucinous carcinoma)

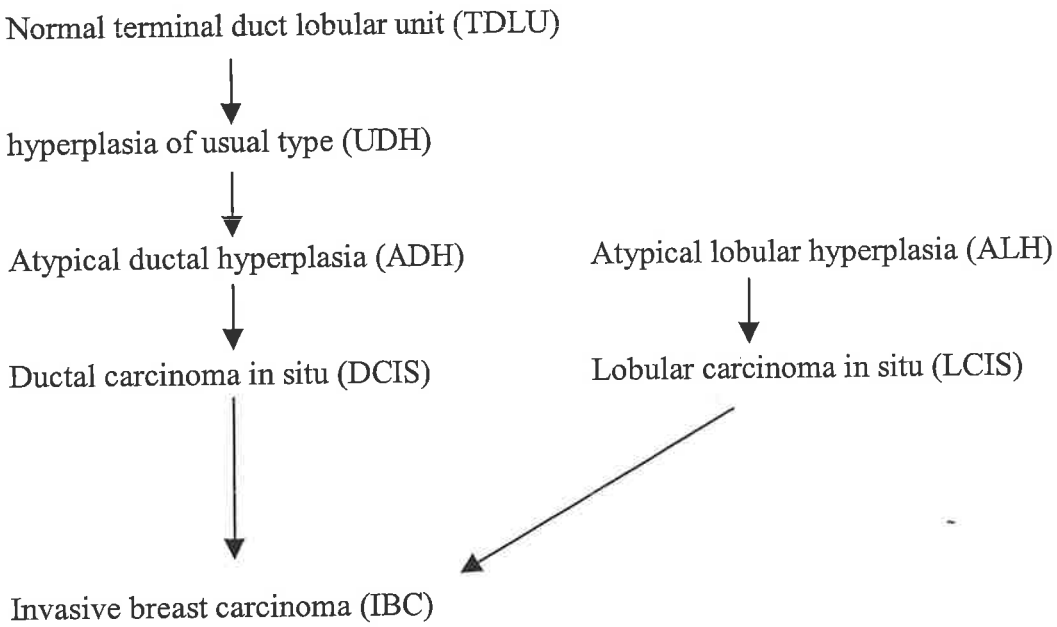

Figure 1.2 Putative multistep process of breast carcinogenesis. Figure derived from Krishnamurthy and Sneige (2002).

5. Tubular carcinoma

6. Other rare types

1.3 Tumor markers

Breast cancer is a complex disease with marked heterogeneity of disease course and clinical outcome. Tumor characteristics or markers have been used to improve risk assessment, early tumor detection, differential diagnosis, prognosis, therapeutic approach, and disease monitoring. Early studies utilized the conventional markers of tumor size, tumor grade, histologic type, lymph node involvement, and hormone receptor status. However, the conventional markers are limited in their ability to predict those patients with node-negative disease, who will relapse. Although approximately 70% of these node-negative patients survive without additional treatment after initial surgical resection, an unidentifiable 30% of these women are candidates for aggressive adjuvant treatment (Bland et al., 1998). Several new markers based on molecular and biochemical studies have been developed in an effort to provide better information for management and therapeutic decisions in breast cancer. These markers identify the presence of genetic mutations (p53, bcl-2, c-myc, nm23), increased cell proliferation (Ki-67, S-phase fraction), protease production (cathepsin-D, plasminogen activators, matrix metalloproteinases), growth factors and receptors (EGFR, c-erbB-2), tumor angiogenesis, tumor adhesion molecules, and others (Mirza et al., 2002, Leong and Lee, 1995).

1.3.1 Conventional markers

Tumor size. Tumor size is determined by measuring at least two dimensions with the greatest dimension being used for assessing disease stage. Increased tumor size is associated with decreased survival in node-negative patients (Carter et al., 1989, Saimura et al., 1999). Ninety percent of patients with tumors smaller than 1.0 cm and without

evidence of nodal involvement have disease free survival of 10 years (Rosen et al., 1993, Kollias et al., 1997).

Tumor grade. Most grading systems are based on the degree of abnormality in glandular configuration, number of mitoses per high power field, and degree of nuclear atypia eg modified Bloom and Richardson system (Elston & Ellis, 1993). Tumor grade has been reported to be related to poor survival in node-negative breast cancer patients (Fisher et al., 1988, Reed et al., 2000, (Mirza et al., 2002).

Histological type. Survival outcome varies with histological type of breast cancer. The 30 year survival rate was found to be approximately 74% for patients with intraductal carcinoma, 65% for papillary carcinoma, 34% for infiltrating lobular carcinoma, and 29% for infiltrating ductal carcinoma.

Lymph node involvement. Axillary lymph node metastasis is the most reliable marker of outcome for treatment in breast cancer. Approximately 70% of patients with lymph node-positive disease will develop a recurrence within 10 years, compared with 20-30% of patients without lymph node involvement (Fisher et al., 1993). The number of nodes involved is reportedly associated with prognosis. Patients presenting with 4 or more involved nodes have a worse prognosis than patients with fewer than 4 (Fitzgibbons et al., 2000).

Hormone receptor status. Expression of estrogen and progesterone receptors (ER and PR) as measured by either radioligand binding assay of tumor extracts or immunohistochemistry in tissue sections, is a useful predictor of response to endocrine therapy and patient prognosis. As PR expression is regulated by estrogen, most PR positive cancers are also ER positive. A negative ER and PR status has been associated with

decreased survival in node-negative breast cancer patients (Fisher et al., 1988, Pichon et al., 1996, Seshadri et al., 1996).

1.3.2 Other tumor markers

c-erbB-2 (Her2/neu). The c-erbB-2 oncogene is located on chromosome 17q21 and encodes a transmembrane glycoprotein receptor, p185. This protein has partial homology with epidermal growth factor receptor and shares intrinsic tyrosine kinase activity (Coussens et al., 1985). Amplification of c-erbB-2 occurs in 10-30% of breast cancer and its correlation with survival outcomes in node-negative patients remains controversial (Clark and McGuire, 1991, Andrulis et al., 1998, Mirza et al., 2002). However, c-erbB-2 overexpression is suggested to be of prognostic value, with an anti-c-erbB-2 monoclonal antibody currently available as a novel anticancer drug, Herceptin (Cobleigh et al., 1999). This drug has been shown to be effective in 20% of patients with recurrent breast cancers demonstrating overexpression of c-erbB-2. In addition, the c-erbB-2 positivity predicts response to other adjuvant therapy regimens, such as, a significantly improved response in patients with c-erbB-2-positive tumors treated with high-dose systemic adjuvant therapy with doxorubicin (Muss et al., 1994, Paik et al., 1998).

p53. p53 is a tumor suppressor gene situated in the short arm of chromosome 17. It codes for a 53-kd nuclear phosphoprotein involved in cell cycle regulation (Levine, 1997). Mutation of the p53 gene leading to p53 protein accumulation has been found in about one third of breast cancers (Davidoff et al., 1991, Thor et al., 1992). Studies of node-negative breast cancers have indicated a poor prognosis for patients with p53 gene alteration (Falette et al., 1998) and p53 protein overexpression (Allred et al., 1993, Andersen et al., 1993). p53 alterations also identify patients responsive to chemotherapy and radiotherapy (Bergh et al., 1995, Hawkins et al., 1996). Importantly, patients with germline p53

mutation (Li-Fraumeni syndrome) have an increased incidence of breast cancers compared to patients with somatic mutation of p53 (Glebov et al., 1994, Kleihues et al., 1997). An apparent linkage between expression of p53 and BRCA1 in familial breast cancer has been demonstrated (Sobol et al., 1997).

Ki-67 is a nonhistone nuclear protein detectable at all stages of the cell cycle, except G0 (Gerdes et al., 1984). The proportion of cell nuclei immunoreactive for Ki-67 in tissue sections is therefore a marker for cell proliferation which can be used to determine rate of tumor growth. Tumors with high levels of Ki-67 are inversely correlated with ER status and have a worse prognosis for node-negative breast patients (Veronese and Gambacorta, 1991, Molino et al., 1997, Brown et al., 1996, Sahin et al., 1991).

S-phase fraction is a measurement of cell proliferation utilizing the proportion of cells synthesizing DNA, as determined by flow cytometry. Increased S-phase fraction has been associated with poor outcome in breast cancer (Balslev et al., 1994, Bryant et al., 1998).

1.4 Structural components of the breast stroma which impact on cancer progression

1.4.1 Extracellular matrix constituents in breast cancer

The secretory acini of the mammary gland are surrounded by a supportive stromal tissue containing fibroblasts, adipose cells, blood vessels, cells of the immune system, and amorphous extracellular matrix (ECM). The ECM is composed of a variety of macromolecules that interact with each other and with adjacent cells. As a result of this interaction, the matrix molecules provide structural integrity to the tissues and also mediate growth regulation, cellular migration, and differentiation of cells. The ECM components in breast undergo change during preadult development, estrous cycling, pregnancy, lactation, and glandular involution. Changes in expression of the major ECM components during

carcinogenesis of the breast, including collagens, glycoproteins, and various glycosaminoglycans, are shown in Table 1.1.

1.4.2 Proteoglycan in breast cancer

Proteoglycans are a heterogenous family of macromolecules. They provide structural integrity to tissues, but also mediate cell proliferation, differentiation, and migration (Kawashima et al., 2000). Characteristically, proteoglycans consist of a core protein to which one or more sulfated glycosaminoglycan (GAG) side chains are covalently linked. The diversity of proteoglycans, different molecular constructions and functions, are dependent on differential expression of genes encoding core proteins as well as variations of GAG components (Bandtlow and Zimmermann, 2000). The GAGs are large unbranched polysaccharides of repeating disaccharide units. Based on the disaccharide structure, GAGs are classified into chondroitin sulfate (CS), dermatan sulfate (DS), keratan sulfate (KS), heparin/heparan sulfate (HS), and nonsulfated hyaluronan (HA) (Bandtlow and Zimmermann, 2000). Due to carrying sulfate or carboxyl groups on their structure, the GAGs are highly negatively charged permitting them to interact with various positively charged molecules such as growth factors, cytokines, and chemokines (Faham et al., 1996, Spillmann et al., 1998, Bandtlow and Zimmermann, 2000, Schlessinger et al., 1995).

Matrix proteoglycans, ie those defined on the basis of their secretion into the pericellular milieux, are divided into three groups: the basement membrane proteoglycans, the hyalectans, and the small leucine-rich proteoglycans (Iozzo, 1998). The basement membrane proteoglycan group is comprised of perlecan, agrin, and bamacan, which are localized to basement membranes underlying vascular and epithelial structures of mammalian organisms. The hyalectan group refers to proteoglycans which contain a lectin

Table 1.1. ECM constituents with altered expression in breast tumors and carcinoma cells (Lochter and Bissell, 1995).

Collagens		Glycoproteins		Glycosaminoglycans	
Type I collagen	+	Laminin	-	Hyaluronan	+
Type I-trimer collagen	+	Fibronectin	+	Chondroitin sulphate	+
Type III collagen	+	Vitronectin	+	Dermatan sulphate	-
Type IV collagen	-	Elastin	+	Heparan sulphate	-
Type V collagen	+	Thrombospondin	+		
OF/LB collagen*	+	Tenascin	+		

ECM constituents are present more (+) or less (-) abundantly in breast tumor tissues or tumor-derived cell lines than in normal breast tissues or derived epithelial/stromal cell lines.

* OF/LB collagen = onco-fetal, laminin-binding collagen

domain and interact with hyaluronan, including versican, aggrecan, neurocan, and brevican. The family of small leucine-rich proteoglycans contains at least nine members, viz decorin, biglycan, fibromodulin, lumican, keratocan, proline arginine-rich end leucine-rich repeat protein (PRELP), osteoherin, epiphycan, and osteoglycin. In addition to the widely distributed matrix proteoglycans, there are a number of cell surface proteoglycans such as syndecan, thrombomodulin, and fibroglycan (Hardingham and Fosang, 1992).

Changes in the tissue content of proteoglycans and composition of GAGs have been reported between normal and neoplastic human breast tissue (Alini and Losa, 1991). The overall proteoglycan content is increased 2-fold in the extracellular matrix of breast cancer tissue (Alini and Losa, 1991). The levels of CS increase in tumor tissues, whereas the amount of DS decreases. High levels of hyaluronic acid are also detectable in breast cancer (Takeuchi et al., 1976).

1.4.2.1 Structure and function of versican

Versican, a CS proteoglycan, is grouped in the family of HA-binding proteoglycans, termed hyalectins (Iozzo, 1998). The primary structure of versican, analyzed from a human fibroblast cDNA library, consists of a 400 kDa core protein of 2409 amino acids and carrying 12 to 15 CS side chains (Figure 1.3A) (Zimmermann and Ruoslahti, 1989). Its structure contains 3 domains: the N terminal region (G1 domain), the central domain, and the C terminal globular region (G3 domain). The G1 domain consists of an immunoglobulin-like loop region and two link protein-like tandem repeats, which bind HA (Figure 1.3B). The central core protein domain contains serine residues that carry the GAG side chains through a carbohydrate linker oligosaccharide including xylose. The G3 domain contains two epidermal growth factor-like repeats, a lectin-like sequence and a complement regulatory protein (CRP)-like domain. Several carbohydrates as well as

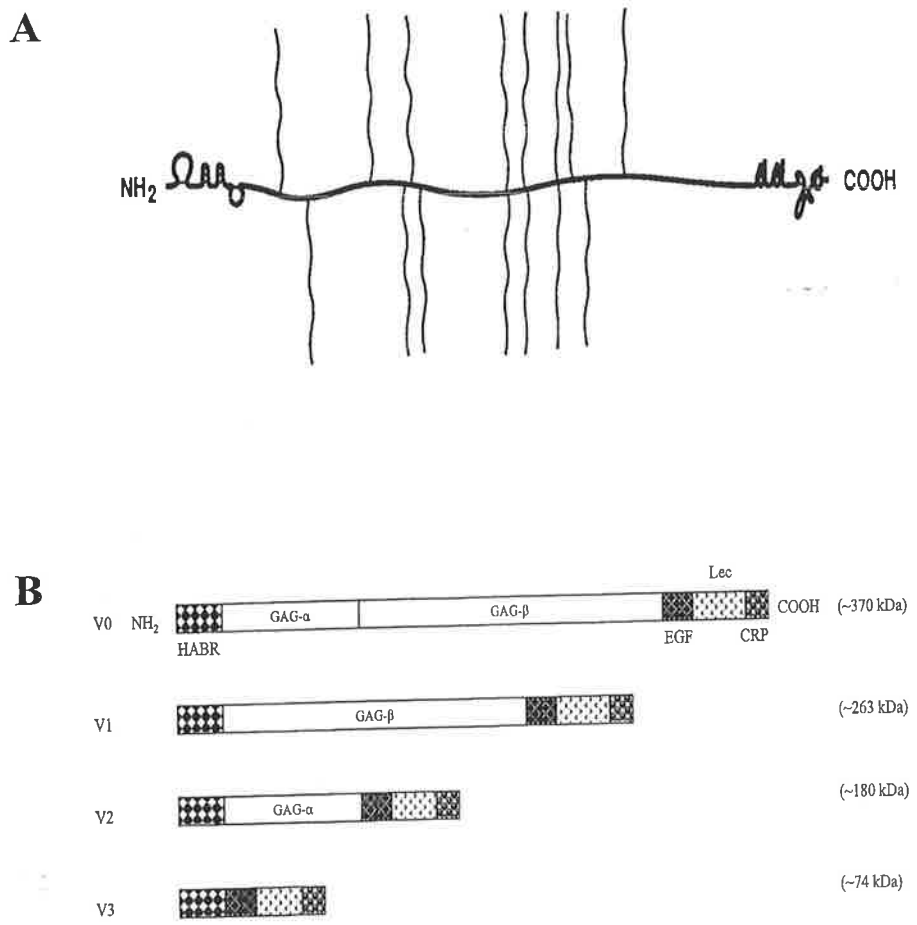

Figure 1.3 A. Structural model of versican consists of a core protein (thick line) with attached CS side chains (wavy lines).

B. Versican isoforms are generated by alternative splicing of the mRNA transcript. HABR = HA-binding region, GAG-α and GAG-β = glycosaminoglycan attachment regions, EGF = two epidermal growth factor-like domains, Lec = a lectin binding domain, and CRP = complement regulatory protein-like domain. Figure derived from LeBaron (1996).

tenascin-R bind versican through the G3 domain (Aspberg et al., 1995). The versican gene (CSPG2) is localized on the long arm of human chromosome 5 (5q12-5q14) and is encoded by 15 exons (Iozzo et al., 1992). As a result of alternative splicing in the two large exons encoding the GAG attachment sites, four isoforms are detected in mammals: V0, V1, V2, and V3 (Zimmermann et al., 1994). The GAG attachment sites, GAG-α and GAG-β, are encoded by exon 7 and exon 8, respectively. V0 is the largest isoform and contains both GAG-α and GAG-β. V1 contains only GAG-β, and V2 only GAG-α. V3 lacks both GAG-α and GAG-β (Zimmermann et al., 1994, Zako et al., 1995). The estimated molecular weights for the core proteins of the four splice variants are approximately 370, 263, 180, and 74 kDa for V0, V1, V2, and V3, respectively (Figure 1.3B) (Lebaron, 1996). Expression of the versican gene is regulated by a promoter that contains a TATA box and potential binding sites for transcription factors such as AP2, SP1, CCAAT enhancer-binding protein, cyclic AMP-responsive element, and CCAAT binding transcription factor (Naso et al., 1994). Additionally, up-regulation of versican gene expression was found in skin and gingival human fibroblasts in response to TGF-β (Kahari et al., 1991). Enhanced versican expression is also induced by combination of EGF, PDGF, and TGF-β in fibroblasts (Tiedemann et al., 1997).

Several studies suggest that versican may play a role in cellular adhesion, migration, and proliferation by promoting an interaction between cell surfaces and other extracellular matrix molecules (Zimmermann and Ruoslahti, 1989). Versican is regarded as an anti-adhesive molecule, based on studies demonstrating its ability to interfere with the attachment of embryonic fibroblasts to collagen type I, fibronectin, and laminin (Yamagata et al., 1989). Additionally, studies conducted at the confocal microscopic level indicate that areas of the pericellular matrix rich in versican are excluded from focal adhesion contacts

of cultured fibroblasts with the underlying substratum (Yamagata et al., 1993). The anti-adhesive activity of versican is regulated through the G1 domain (Ang et al., 1999, Yang et al., 1999). However, versican also possesses an adhesive function, promoting cell adhesion through the C terminal domain. Interaction of the C terminal domain of versican with β_1-integrin activates focal adhesion kinase (FAK), mediates cell adhesion, and protects against apoptosis in glioma cells (Wu et al., 2002). Versican also binds to adhesion molecules such as L and P selectins, present on the surface of inflammatory leukocytes (Kawashima et al., 1999, Kawashima et al., 2000). This binding is mediated through the CS chains. Thus versican could be one of the extracellular components involved in inflammatory responses.

In the nervous system, embryonic tissues that express versican act as a barrier to neural crest cell migration and axonal outgrowth (Landolt et al., 1995). Overexpression of versican found in Splotch mice carrying a mutation in the Pax 3 gene transcriptional factor is associated with defective neural crest migration pathways (Henderson et al., 1997). A recent study has shown that upregulation of versican following CNS injury prevents nerve regeneration (Asher et al., 2002). Animals treated with chondroitinase ABC lyase to degrade chondroitin sulfate after spinal cord injury demonstrated enhanced regeneration of both ascending and descending corticospinal-tract axons (Bradbury et al., 2002). Expression of a versican mini-gene in NIH3T3 fibroblasts stimulated cell proliferation via EGF-like motifs in the G3 domain, and this effect could be blocked by deletion of the G3 domain or antisense oligonucleotides to the EGF receptor (EGFR) (Zhang et al., 1998b). These results suggest that versican EGF-like motifs may enhance cell proliferation through a direct or indirect interaction with EGFR. Furthermore, expression of a versican G1 construct in NIH3T3 fibroblasts reduced cell adhesion and increased cell growth, supporting the hypothesis that versican stimulates cell proliferation through its ability to

decrease cell adhesion (Yang et al., 1999). In vascular smooth muscle cells, PDGF, a mitogen and chemotactic agent, upregulates HA and versican synthesis thereby promoting formation of pericellular matrix (Evanko et al., 2001). Pericellular matrix, rich in HA and versican, is required for cell proliferation and migration by diminishing cell surface adhesion and affecting cell shape changes (Evanko et al., 1999).

Versican binds several different molecules within matrix, some involved in ECM assembly. The N terminus of versican (G1 domain) is structurally similar to the HA binding region of CD44, link protein, and the N-terminus of the cartilage proteoglycan, aggrecan. Whereas the binding of versican to HA is mediated through the N terminal G1 domain, versican binds CD44 through its CS chains (Kawashima et al., 2000). This 3-way binding might stabilize HA-versican aggregates associated with the cell surface. In addition, versican has been shown to interact with tenascin-R, a member of the tenascin family of glycoproteins expressed specifically in the nervous system, through the versican C-type lectin domain (Aspberg et al., 1995). The highly selective binding of versican to tenascin-R together with localization of both versican and tenascin-R in similar tissues lends support to the tenet that this interaction is of biological significance. The C-type lectin domain of versican also interacts with the fibrillar ECM protein fibulin-1 and fibulin-2. Again these molecules coexist with versican in tissues such as blood vessels, skin, and the developing heart (Aspberg et al., 1999, Olin et al., 2001). Both fibulin-1 and -2, versican, and HA are produced in endocardial cushion tissue, suggesting that fibulin may be implicated in organization of HA-versican complexes within the ECM of the developing heart (Miosge et al., 1998). The heart defect (hdf) mouse arose from a transgene insertional mutation in versican gene (Mjaatvedt et al., 1998). The loss of versican expression in the homozygous hdf mouse was associated with the failure of the endocardial cushion formation.

Versican has been found in both embryonic and adult tissues. In human adult tissues, versican is detected in loose connective tissues of various organs, particularly in association with the elastic fiber network (Bode-Lesniewska et al., 1996). Moreover, versican is present in smooth muscle, cartilage, the central and peripheral nervous system, blood vessel wall, dermis and in the proliferative zone of the epidermis (Bode-Lesniewska et al., 1996, Yao et al., 1994, Zimmermann et al., 1994).

Elevated expression of versican levels has been described in many human cancers, including breast cancer (Nara et al., 1997, Brown et al., 1999, Ricciardelli et al., 2002), prostate cancer (Ricciardelli et al., 1998), melanoma (Touab et al., 2002), gastric carcinoma (Theocharis et al., 2003), brain tumors (Paulus et al., 1996), and ovarian cancer (Voutilainen et al., 2003). The expression of versican was detectable in dysplastic nevi, primary and metastatic melanomas, but not in benign melanocytic nevi (Touab et al., 2002). Furthermore, purified versican from astrocytoma cells stimulated melanoma cell growth and inhibited melanoma cell adhesion to fibronectin and collagen type I (Touab et al., 2002). Therefore, versican may facilitate cell detachment and proliferation. The increased versican in human gastric carcinoma was found to contain increased amounts of 6-sulphated and non-sulphated disaccharides as compared to normal gastric mucosa (Theocharis et al., 2003). Versican is also enriched in stroma of ovarian cancer, but does not reach significance as an independent predictor of outcome for patients (Voutilainen et al., 2003). Conversely, expression of stromal versican is an independent predictor in prostate cancer (Ricciardelli et al., 1998). In breast tumors, versican is present in the proliferating mesenchymal cells localized to the peritumoral stromal tissue, especially at the peripheral invasive areas (Nara et al., 1997). The high level of versican expression in peritumoral stroma has been shown to correlate with early relapse in node-negative breast

cancer patients (Ricciardelli et al., 2002). However, the biological functions of versican in breast cancer remain unknown.

1.4.3 Tenascin

Tenascin-C (TN-C) is a large glycoprotein component of extracellular matrix, a hexamer of similar subunits joined at their amino terminus by disulfide bonds (Erickson and Bourdon, 1989, Natali and Zardi, 1989, Chiquet-Ehrismann, 1990). TN-C also has been known as myotendinous antigen, cytotactin, neuronectin, $J1_{220/200}$, and TN (Jones and Jones, 2000a). Each monomeric unit of TN-C has multidomains comprising a TA (TN assembly) domain, a series of epithelial growth factor (EGF)-like repeats, a variable number of fibronectin type III (FN-III) domains, and a C terminus with homology to the globular domains of the β and γ chains of fibrinogen (Figure 1.4) (Siri et al., 1991, Sriramarao and Bourdon, 1993, Mighell et al., 1997, Hindermann et al., 1999). The TA domain is responsible for hexamer assembly, while the EGF-like repeats are anti-adhesive for fibroblasts, neurons and glia (Jones and Jones, 2000b). The fibrinogen-like domain interacts with other ECM, cell surface proteins (such as collagen, integrin, heparin) and cell surface chondroitin sulfate (Jones and Jones, 2000b).

Although human TN-C is coded by a single gene, alternative splicing of the FN-III repeats within the TN-C mRNA precursor generates structurally and functionally different TN-C isoforms. In TN-C, there are eight conserved FN-III repeats (Figure 1.4B, designated as number 1-8) and nine alternatively spliced FN-III repeats (Figure 1.4B, designated as letter A-D that inserted between the conserved repeat 5 and 6) (Jones and Jones, 2000a). There are two predominant isoforms: the larger isoform contains alternatively spliced FN-III

A

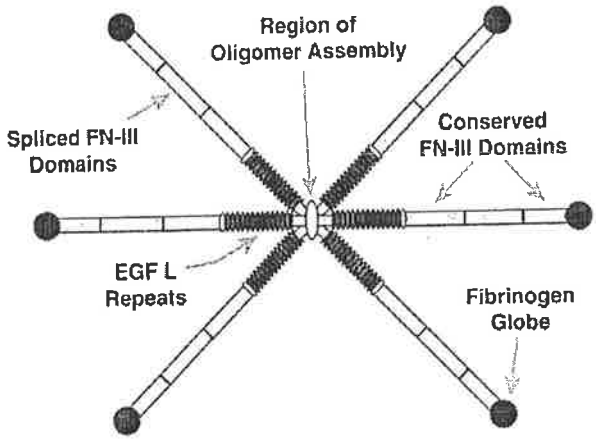

B

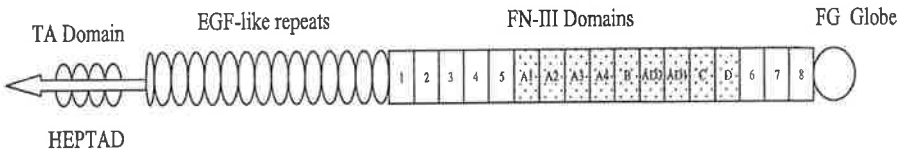

Figure 1.4 A. A model of the TN-C hexabrachion.

B. Schematic representation of the human TN-C subunit. The TN assembly (TA) domain links six polypeptide TN chains via the heptad repeat regions (small ovals). Terminal cysteine residues (arrowhead) may allow individual polypeptides to form hexamers. The human TN subunit contains 14 + 1/2 EGF-like repeats (ovals), FN-III domains (light and dotted boxes), and a fibrinogen globe at the C terminus. The dotted boxes represent FN-III domains undergoing alternative splicing.

Figure derived from Jones and Jones (2000a).

repeats, the smaller isoform lacking all FN-III repeats (Gulcher et al., 1989). The larger isoform is much more sensitive to matrix metalloproteinases than the smaller isoform (Siri et al., 1995). The large isoform appears to be expressed mainly at the onset of cellular processes that involve cell migration, proliferation, and tissue remodeling eg in neoplasia, wound healing, and during development (Chiquet-Ehrismann et al., 1986, Borsi et al., 1992, Hindermann et al., 1999, Kaplony et al., 1991). At least 8 splice variant transcripts for human TN-C have been described (Sriramarao and Bourdon, 1993).

The precise role of TN-C in ECM is not clearly understood. A wide spectrum of functions including cell adhesion/anti-cell adhesion, promotion/regulation of cell migration, and stimulation/inhibition of cell growth have been proposed for TN-C (Erickson and Bourdon, 1989, Chiquet-Ehrismann, 1990). These activities suggest that TN-C may play a critical role in tumor-matrix interaction, potentially in regulation of tumor proliferation, invasion, and metastasis. The most consistently demonstrated function of TN-C appears to be its anti-adhesive activity. *In vitro*, TN-C inhibits fibroblast adhesion to fibronectin. Monoclonal antibodies to TN-C neutralize the inhibitory capacity of TN-C for cellular FN binding (Chiquet-Ehrismann et al., 1988). Reportedly, recombinant TN-C fragments containing the EGF-like repeats are anti-adhesive, whereas TN-C fragments containing the distal FN-III repeats adhere to cells (Spring et al., 1989). Cell binding is probably achieved via specific binding of the RGD sequence within the third FN III repeat of TN-C to cellular integrins: $\alpha v\beta 3$, $\alpha v\beta 6$, $\alpha 9\beta 1$, $\alpha v\delta$, and $\alpha 8\beta 1$ (Crossin, 1996). Alternatively, as TN-C is a heparin binding protein, TN-C may bind to heparan sulfate proteoglycans located on the cell membrane.

In breast tissues, TN-C is immunolocalized in the human adult resting and aging breast to thin, irregular bands surrounding ducts and acini, whereas thick continuous bands of TN-C

staining were detected around ductal and acinar structures in all variants of fibrocystic disease and carcinoma in situ (Koukoulis et al., 1991, Howeedy et al., 1990). Several studies report markedly enhanced expression of TN-C in human mammary carcinomas (Gould et al., 1990, Moch et al., 1993, Shoji et al., 1992). Noteably, prominent stromal TN-C immunoreactivity was present around clusters or individual tumor cells in infiltrating ductal carcinomas (Shoji et al., 1992, Shoji et al., 1993, Moch et al., 1993). This is consistent with recent findings demonstrating universal TN-C expression in the periductal stroma of patients with preinvasive cancer and invasive breast cancer (Goepel et al., 2000). Benign lesions showed weaker TN-C immunoreactivity than malignant tissues, whereas TN-C was undetectable in normal breast tissue (Goepel et al., 2000). In invasive breast carcinoma, the larger TN-C isoform (330 kDa) is expressed at levels 10-fold higher than in normal breast tissue and similar results were observed in phyllodes tumors and in some fibroadenomas with high stromal cellularity (Borsi et al., 1992). It has been reported that expression of two TN-C isoforms, one containing domain D and the other containing both domain B and D, was significantly associated with invasive breast carcinoma (Adams et al., 2002). These isoforms were also identified in a subset of ductal carcinoma in situ (DCIS). All results suggest that TN-C isoforms may be used as a predictor for tumor progression of breast cancer.

The majority of immunohistochemical investigations have documented that TN-C staining was intensely present in stroma surrounding breast cancer cells, suggesting that TN-C is most likely produced by mesenchymal fibroblasts (Shoji et al., 1992, Moch et al., 1993, Iskaros et al., 1998). More recently however, cytoplasmic TN-C staining has been detected within breast cancer cells (Ishihara et al., 1995, Tokes et al., 1999). The structure and function of epithelial TN-C may be possibly different from that of the mesenchymal TN-C. It has been shown that patients with expression of TN-C in cancer cells exhibited shorter

survival than patients with TN-C-negative cancer cells, irrespective of whether their tumors were positive or negative for stromal TN-C. In turn, patients with stromal TN-C-positive cancers showed poorer survival and more frequent metastasis than patients with stromal TN-C-negative cancers (Ishihara et al., 1995).

Four other proteins: TN-R, TN-X, TN-W, and TN-Y have the consecutive arrangement of domains that was found in TN-C (Jones and Jones, 2000a). TN-R (also termed restrictin and $J1_{160/180}$) has been shown to be specific for central and peripheral nervous system tissues and its expression partially overlaps with that of TN-C (Chiquet-Ehrismann, 1995, Jones and Jones, 2000a). TN-X is prominently found in skeletal and heart muscle and connective tissues (Chiquet-Ehrismann, 1995, Jones and Jones, 2000a). TN-W was expressed prominently in neural crest pathway in the zebrafish and colocalized with TN-C (Weber et al., 1998). TN-Y was expressed in connective tissues and has been shown to modulate muscle cell growth (Tucker et al., 1999).

1.4.4 Hyaluronan and its receptors

1.4.4.1 Hyaluronan (HA)

Hyaluronan (hyaluronic acid or HA) is an unbranched glycosaminoglycan synthesized from disaccharide repeats of D-glucuronic acid and N-acetyl-D-glucosamine that are linked with β1-3 and β1-4 bonds (Figure 1.5A) (Laurent and Fraser, 1992). Unlike other GAGs, HA is not covalently attached to a protein core and is unsulfated. A single molecule of HA can have a molecular mass of up to 10×10^6 Da (Noble, 2002). In contrast to other GAGs, HA is not synthesized in the Golgi but at the inner face of the plasma membrane and nascent HA is directly translocated into the ECM (Luke and Prehm, 1999). The HA synthases (HASs) have been proposed to be responsible for synthesis of HA. Three mammalian enzymes have been cloned: HAS1, HAS2, and HAS3 (Spicer and McDonald,

A

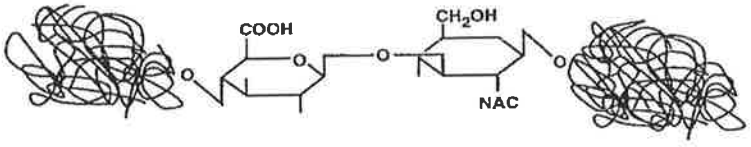

B

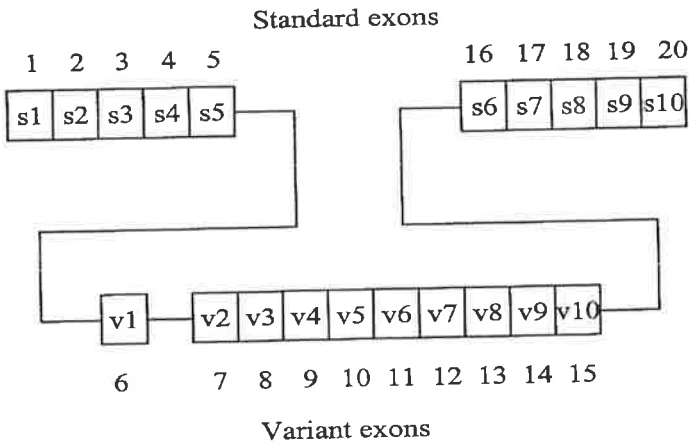

Figure 1.5 A. Schematic representation of the structure of hyaluronan. The linear polymer is made up of a repeating disaccharides unit consisting of β1,4-glucuronic acid linked β1,3 to N-acetylglucosamine. The native molecule entangles and forms a random coil in solution. Figure derived from Knudson (1995).

B. Schematic representation of the structure of the CD44 gene. The standard exons (s1-s10) encode the standard protein isoform, CD44s. The exons s1-s5 is in the extracellular domain and contain HA-binding domain, whereas exon s18 is in the transmembrane domain and exon s19 and exon s20 are in the cytoplasmic domain. Variably spliced exons v1-v10 in the proximal extracellular domain can be inserted between exons s5 and s6.

1998). Although three separate genes encode the three HAS isoforms, the isoforms show a high homology of amino acid sequence. Expression of different HAS isoforms is associated with various tissues and regulated by growth factors and cytokines (Recklies et al., 2001).

HA is distributed in extracellular matrix and on the cell surface (Knudson and Knudson, 1993). It has been reported that an increased deposition of HA into matrix correlates with various physiological processes including tissue morphogenesis, wound repair, inflammation, cell motility, and tumor invasion (Laurent and Fraser, 1992, Turley, 1992, Sherman et al., 1994). HA has been proposed to exert its effect on cells by interaction either with HA-binding proteins (ie receptors) on the cell surface or with HA-binding proteins (HABPs) within the ECM. HABPs or hyaladherins are divided into the Link module superfamily and non-Link module hyaladherins. The Link module superfamily consists of members containing Link module. These members include link protein, aggrecan, versican, neurocan, brevican, CD44, tumor-necrosis-factor-stimulated gene-6 (TSG-6) and lymphatic vessel endothelial HA receptor-1 (LYVE-1) (Day and Prestwich, 2002). The HA-binding domains from Link module-containing proteins can be subdivided into three groups: type A (e.g., TSG-6), B (e.g., CD44), and C (e.g., link protein). The non-Link module hyaladherins are Inter-α-inhibitor (IαI), CD38, sialoprotein associated with cones and rods (SPACR), SPACRCAN (interphotoreceptor matrix HA-binding proteoglycan synthesized by photoreceptors and pinealocytes), and receptor for hyaluronate-mediated motility (RHAMM) . In addition to RHAMM, there are three other HABPs found within cells, namely CDC37 (cell cycle control protein), P-32 (a protein co-purified with pre-mRNA splicing factor SF2), and intracellular HABP4 (IHABP4) (Day and Prestwich, 2002).

HA exhibits a negative charge due to its component carboxyl groups, leading to an ability to attract water molecules. The HA molecules entangle and form a random network of chains. As a consequence of these properties, HA forms solutions of high viscosity with resultant effects on molecular exclusion, flow resistance, and osmotic pressure, (Laurent and Fraser, 1992). HA can bind to other matrix molecules, eg cartilage proteoglycan, aggrecan. HA is specifically bound to aggrecan and this interaction is stabilized by link protein (Kohda et al., 1996). Without link protein, the aggregate cannot be retained in cartilage. Evidence in support of this is that mice lacking link protein died shortly after birth as a consequence of severe defects in cartilage development (Watanabe and Yamada, 1999). Various cell types (eg fibroblasts, smooth muscle cells, chondrocytes) in tissue culture are surrounded by pericellular coats rich in HA (Knudson et al., 1996, Blom et al., 1995, Evanko et al., 2001). The coats are visualized by the exclusion of particles such as red blood cells or bacteria (Clarris and Fraser, 1968, Knudson, 1998). In addition to HA, the coats of vascular smooth muscle cells are rich in versican (Evanko et al., 1999). The formation of pericellular coats has been associated with cell motility and division. Removal of this coat by competitive HA oligosaccharides that block the binding of HA to the cell surface prevented pericellular coat assembly and inhibited cell division and migration (Evanko et al., 1999). It has been suggested that the coats may also protect cells from viral infections and cytotoxic effects of lymphocytes (Patterson et al., 1975, McBride and Bard, 1979, Knudson and Knudson, 1993).

Using histochemical staining with specific HA affinity probe, many epithelial tumors show increasing HA within the surrounding connective tissue matrix (Ropponen et al., 1998, Setala et al., 1999, Bertrand et al., 1992). HA is produced by both epithelial tumor cells and stromal cells. In addition, tumor cells can also induce stromal cell synthesis of HA (Knudson et al., 1984). Elevated levels of stromal HA expression are strongly correlated

with unfavorable outcome for patients with breast cancer (Auvinen et al., 2000). Accumulation of stromal HA in breast cancer was elevated in comparison to normal tissue and benign lesions, especially in peripheral invasive areas (Ponting et al., 1993). In addition, elevated expression of stromal HA combined with HA expression in cancer cells was related to poor survival for breast cancer patients (Auvinen et al., 2000).

The interaction of HA with cells influences cell behavior. There are at least three major influences of HA on normal and tumor cell behavior. These are its physiological properties, its interaction with various HA-binding macromolecules in the assembly of pericellular and extracellular matrices, and its effects on cell signaling and behavior. The concentration of HA in tissues peaks, particularly in ECM surrounding proliferating and migrating cells, during embryonic development, regeneration, healing, as well as tumor formation. As a result of its promotion of tissue hydration and associated increase in osmotic pressure, HA creates a milieux favorable for mitotic cell rounding and cell movement. A recent study showed that HA promotes glioblastoma cell migration within a fibrin gel by increasing hydration and consequently the porosity of the gel (Hayen et al., 1999). All of these results suggest that the deposition of HA facilitates tumor cell migration *in vivo*. Increasing HA synthesis correlates with increased HAS activity. HAS activity peaks at mitosis, at which time HA is enriched in intracellular compartments and in the pericellular matrix. Promotion of cancer progression by increased HA production has been reported. Expression of HAS1 by transfection into mutant mouse mammary carcinoma cells defective in HAS activity rescued HA production, formation of pericellular matrix and pronounced lung metastasis after injection in mice (Itano et al., 1999a). In addition to its functions in tissue hydration and assembly of matrices, HA exerts effects on cell behavior by interaction with cell surface receptors, such as CD44 and RHAMM, or by sustained attachment to HAS across the plasma membrane. Most studies to date have

focused on HA functions within the ECM and at the cell surface, although HA is also located intracellularly (Evanko et al., 1999). Intracellular HA-binding proteins have been identified and these proteins interact with extra-cellular-regulated kinase (Zhang et al., 1998a).

1.4.4.2 CD44

CD44 is a family of transmembrane glycoproteins that function mainly as receptors for HA. The CD44 molecule is encoded by a single gene, mapped to the short arm of human chromosome 11. The gene comprises 20 exons and forms two groups. One group contains exons 1-5 (s1-s5) and exons 16-20 (s6-s10) spliced together to form a single transcript known as the standard isoform (ie CD44s) (Figure 1.5B). The other group contains the variable exons 6-15 (frequently referred to as v1-v10) that are alternatively spliced between the standard exons ie at an insertion site between exon 5 and 16 (Goodison et al., 1999). The products containing the variable exons are designated CD44v. As a result of this alternative splicing, a myriad of CD44 variants can be generated. In the human CD44 gene however, exon 6 contains a stop codon, therefore there is no CD isoform containing v1 expression.

The protein structure of CD44 consists of three domains: the extracellular domain, which binds to HA; the transmembrane domain, which is responsible for the lymphocyte homing; and the C-terminal cytoplasmic domain, which mediates the interaction with cytoskeleton (Rudzki and Jothy, 1997, Underhill, 1992). The N-terminal or extracellular HA-binding domain encoded by exons 1 to 5 is highly conserved between numerous HA-binding proteins, and across the mammalian species. There are at least three binding sites on the CD44 molecule for HA. One is encoded by exon 2 and has homology with cartilage link

protein. The other two sites overlap within exon 5. The HA binding sites are designated B(X7)B, consisting of clusters of seven basic amino acids flanked by specific arginine or lysine residues (Rudzki and Jothy, 1997).

Interaction of CD44 with HA modulates cell adhesion, proliferation, migration, and angiogenesis (Lesley et al., 1993, Bourguignon et al., 1998, Lokeshwar et al., 1996). Various biological pathways are activated through HA binding to CD44, via specific intermediate molecules (Figure 1.5C). Stimulation of the CD44-associated cell surface protein $p185^{HER2}$ tyrosine kinase leads to increased tumor cell growth (Bourguignon et al., 1997). Binding of HA also stimulates the intracellular domain of CD44 to interact with the oncogenic protein c-Src kinase, leading to increased cell proliferation, spreading, and migration in many cell types (Broome and Hunter, 1996, Kaplan et al., 1995, Bourguignon, 2001). c-Src kinase activation increases phosphorylation of the cytoskeletal protein, cortactin, leading to reduced cross-linking of filamentous actin in vitro (Bourguignon et al., 2001). This finding suggests that the CD44 molecule provides a direct linkage between the ECM HA and the cytoskeleton. Rho-like GTPases such as RhoA and Rac1 also participate as signaling intermediaries between CD44 and cytoskeletal proteins. Binding of HA promotes CD44 activation of Rac1 signaling, a pathway known to produce reorganization of the actin cytoskeleton with associated membrane ruffling, cellular projection, cell motility, and cell transformation (Nobes and Hall, 1995, Bourguignon et al., 2000b). Activation of Rac1 is achieved by binding of the intracellular domain of CD44 to guanine nucleotide exchange factor (eg Tiam1) inducing cytoskeleton-mediated changes to cell shape, cell adhesion, and cell motility (Nobes and Hall, 1995, van Leeuwen et al., 1995). Linkage between HA and the CD44v3 isoform, thereby activating Tiam1-Rac1 signaling, reportedly promotes cytoskeleton-mediated tumor cell migration and breast cancer progression (Bourguignon et al., 2000b). The intracellular domain of CD44 exhibits

C

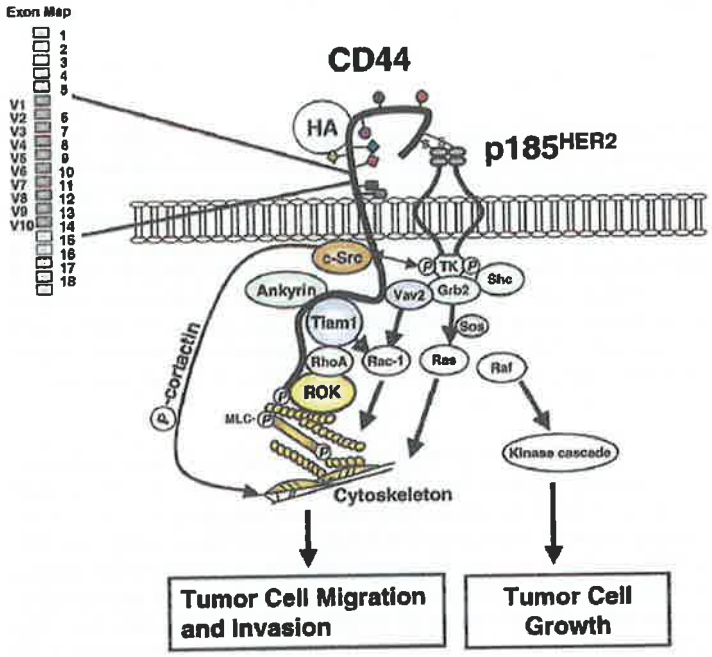

Figure 1.5 C. A model for HA-dependent, CD44-specific signaling pathways. HA binds CD44 at distal extracellular domain and promotes activation of both tyrosine kinase (TK) activity of $p185^{HER2}$ and c-Src kinase. c-Src phosphorylates cortactin involving actin cytoskeletal filament. The binding of HA to CD44 also activates signal proteins such as RhoA, Tiam1, Rac1, Vav2, and cytoskeletal proteins including ankyrin. Activation of these signaling pathways together influences tumor cell migration and invasion. Additionally, current model suggests that the interaction between CD44 and its selected binding partners play a role in coordinating "cross-talk" among various intracellular signaling pathways (eg. Rho/Ras signaling and receptor-linked $p185^{HER2}$/c-Src tyrosine kinase pathways) leading to the concomitant onset of multiple functions including tumor cell adhesion, proliferation, migration, and invasion. MLC, myosin light chains. Figure derived from Turley et al. (2002).

binding sites for ERM (ezrin/radixin/moesin) cytoskeletal proteins and ankyrin, also leading to interaction with the underlying actin cytoskeleton (Lokeshwar et al., 1996, Zhu and Bourguignon, 2000, Tsukita et al., 1994). The ankyrin binding domain in CD44 is required for HA-mediated binding and cell adhesion (Lokeshwar et al., 1994), and promotes tumor cell migration (Zhu and Bourguignon, 2000). In addition, the interaction of ankyrin with Tiam1 promotes Rho GTPase activation and cytoskeletal changes observed in metastatic breast tumor cell invasion and migration (Bourguignon et al., 2000a).

Expression of CD44 is found in a wide variety of normal cell types including haemopoietic cells, transitional epithelial cells, dermal fibroblasts, articular chondrocytes, and neural glial cells. Most normal epithelial and non-epithelial tissues express the CD44s isoform. Expression of the CD44 variant isoforms is far more restricted in normal than in malignant tissues (Wielenga et al., 1993, Rudzki and Jothy, 1997). Expression of the CD44v6 isoform has been found in metastatic rat pancreatic carcinoma cells. Transfection of CD44v6-containing plasmids bestowed non-metastatic rat pancreatic carcinoma cells with the ability to form distant metastases (Gunthert et al., 1991). Furthermore, antibody specific for this variant inhibited formation of secondary neoplastic foci when co-injected with metastatic tumor cells (Seiter et al., 1993), supporting the notion that CD44 v6 variants are involved in tumor progression. Expression of CD44 variants has been implicated in the early stages of breast carcinogenesis and in promotion of breast cancer development (Bankfalvi et al., 1998, Iida and Bourguignon, 1997). However, the relationship between CD44 variants and clinical outcome for patients with breast cancer is unclear.

1.4.4.3 RHAMM (Receptor for HA mediated motility)

RHAMM has been described as the HA-binding protein of the cell surface hyaluronate receptor complex (HARC) that mediates HA-induced motility (Turley et al., 1991,

Hardwick et al., 1992). This complex appears at the cell surface or is released as soluble proteins of 72, 68, 58, and 52 kDa (Turley et al., 1987). Antibodies raised against the 52 and 58 kDa proteins containing the HA-binding domain block migration of cells in response to HA (Hardwick et al., 1992). Unlike other hyaladherins, RHAMM lacks transmembrane domain. It has been speculated that RHAMM is anchored in the membrane by accessory molecules (Hardwick et al., 1992, Turley, 1992).

RHAMM is distributed on the cell surface, in cytoplasm, cell nucleus, mitochondria, and cytoskeleton (Hardwick et al., 992, Wang et al., 1996, Entwistle et al., 1995, Masellis-Smith et al., 1996, Lynn et al., 2001, Assmann et al., 1998). By cDNA sequence, two binding motifs for HA located near the carboxyl terminus (amino acids 401-411 and 423-432) have been detected in RHAMM (Yang et al., 1993, Yang et al., 1994). These sites contain B(X7)B motifs in common with the sites in various HA-binding proteins, such as link protein, versican, aggrecan, and CD44 (Yang et al., 1994).

RHAMM is encoded within one gene (Spicer et al., 1995) with extensive alternative splicing of RNA or post translational processing of protein to produce multiple forms of RHAMM proteins. The murine RHAMM gene spans 20 kb at least and comprises 14 exons (Figure 1.5D) (Entwistle et al., 1995). A minor transcript coding alternatively spliced exon 4, namely RHAMM1v4, encodes a 73 kDa protein (Entwistle et al., 1995) which produced transformation and metastasis formation when overexpressed in immortalized murine fibroblasts (Hall et al., 1995).

Recent studies have reported a protein named intracellular hyaluronic acid binding protein (IHABP) (Hofmann et al., 1998b, Assmann et al., 1998, Fieber et al., 1999). The IHABP gene was characterized in murine and human indicating that RHAMM cDNA is a part of IHABP cDNA. The murine IHABP gene consists of 18 exons and spans over nearly 30 kb.

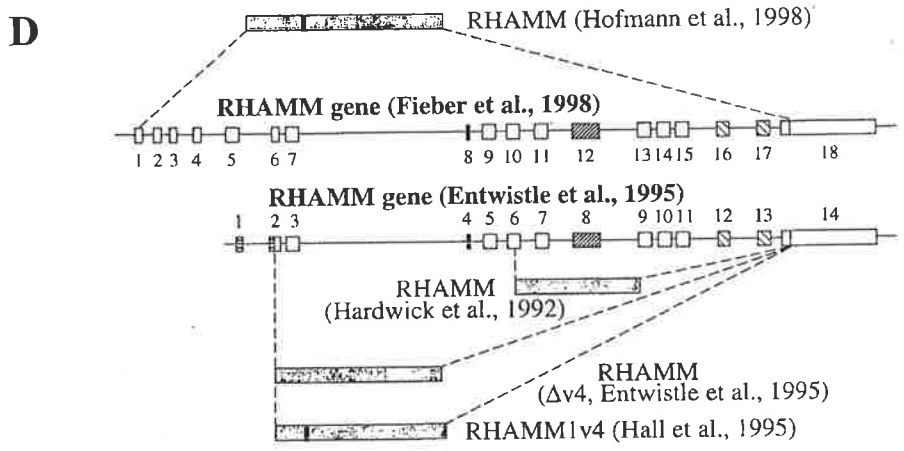

Figure 1.5 D. Schematic diagram of the structure of the RHAMM gene. Comparison of murine RHAMM open reading frames from cDNA isolates and the genomic structure. The murine RHAMM gene consists of 14 exons by Entwistle(Entwistle et al., 1995) and 18 exons by Fieber (Fieber et al., 1998). The exon 1 (Entwistle) matches part of exon 5 (Fieber). Exon 8 (Entwistle) and exon 12 (Fieber) are repeat regions indicated by hatched boxes. The HA-binding sites shown as the sparsely hatched boxes are in exon 12 and 13 (Entwistle) as well as exon 16 and 17 (Fieber). Comparison of the deduced peptide sequence of murine IHABP and murine RHAMM : RHAMM (IHABP) protein 95 kDa (Hofmann et al., 1998b), RHAMM1v4 protein 73 kDa (Entwistle et al., 1995, and Hall et al., 1995) and RHAMM protein 52, 58 kDa (Hardwich et al., 1995) (Turley et al., 1998). Figure derived from Hofmann et al. (1998a).

The first five exons encode IHABP specific sequence. Exon 6-18 of the genomic structure of IHABP is identical to the genomic structure published for RHAMM (figure 1.5D).

Several studies have focused on the function of RHAMM. RHAMM has been implicated mainly in cell motility. A variety of cells have been shown to require RHAMM for locomotion such as fibroblasts, epithelial cells, smooth muscle cells, macrophages, B cells, T cells and malignant myeloma cells (Turley et al., 1993, Masellis-Smith et al., 1996, Wang et al., 1998, Teder et al., 1995, Abetamann et al., 1996). Antibody-blocking studies have established that cell surface RHAMM is required for cell motility in response to HA (Turley, 1992, Turley et al., 1993), PDGF (Zhang et al., 1998a), TGF-β1 (Samuel et al., 1993), and ras oncogene (Hall et al., 1995). Additional studies have indicated that binding of HA by cell surface RHAMM results in signal transduction and focal adhesion turnover that are essential for cell motility (Hall et al., 1994).

RHAMM overexpression has been observed in human B cell malignancies, carcinoma of lung, pancreas, and breast (Teder et al., 1995, Abetamann et al., 1996, Turley et al., 1993, Masellis-Smith et al., 1996, Wang et al., 1998). In pancreatic cancer cell, RHAMM mRNA is overexpressed in a panel of human pancreatic cell lines exhibiting a poorly differentiated phenotype and a high metastatic potential when injected into nude mice (Abetamann et al., 1996). In addition, it has been reported that the highest HA concentration in primary pancreatic tumors was found at the interface between the tumor and normal tissue (Fries et al., 1994). RHAMM may promote invasion of pancreatic cells into the surrounding tissue by increasing cell motility in response to HA. RHAMM overexpression is present in primary breast cancers with lymph node metastases (Wang et al., 1998). These results suggest that RHAMM overexpression could be a useful prognostic indicator for breast cancer progression.

Statement of Aims

Versican, a family member of the large chondroitin sulfate proteoglycans, is a recognized modulator of matrix attachment and motility for mesenchymal cells. It is also a candidate prognostic marker and potential therapeutic target for cancers derived from mesenchymal cells. Recent studies from this laboratory have indicated that elevated expression of versican in peritumoral stroma predicts disease progression for men treated with surgery for early stage prostate cancer (Ricciardelli et al., 1998). Since the prominent actions of versican include anti-cell adhesion, the presence of increased versican levels may facilitate cancer cell migration through ECM. Apart from its presence at the invasive edge of breast cancers, little is known about versican expression in breast cancer tissues (Nara et al., 1997). The fact that versican is able to interact with HA and localizes with TN, both of which have been implicated as predictors of outcome for breast cancer suggests that the expression of versican may also be a candidate prognostic marker for breast cancer. This thesis presents observations regarding the expression, regulation and biological functions of versican in breast cancer.

The specific aims of this study were:

Aim 1. To determine the sites and level of accumulation of versican, chondroitin sulfate, TN and HA in breast cancer tissues, and to determine which of these components is the strongest predictor of outcome for women with node-negative breast cancers.

Aim 2. To determine whether breast cancer cells regulate versican secretion by stromal fibroblasts *in vitro*, and to investigate candidate soluble mediators produced by breast cancer cells.

Aim 3. To determine whether versican purified from fibroblast CM is able to modulate breast cancer cell adhesion and migration on ECM components *in vitro*.

Aim 4. To investigate whether breast cancer cells can utilise fibroblast CM, known to contain HA and versican to assemble a pericellular matrix sheath *in vitro*.

Chapter 2

Expression of Extracellular Matrix Components Versican, Chondroitin Sulfate, Tenascin-C and Hyaluronan, and Their Association with Disease Outcome in Node-Negative Breast Cancer

2.1 Introduction

The extracellular matrix (ECM) provides a physical framework for cellular attachment and participates in the normal physiological regulation of cell proliferation, migration, and differentiation. Consequently, components of ECM have become a major focus for studies examining pathological correlates of outcome for a number of cancer types. For example, disease relapse for patients with node negative breast cancer was recently associated with elevated expression of the chondroitin sulfate proteoglycan, versican in the peritumoral stromal tissue (Ricciardelli et al., 2002). Individual matrix components do not exist in isolation however, but rather function as a complex due to the numerous binding associations and biological interactions of these molecules. *In vivo*, versican binds to the linear unsulfated glycosaminoglycan hyaluronan (HA) via the amino terminal tandem repeat peptide sequence of versican, which is homologous to link protein and has inherent affinity for HA (Lebaron et al., 1992). In addition, versican also binds to the hexameric glycoprotein TN-R, possibly via interaction between the lectin domain of versican with either a carbohydrate moiety on TN (Aspberg et al., 1995) or with the fibronectin type III repeats within TN (Aspberg et al., 1997). TN-R has substantial sequence similarity with TN-C and its expression overlaps with that of TN-C (Norenberg et al., 1992). TN-C was found to co-localize with versican in precartilaginous mesenchyme and in connective tissue underlying epithelia (Perides et al., 1993). Individual reports have cited increased

levels of versican, HA or TN-C within neoplastic stroma of breast cancer, accumulating particularly at the leading edges of invasive foci (Nara et al., 1997, Jahkola et al., 1996, Ponting, 1993). In addition to the observations for versican, both HA and TN-C have been associated with disease outcome for breast cancer (Auvinen et al., 2000, Adams et al., 2002). Thus not only are all three molecules coincident *in situ* and apparently associated with clinical outcome from breast cancer, but from a functional viewpoint, they have all been identified as modulators of cellular attachment and motility (Chiquet-Ehrismann, 1990, Braunewell et al., 1995, Evanko et al., 1999). However, it is not clear whether these matrix factors assemble in a stoichiometric relationship, nor which of these matrix factors might have the greatest importance with respect to determination of patient outcome from disease.

The focus of this study was therefore, to individually examine the sites and level of accumulation of versican, chondroitin sulfate, TN-C, and HA in breast cancer tissues, and to determine which of these components within the matrix complex is the strongest predictor of outcome for women with node negative disease.

2.2 Materials and Methods

2.2.1 Materials

Monoclonal anti-TN2 (TN-C) against human tenascin hexabrachion structure and peroxidase-conjugated streptavidin were purchased from Dako (Denmark). Monoclonal anti-CS56 reactive for chondroitin sulfate, chondroitinase ABC, 3,3'-diaminobenzidine tetrahydrochloride (DAB), Streptomyces hyaluronidase were from Sigma Chemical Co (St Louis, MO). Avidin-biotin-peroxidase complex (ABC), biotinylated goat anti-mouse IgG secondary antibody, and biotinylated goat anti-rabbit IgG secondary antibody were from Vector Labs (Irvine CA). Rabbit anti-human versican was supplied by Dr R LeBaron, University of Texas San Antonio, USA. A biotinylated complex of bovine cartilage aggrecan HA-binding region and link protein (bHABC) was described in previous study (Tammi et al., 1994). Histogrip-coated slides were from Zymed Labs (San Francisco CA). DPX was from BDH Labs (UK).

2.2.2 Patients and tissue samples

A retrospective cohort of 86 women who underwent surgery for primary breast cancer between 1987 and 1991 was assembled with approval from the Research Ethics Committee of Flinders Medical Centre, Adelaide, South Australia. All patients were node-negative and all tumor tissue samples were diagnosed as infiltrating ductal carcinoma. Thirty five patients were in common with our previously reported cohort (Ricciardelli et al., 2002). No patients in either cohort had previously received chemotherapy, hormonal therapy, individually or in combination. The breast tumor tissue samples were graded according to the modified Bloom and Richardson system. Steroid receptor status was routinely assessed using the radioligand binding assay (Horsfall et al., 1986). Clinical and pathological data for the cohort is summarized in Table 2.1.

Table 2.1. Clinical and pathological characteristics of 86 patients with node-negative, infiltrating ductal carcinoma .

Characteristic		
Median age (range)		63 (28-82) years
Median follow-up (range)		65.5 (11-116) months
Menopausal status		
	Pre-menopausal	15
	Post-menopausal	68
	Unknown	3 (45, 46, 47 years)
Tumor grade		
	Grade I	13
	Grade II	34
	Grade III	39
Tumor size		
	<20 mm	47
	≥20 mm	39
Stage		
	1	46
	2a	39
	2b	1
Hormonal status		
	ER <10 fmol/1mg protein	32
	ER ≥10 fmol/1mg protein	54
	PR < 10 fmol/1mg protein	42
	PR ≥ 10 fmol/1mg protein	44
Recurrence		
	Non relapse	58
	Relapse	28
Death during follow-up		
	Alive	59
	Breast cancer	18
	Other causes	9

2.2.3 Immunohistochemical staining of breast tissue

Sections (4 μm) from archival formalin-fixed paraffin-embedded tissue blocks were mounted on Histogrip-coated slides and baked for either 60 min or overnight at 50-60°C. They were then deparaffinized in xylene, rehydrated in ethanol, and rinsed in PBS, pH 7.4. Endogenous peroxidase was blocked using 0.3% H_2O_2 in PBS for 5 min. To detect antigenicity of versican, the sections were predigested with chondroitinase ABC (0.5 U/ml in 0.1 M Tris acetate buffer pH 7.8, 0.1% BSA) 90 min at room temperature. After blocking nonspecific binding sites with 10% goat serum, the sections were incubated with rabbit anti-human versican (1:1000) overnight at 4°C, followed by addition of biotinylated goat anti-rabbit IgG secondary antibody (1:400) and peroxidase-conjugated streptavidin (1:500). After each step, the sections were washed with PBS twice for 5 min. To detect chondroitin sulfate, tissue sections were blocked with goat serum, followed by incubation with monoclonal mouse antibody CS56 (1:500) 60 min at room temperature. Subsequently, biotinylated goat anti-mouse IgG secondary antibody (1:400) and peroxidase-conjugated streptavidin were applied to the sections. To detect TN-C, tissue sections were digested with 0.1% pepsin in 0.01 M HCl 60 min at 37°C prior to blocking with 10% normal horse serum. Sections were then incubated with monoclonal mouse antibody TN2 (1:400) for 120 min at room temperature, followed by biotinylated horse anti-mouse IgG secondary antibody (1:400), and then avidin-biotin-peroxidase complex (1:200). To detect HA, tissue sections were blocked for non-specific binding with 1% BSA in PBS, incubated with bHABC probe (2.5 μg/ml, diluted in 1% BSA in PBS) overnight at 4°C, and then treated with avidin-biotin-peroxidase complex as previously reported (Tammi et al., 1994). The specificity of staining for HA was examined using tissue sections predigested with Streptomyces hyaluronidase in the presence of protease inhibitors.

Visualization of all the various immunoreactions was achieved using diaminobenzidine tetrahydrochloride and hydrogen peroxide (0.03% in 50 mM Tris-HCl, pH 7.6) for 6 min. Sections were rinsed in tap water, counterstained with hematoxylin, dehydrated through graded alcohols, cleared in xylene and mounted using DPX .

2.2.4 Evaluation of staining

The level of immunostaining for versican, chondroitin sulfate, and TN-C was measured using an automated image analysis system (VideoPro 32; Leading Edge P/L, Marion, South Australia) as previously described (Ricciardelli et al., 2002). Twenty images from random areas from each breast cancer tissue section were captured at 66x magnification and edited using VideoPro 32 software. The images included both epithelial and stromal areas. Epithelial areas were evaluated visually and recorded for each matrix component. Epithelial areas were then edited from the captured images, retaining only the stromal areas for image measurement. The following image measurements were recorded for the stromal tissue: total area and immunostained area (in pixels), and absorbance (ie reciprocal of optical density, OD in arbitrary density units) which represents the intensity of staining for each matrix component. The mean IOD (MIOD) was determined from the formula: stained area x integrated absorbance / divided by total area, for each section, and then the mean was calculated for the 20 images from each patient. Quality assurance of staining intensity measurement was achieved by the inclusion of intra- and inter-run control slides of known staining level within each staining run. In this study, the coefficient of variation in staining was below 10%, and no corrective modulation of intensity values was undertaken.

The intensity of HA in peritumoral stromal tissue was graded visually as weak (+), moderate (++), and strong (+++). The expression of HA in breast cancer cells was classified as 'negative' when < 5% of cancer cells were stained, 'weak' when 5-40% cells stained, 'moderate' when 41-70% cells stained, and 'strong' when 71-100% cells stained.

2.2.5 Statistical analysis

Statistical analysis was performed using SSPS 10 for Windows software (SPSS Inc., Chicago, IL). The relationship between clinicopathological variables and the expression (MIOD) of extracellular matrix components was determined using Spearman's rho correlation and Pearson Chi-square or Fisher's exact test. Spearman's rho analysis was also used to test for correlation between expression levels of the individual extracellular matrix components. Relapse-free survival was defined as the time from the date of diagnosis of disease to the date of disease recurrence (local or systemic). Overall survival was defined as the time from diagnosis of disease to death from breast cancer. Cox regression was used to correlate risk of relapse and death with the level of expression of individual matrix components. Kaplan-Meier product limit plots and log rank tests were used to compare the rates of relapse or death for groups of patients dichotomized for high or low expression of matrix component. Statistical significance was set at $P < 0.05$.

2.3 Results

2.3.1 Immunolocalization and expression of versican, CS, TN-C and HA

Staining for the individual extracellular matrix components was performed in 86 patients. After staining, some cases were excluded due to insufficient residual tumor area for adequate analysis. Available for analysis were 85 cases for versican staining, 85 cases for CS staining, 81 cases for TN-C staining, and 79 cases for HA staining.

Versican immunoreactivity was observed in the peritumoral stromal matrix of all breast cancer tissues examined (Figure 2.1A). The intensity of staining varied between patient samples, the median (range) concentration of versican in peritumoral stromal tissue being 8.68 (1.82-24.48) density units per pixel. In non-malignant breast tissue areas of breast cancer specimens, versican was either absent or presented as a thin discontinuous band of weak staining of the periductal stroma (not shown). Versican immunoreactivity was not observed in either cancer cells or the non-malignant epithelial cells in any of the specimens.

Chondroitin sulfate immunoreactivity (epitope CS56) was observed predominantly in the peritumoral stromal tissue of all breast cancer tissues examined (Figure 2.1B), the median (range) concentration of CS being 17.0 (7.1-25.6) density units per pixel. In 10 of the 85 (12%) specimens, membranous and cytoplasmic staining of the malignant epithelial cells was evident (Figure 2.1C, D). Weak immunostaining for chondroitin sulfate was observed within the basement membrane of non-malignant glands and in the surrounding collagenous stromal matrix (Figure 2.1E). Chondroitin sulfate was also present in nerve bundles, and the adventitia of arteries (Figure 2.1F, G). Chondroitin sulfate was not detected in normal ductal epithelial cells.

TN-C immunoreactivity was observed in the peritumoral stroma of all breast cancer tissues examined (Figure 2.1H), the median (range) concentration of TN-C being 19.4 (3.5-

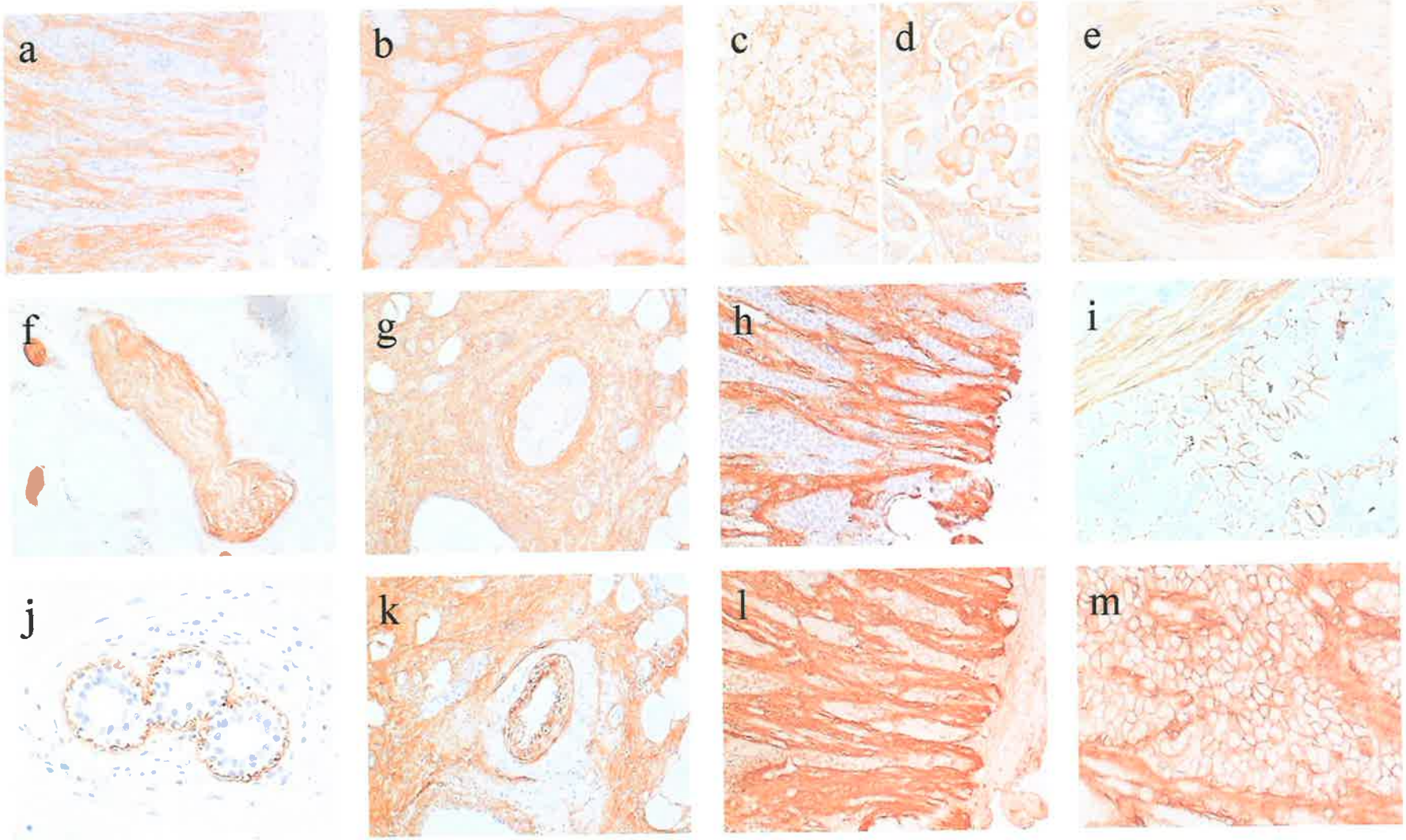
a
b
c
d
e
f
g
h
i
j
k
l
m

34.7) density units per pixel. TN-C immunoreactivity was observed in the cytoplasm and cell membrane of the malignant epithelial cells in only 3/81 (4%) of patients (Figure 2.1I). TN-C was also detected as a thin band of weak immunoreactivity surrounding normal ducts, and in the endothelial and smooth muscle cells of blood vessels within normal breast tissue (Figure 2.1J, K). No TN-C expression was detected in normal ductal epithelial cells.

Staining for HA was present in the peritumoral stromal tissue of all specimens of breast carcinoma, with variable intensity between tumors (Figure 2.1L). Weak HA staining of the stromal tissue was observed in 10/79 (13%) of tumors, moderate staining in 17/79 (21%), and strong staining in 52/79 (66%). HA was also detected in the malignant epithelial cells of 65/79 (82%) specimens (Figure 2.1M). In 42 of these specimens, HA was detected in more than 40% of the carcinoma cells. HA staining was associated with the plasma membrane in 40/65 specimens, with the plasma membrane and within the cytoplasm in 16/65 specimens, and with the plasma membrane and within the cytoplasm and the nucleus in 9/65 patients.

2.3.2 Relationship between expression of the individual ECM components, and their relationship with clinicopathological features of node-negative primary breast cancer

The relationships between the concentrations of the individual matrix components in peritumoral stromal tissue are shown in Table 2.2. Significant associations were detected between the levels of versican and CS (Figure 2.2, $r = 0.334$, $P = 0.002$), and between the levels of TN-C and HA in stroma ($r = 0.322$, $P = 0.005$). The relationships between the concentrations of versican, CS, TN-C and HA and patient clinicopathological factors (tumor size, grade, stage, and steroid receptor status) are shown in Table 2.3. The level of versican staining of peritumoral stromal tissue was not related to any of the clinicopathological factors examined, whereas increased expression of CS within peritumoral stroma was correlated with increased tumor grade ($P = 0.018$). Increased

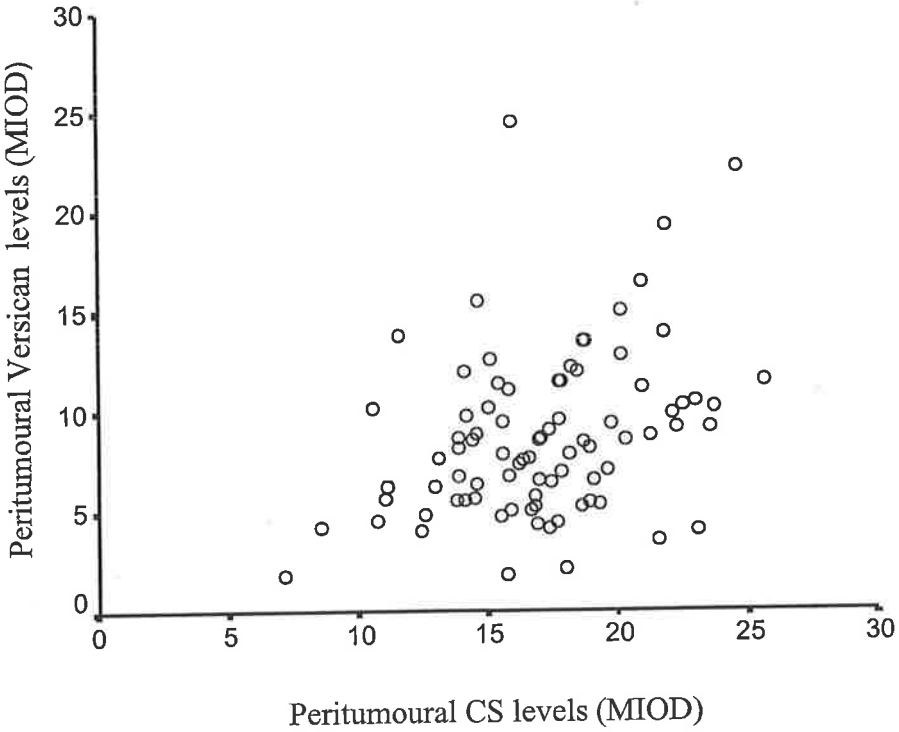

Figure 2.2. Correlation of immunostaining for versican and CS in node-negative, primary breast cancer. Concentration (MIOD) expressed in density units/pixel. Spearman rho analysis, r = 0.334, P = 0.002.

Table 2.2. Correlation between versican, TN-C, CS, and HA (Spearman's rho correlation)

Versican and CS	r=0.334	P=0.002*
Versican and TN-C	r=0.046	P=0.684
CS and TN-C	r=0.204	P=0.068
Versican and HA in stroma	r=-0.068	P=0.552
CS and HA in stroma	r=0.207	P=0.069
TN-C and HA in stroma	r=0.322	P=0.005*

* = Statistically significant at P<0.05

Table 2.3. Association of extracellular matrix components with clinicopathological parameters in node-negative breast cancer.

Variables	Versican (n=85)	CS (n=85)	TN-C (n=81)	HA in stroma (n=79)	HA in cancer (n=79)
Tumor size	r=0.004 P=0.969	r=-0.023 P=0.837	r=0.318 P=0.004*	r=0.274 P=0.015*	r=0.045 P=0.69
Tumor grade	r=0.012 P=0.912	r=0.256 P=0.018*	r=0.402 P=0.0001*	r=0.394 P=0.001*	r=0.306 P=0.006*
Tumor stage	r=0.020 P=0.859	r=-0.005 P=0.964	r=0.303 P=0.006*	r=0.219 P=0.052	r=0.009 P=0.939
ER level	r=0.084 P=0.443	r=-0.025 P=0.820	r=-0.273 P=0.014*	r=-0.06 P=0.600	r=-0.145 P=0.203
PR level	r=0.165 P=0.677	r=0.69 P=0.130	r=-0.197 P=0.077	r=-0.119 P=0.298	r=-0.048 P=0.677

r = Spearman correlation coefficient
All variables except tumor grade, tumor stage, HA in stroma and HA in cancer were continuous variables
* =statistically significant at P<0.05

expression of TN-C in peritumoral stromal tissue was significantly associated with increased tumor size (P = 0.004), tumor grade (P = 0.001), stage (P = 0.006), and was inversely related to ER status (P = 0.014). Increased expression of HA in peritumoral stromal tissue was significantly associated with increased tumor size (P = 0.015) and grade (P = 0.001), but not tumor stage (P = 0.052). Expression of HA by cancer cells correlated with tumor grade only (P = 0.006).

Versican and tenascin expression were also analyzed as dichotomized variables using the Chi-squared analysis. Versican expression (cut point MIOD <13 vs ≥13 density units per pixel) (Table 2.4) was associated with PR status (P = 0.015), but not with other factors tested. The cut point for versican was determined previously to be in the range of MIOD 13-14 density units per pixel (Ricciardelli et al., 2002). Stromal TN-C expression (cut point MIOD <19.4 vs ≥19.4 density units per pixel) (Table 2.4) was significantly associated with tumor size (P = 0.014), grade, (P = 0.004), and stage (P = 0.008). Because there was no established MIOD cut point for TN-C, the median MIOD for the cohort was used.

2.3.3 Prediction of disease outcome based on immunoreactivity of the ECM components

An increased risk of relapse was predicted by increasing tumor size (P = 0.036), and by high levels of versican expression when tested as either a continuous (P = 0.047) or a dichotomized variable (cut point MIOD <13 vs ≥13 density units per pixel, P = 0.007) (Table 2.5A). A relative risk of 1.08 for versican as a continuous variable signifies that the risk of relapse increases by 8% for each unit increase in versican content. A relative risk of 3.12 for versican as a dichotomized variable signifies a 3-fold increase in risk for patients with high versican content over those with low versican content. TN-C levels did not predict relapse-free survival. An increased risk of death was predicted by increasing tumor size (P = 0.050) and high levels of TN-C expression, when tested as either a continuous (P

Table 2.4. Correlation of versican cut off <13 vs ≥13, and TN-C cut off <19.4 vs ≥19.4 with established prognostic factors for breast cancer (Pearson Chi-square[a] or Fisher's exact test[b]).

		Versican		TN-C	
		<13	≥13	<19.4	≥19.4
Tumor size	< 20	41	5	27	16
	≥ 20	34	5	13	25
		p =1.00[b]		p =0.014 [b]*	
Grade	I	12	1	11	2
	II	28	5	17	14
	III	35	4	12	25
		p = 0.720[a]		p = 0.004[a]*	
Stage	1	40	5	27	15
	2a	34	5	12	26
	2b	1		1	
		p = 0.908[a]		p =0.008[a] *	
ER status					
ER <10 fmol/1mg protein		31	1	13	18
ER ≥10 fmol/1mg protein		44	9	27	23
		p = 0.082 [b]		p = 0.362 [b]	
PR status					
PR < 10 fmol/1mg protein		41	1	17	23
PR ≥ 10 fmol/1mg protein		34	9	23	18
		p = 0.015 [b] *		p = 0.269 [b]	

* = statistically significant at P<0.05

Table 2.5
A. Univariate Cox Regression analyses for disease-free survival and overall survival

Variable	Disease-free survival			Overall survival		
	Relative risk	95% CI	P value	Relative risk	95% CI	P value
Tumor size (n=86)[a]	2.27	1.06-4.87	0.036*	2.67	1.00-7.10	0.050*
Grade						
Grade I (n=13)	1.00			NT		
Grade II (n=34)	0.44	0.10-1.97	0.282			
Grade III (n=39)	1.49	0.69-3.23	0.314			
ER status (n=86)[b]	1.34	0.60-2.99	0.472	0.744	0.29-1.92	0.541
PR status (n=86)[c]	1.88	0.87-4.09	0.111	1.14	0.45-2.89	0.786
Versican (n=85)[d]	1.08	1.00-1.16	0.047*	1.06	0.96-1.17	0.255
Versican (n=85)[e]	3.12	1.37-7.11	0.007*	NT		
CS (n=85)[f]	1.07	0.97-1.19	0.168	1.09	0.95-1.24	0.206
TN-C (n=81)[g]	1.04	0.99-1.09	0.128	1.07	1.00-1.14	0.024*
TN-C (n=81)[h]	NT			3.80	1.25-11.55	0.019*
HA in stroma						
weak (n=10)	1.00			1.00		
moderate (n=17)	1.21	0.30-4.88	0.788	0.895	0.15-5.36	0.904
strong (n=52)	1.01	0.29-3.50	0.986	0.945	0.20-4.37	0.942
HA in cancer cells (n=79)	0.948	0.36-2.53	0.916	0.936	0.26-3.32	0.919

B. Multivariate analysis of tumor size, versican and TN-C immunostaining for disease-free survival and overall survival

Variable	Disease-free survival (n=85)			Overall survival (n=81)		
	Relative risk	95% CI	P value	Relative risk	95% CI	P value
Tumor size[a]	2.34	1.09-5.08	0.030*	1.96	0.72-5.33	0.187
Versican[e]	3.36	1.46-7.73	0.004*	NT		
TN-C[h]	NT			3.28	1.06-10.18	0.040*

a = Tumor size(mm) as a dichotomous variable cut point <20 vs ≥20
b = ER status (fmol/mg protein)as a dichotomous variable cut point <10 vs ≥10
c = PR status (fmol/mg protein)as a dichotomous variable cut point <10 vs ≥10
d = Versican immunostaining (MIOD units) as continuous variable
e = Versican immunostaining (MIOD units) as dichotomous variable, cut point <13 vs ≥13
f = CS immunostaining (MIOD units) as continuous variable
g = TN-C immunostaining (MIOD units) as continuous variable
h = TN-C immunostaining (MIOD units) as dichotomous variable, cut point <19.4 vs ≥19.4
NT = not tested, as not significant as continuous variable in univariate analysis
* = Statistically significant at $P < 0.05$

= 0.024) or a dichotomized variable (cut point MIOD <19.4 vs ≥19.4 density units per pixel, P = 0.019). Versican levels in peritumoral stromal tissue did not predict overall survival. Neither the level of CS nor HA predicted relapse-free survival and overall survival in this cohort of node-negative breast cancer patients. Multivariate analysis was conducted only on those variables significant in univariate analysis, hence non significant variables were "not tested". Multivariate analysis comparing risks of relapse for tumor size and versican concentration indicated that these variables independently predicted relapse (Table 2.5B). Multivariate analysis comparing risks of death for tumor size and TN-C concentration indicated that TN-C was the stronger predictor of overall survival (Table 2.5B).

The rates of relapse and death in this cohort were investigated using Kaplan-Meier Product Limit and Log Rank tests for tumor size dichotomized at 20mm (Figure 2.3). The rates of relapse and death were greater for the group of patients with tumors ≥20mm (Figure 2.3A, B) (relapse-free survival at 5 years was 79% versus 58%, overall survival at 5 years was 90% versus 68%, for patients with tumor size <20mm and ≥20mm, respectively). Versican and TN-C levels were investigated as dichotomized variables by Kaplan-Meier test for rates of relapse and death, respectively (Figure 2.3C, D). The rate of relapse was greater for the group of patients with versican levels MIOD ≥13 (relapse-free survival at 5 years, 74% versus 35% for patients with versican levels MIOD <13 and ≥13 respectively). The rate of death was greater for the group of patients with TN-C levels MIOD ≥19.5 (overall survival at 5 years, 92% versus 66% for patients with TN-C levels MIOD <19.5 and ≥19.5 respectively).

Because tumor size and versican concentration were independent variables in Cox multivariate analysis, combined scores for these variables were compared between patient

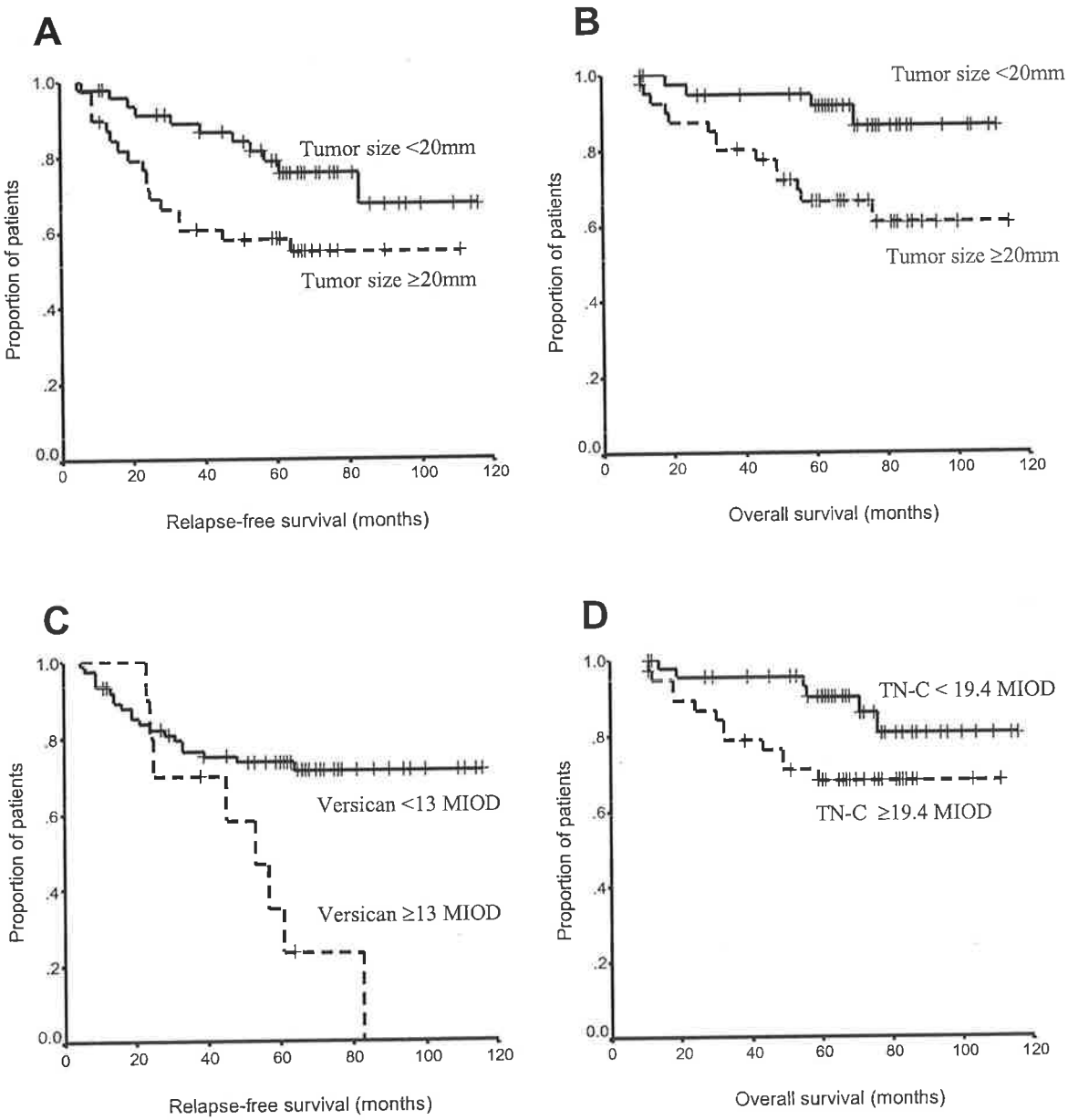

Figure 2.3. Kaplan-Meier plots for relapse-free survival (RFS) and overall survival (OS) in node-negative breast cancer patients.

A. Relapse-free survival, variable tumor size, n = 86, cut point <20 mm vs ≥20 mm, number of relapses 11/47 (23.4%) vs 17/39 (43.6), log rank statistic 4.69, P = 0.030.

B. Overall survival, variable tumor size, n = 86, cut point <20 mm vs ≥20 nm, number of deaths 6/47 (12.7%) vs 12/39 (30.8), log rank statistic 4.17, P = 0.041.

C. Relapse-free survival, variable stromal versican concentration, n = 85, cut point MIOD <13 vs ≥13 density units/pixel, number of relapses 20/75 (26.7%) vs 8/10 (80%), log rank statistic 8.22, P = 0.004.

D. Overall survival, variable stromal TN-C concentration, n = 81, cut point MIOD <19.4 vs ≥ 19.4 density units/pixel, number of deaths 4/40 (10%) vs 14/41 (34.1%), log rank statistic 6.44, P = 0.011.

subgroups in Kaplan Meier plots, to determine whether a more robust prediction of the rate of relapse for patients with node-negative, primary breast cancer could be achieved. Figure 2.4 illustrates that patients with small tumors and low versican concentration experienced fewer relapses than patients with large tumors and low versican level. In contrast, patients with high versican concentration, irrespective of tumor size, experienced a high rate of relapse (relapse-free survival at 5 years, 82% versus 64% versus 35% for the groups of patients with low versican and small tumors, low versican and large tumors, high versican irrespective of tumor size, respectively).

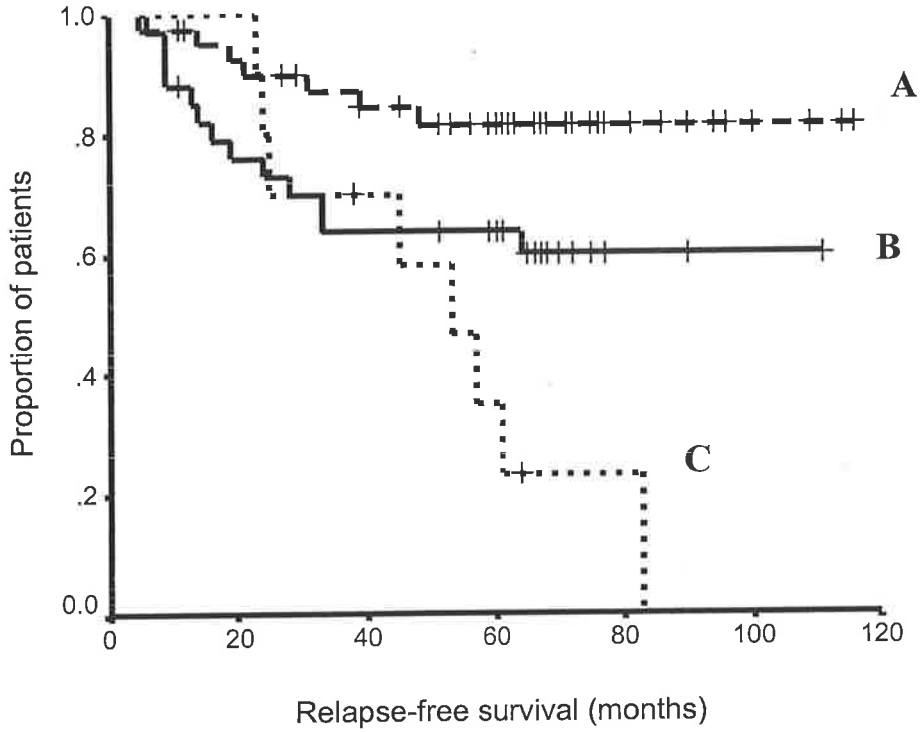

Figure 2.4. Kaplan-Meier plot for RFS in node-negative breast cancer patients, according to tumor size and versican concentration. N = 85, cut points tumor size < 20 mm vs ≥ 20 mm, stromal versican conentration, MIOD < 13 vs ≥ 13 density units/pixel. Patient groups were A, tumor size < 20 mm and versican concentration < 13 density units/pixel, number of relapses 7/41 (17%). B, tumor ≥ 20 mm and versican concentration < 13 density units/pixel, number of relapses 13/34 (38%). C, versican concentration ≥ 13 density units/pixel and tumor size < 20 mm or ≥ 20 mm, number of relapses 8/10 (80%). Log rank statistic 11.76, P = 0.0028.

2.4 Discussion

A diagnosis of node-negative primary breast cancer segregates patients into a category of low risk of relapse and death, but uncertainty of individual outcome remains. Although surgery is curative for the majority of women in this category, approximately 30% of patients will relapse with progressive disease. Currently, there is no reliable means to predict those patients who are likely to relapse, and would potentially benefit from more aggressive treatment at diagnosis. It was recently reported that high levels of versican in peritumoral stromal tissue predicted relapse in a cohort of women with node-negative, primary breast cancer (Ricciardelli et al., 2002). Versican is a recognized modulator of cellular adhesion and motility for mesenchymal cells such as fibroblasts, smooth muscle and neural cells (Bode-Lesniewska et al., 1996), and increased expression of versican in their malignant derivatives, eg melanoma and astrocytoma, appears to contribute to a more aggressive phenotype (Ang et al., 1999, Touab et al., 2002). There have been few reports however, regarding the presence of versican and the level of tumor aggression for adenocarcinomas of tissues, such as breast, prostate and ovary (Ricciardelli et al., 1998, Ricciardelli et al., 2002, Voutilainen et al., 2003).

Versican is a CS-proteoglycan and can bind specifically to other matrix molecules, principally HA and tenascin-R, leading to structural aggregations of matrix. CS proteoglycans, HA and TN-C have been individually implicated in modulating cellular adhesion and several reports suggest that these matrix components co-localize within the neoplastic stroma of tumors and the mesenchyme in embryonic tissues (Yamagata et al., 1993, Nara et al., 1997, Morris-Wiman and Brinkley, 1992, Grumet et al., 1994, Gotz et al., 1995). This suggests that these molecules may act in concert to achieve modulation of cellular attachment and motility. The results of our study indicate that, within the putative matrix complex, the concentration of versican is related to the concentration of CS, but not

to the concentrations of TN-C and HA. The correlation between versican and CS suggests that versican is the predominant CS-proteoglycan present in the peritumoral stromal tissue of breast cancer. The variability in the ratio of versican to TN-C and HA between individual patients suggests that the putative matrix complex in peritumoral stroma is not assembled in a fixed ratio of composition. Reinforcing this structural variability, no uniform association is observed between the matrix components and the clinicopathological features of the individual carcinomas. Whereas increased TN-C levels are related to increased tumor size, higher grade and stage, and the absence of estrogen receptors, all accepted features of more aggressive carcinomas, increased versican is independent of these features. The association of TN-C expression with a number of features of tumor aggression is consistent with earlier reports (Ishihara et al., 1995, Iskaros et al., 1998, Ioachim et al., 2002). In agreement with other studies, stromal HA is related only to tumor size and grade, and cancer cell-associated HA is related only to grade (Auvinen et al., 2000).

An examination of the predictive power of the individual matrix components by Cox regression analysis indicated that tumor size predicts both risk of relapse and risk of death, whereas versican and TN-C content of the peritumoral stromal tissue predict only risk of relapse and risk of death, respectively. Neither CS nor HA are predictive of outcome in this cohort of node-negative, primary breast cancer. In agreement with this study, HA expression was not predictive of outcome for the subgroup of node-negative women within a previously published cohort of women with breast cancer (Auvinen et al., 2000) (R Tammi, personal communication). An important finding of this study is that not only is versican concentration independent of tumor size (Spearman correlation), but versican concentration and tumor size are independent predictors of outcome (Cox multivariate analysis) for patients with node-negative breast cancer. Because of this independence, a

robust prediction of outcome can be achieved by combination of tumor size and versican concentration in Kaplan-Meier analysis. Patients with high peritumoral versican concentration experience the highest rate of relapse irrespective of the tumor size (>75% at 5 years). Patients with low versican concentration and small tumors experience the lowest relapse rate (<20% at 5 years).

The scatter of points in the Spearman plot for women with node-negative breast cancer (figure 2, r = 0.334) denoting the ratio of concentration of versican core protein to CS side chains, when compared with the same ratio in men with early stage prostate cancer (r = 0.742, (Ricciardelli et al., 1998), suggests a greater variability in CS proteoglycan type and/or glycosylation level in breast cancer. In support of this observation, the level of chondroitin sulfate in peritumoral stroma in breast cancer is unrelated to risk and rate of relapse, whereas there is a highly significant association in prostate cancer (Ricciardelli et al., 2002). This suggests that there may be a fundamental difference in the expression of CS proteoglycan types between breast and prostate cancers. One example of which is that, unlike prostate cancer cells, 12% of breast cancer specimens contained CS-immunoreactive cancer cells.

This study suggests that within the putative matrix complex of versican, TN-C and HA in peritumoral stromal tissue, versican alone predicts risk of relapse, and may be the principal component responsible for cancer cell metastasis in node-negative, primary breast cancer. The biological role of HA in breast cancer appears less clear. Although HA appears not to be associated with disease outcome in this study of node-negative breast cancer, this molecule is associated with outcome for unselected primary breast cancer patients (Auvinen et al., 2000). Moreover, HA is clearly involved in cellular motility by virtue of its ability to form a pericellular sheath in combination with aggregating proteoglycans, such as versican and aggrecan (Evanko et al., 1999). Although the sheath is anchored by

HA-receptors such as CD44, which have themselves been associated with outcome in breast cancer (Bankfalvi et al., 1998), the existence of sheath relies on its aggregating proteoglycan content (Simpson et al., 2001). To clarify the independent roles of HA and versican, *in vitro* studies need to be performed to determine whether versican promotes motility and invasion of breast cancer cells in the absence of a pericellular sheath of HA.

RHAMM, the other main class of HA receptor that has been reported to be important in promoting tumor progression and dissemination, was considered for staining in this study. Unfortunately, the antiserum to RHAMMv4 (kindly donated by Dr EA Turley) available for preliminary staining was derived using unpurified v4. Non-specific staining was a major problem and evaluation of results was difficult. Thus, detection of RHAMM staining in breast tissues in this study was not performed.

The biological role of TN-C in breast cancer also remains unclear despite its reported anti-adhesive activity, which would favor cell motility and growth promotion (Chiquet-Ehrismann, 1990). TN-C expression has been associated with cell proliferation and may represent a strong marker for local and distant recurrence (Jahkola et al., 1998b). In addition, a series of reports suggest that TN-C expression may be a suitable marker for predicting the invasive potential of premalignant breast lesions, including ductal carcinoma in situ (Adams et al., 2002, Jahkola et al., 1998a, Goepel et al., 2000).

In conclusion, this study has shown that although the extracellular matrix components versican, TN-C and HA appear to be associated in a putative complex with anti- cellular adhesive properties, the ratio of versican content to the other matrix components varies between individual tumors. Within this complex, versican appears to be the sole predictor in matrix for risk and rate of relapse, independent of tumor size, and this would suggest that this molecule has a primary role in breast cancer spread for patients with node negative disease. TN-C, on the other hand, is related to a number of features associated

with tumor aggression and is associated only with risk and rate of death. Its role in progression of breast cancer remains unclear. HA appears from this study to be unrelated to progression of node-negative breast cancer, despite the reported necessity of the versican-cross-linked pericellular sheath of HA for cell motility. Further study is required to determine how these molecules cooperate to control cancer cell metastasis.

Chapter 3

Versican Accumulation in Human Breast Fibroblast Cultures is Increased by Breast Cancer Conditioned Medium

3.1 Introduction

The fact that elevated versican expression in peritumoral stromal matrix was significantly associated with increased risk and rate of relapse in women with node-negative breast cancer (Chapter 2), suggested that the level of versican synthesis by the fibroblast population within the neoplastic stroma may be upregulated by more aggressive cancer cell populations. The mechanism of this upregulation was considered likely to be one of increased versican synthesis based on the work of Brown *et al.* (1999) who demonstrated that the level of versican mRNA expression in stromal cells as determined by *in situ* hybridisation was greater in invasive ductal carcinomas than in normal breast tissue. Due to the difference in spatial localization of the stromal and cancer cell populations, a potential mode of regulation would be by cancer cell mediators, *ie* cancer cell secreted growth factors. Growth factors are important regulators of stromal-epithelial cell interactions within breast cancer (Peres et al., 1987, Cullen et al., 1992, Ellis et al., 1994, Nakamura et al., 1997). It has been recognized that various growth factors are secreted by human breast cancer cell lines, and that these factors demonstrate autocrine and paracrine cell growth enhancing properties. Examples of such cancer cell mediators are transforming growth factor β (TGF-β) (Knabbe et al., 1987), platelet-derived growth factor (PDGF) (Bronzert et al., 1987) and insulin-like growth factor (IGF-1) (Huff et al., 1986). Several polypeptide growth factors have been implicated in the regulation of versican synthesis. Specifically, TGF-β1 has been shown to upregulate versican gene expression in

cultured normal human skin and gingival fibroblasts (Kahari et al., 1991) and in cultured prostate stromal fibroblasts (Sakko et al., 2001). Both TGF-β1 and PDGF-AB enhanced versican synthesis in cultured monkey arterial smooth muscle cells (Schonherr et al., 1991). Moreover, stimulation of cultured human gingival and peridontal ligament fibroblasts by PDGF-BB lead to an increase in mRNA for versican and fibroblast proliferation (Haase et al., 1998). *In vivo* accumulation of versican was demonstrated in the blood vessel intima of patients with atherosclerosis, being located in the extracellular matrix adjacent to both PDGF and TGF-β1-positive cells (Evanko et al., 1998). Elevated expression of vascular endothelial growth factor (VEGF) and basic fibroblast growth factor (bFGF) is correlated with a poor prognosis in patients with invasive breast disease (Relf et al., 1997). These growth factors regulate motility of endothelial cells and pericytes during angiogenesis, but the extent to which an upregulation of versican may be involved is not known. bFGF reportedly upregulates the expression of mRNA for the CSPG decorin in normal and keloid fibroblast cultures but the level of versican mRNA remains constant (Tan et al., 1993). Enhanced versican expression by human lung fibroblasts, HFL-1, is also induced by the combination of epidermal growth factor (EGF), PDGF-BB and TGF-β (Tiedemann et al., 1997). Collectively, these findings support a role for growth factors in the regulation of versican expression. However, the mechanism involved in this enhancement of versican expression in breast tumor stromal tissue is not well understood. The aim of this study was therefore to determine (i) whether versican production by primary cultures of fibroblasts isolated from mammary stroma is enhanced after treatment with cancer cell conditioned medium (CM) or with recombinant growth factors: TGF-β1, PDGF-AB, and bFGF, and (ii), whether the versican-enhancing activity within CM could be attributed to one or more of the above growth factors.

3.2 Materials and Methods

3.2.1 Materials

CMF (calcium and magnesium-free)-Hank's balanced salt solution, RPMI 1640, foetal bovine serum (FBS), trypsin/EDTA, streptomycin, Superscript ™ II RNase H⁻ reverse transcriptase were purchased from Life Technologies (NY, USA). Insulin-transferrin-sodium selenite medium supplement (ITS), collagenase (type II), hyaluronidase (type V), antibiotic antimycotic (A 7292, Penicillin, Streptomycin, Amphotericin B), 3-[4,5-dimethylthiazol-2-y1]-2,5-diphenyltetrazolium bromide (MTT), chondroitinase ABC, ovomucoid, Tris, glycine, goat serum, mineral oil, 3,3'-diaminobenzidine tetrahydrochloride (DAB), and goat anti-mouse IgG -peroxidase were from Sigma Chemical Co (St Louis, MO, USA). UV adhesive 358 was from Loctite LTD (Dublin, Ireland). Tissue culture grade coverslips were from Nunclon (Roskilde, Denmark). Monoclonal antibody cytokeratin (clone AE-1/AE 3) was from Signet (MA, USA). Monoclonal antibody desmin (clone D33), biotinylated goat anti-mouse, peroxidase-conjugated streptavidin were from Dako (Sydney, NSW, Australia). Monoclonal antibody vimentin (clone V9) was from Biogenex Laboratories (San Ramon CA, USA). Random hexamers, versican primers, GAPDH primers were from Bresatec (Adelaide, Australia). 100 bp DNA Ladder was from New English Biolabs Inc (Beverly, MA, USA). RNeasy mini kit was from Qiagen (Hilden, Germany). Taq DNA polymerase was from Perkin Elmer (Norwalk, CT). Recombinant human (rh) TGF-β1, rhPDGF-AB, rhbFGF, chicken anti-human TGF-β1 antibody , rabbit anti-human PDGF antibody, and rabbit anti-human bFGF antibody were purchased from R & D systems (Minneapolis MN, USA). Polyclonal rabbit anti-transferrin was from Rockland (Gillbertsville. PA. USA). Goat anti-rabbit IgG-peroxidase was from Amrad Biotech (Boronia, Victoria, Australia). Monoclonal anti-human large proteoglycan (versican) 2-B-1 was from Seikagaku Corporation (Tokyo,

Japan). Complete protease inhibitor cocktail tablets were from Roche (Mannheim, Germany). Acrylamide and Bradford protein assay were from BioRad Laboratories (Hercules, CA, USA). Nitrocellulose membrane and ECL detection reagent were from Amersham (Buckinghamshire, England). SeeBlue pre-stained protein standard molecular weight markers were from Novex (Carlsbad, CA, USA). All organic salts and solvents were from either Sigma Chemical Co or Ajax Chemicals (Sydney, Australia).

3.2.2 Cell lines

BT 20, MCF-7, MDA-MB-231, and ZR75-1 human breast cancer cell lines were purchased from the American Type Culture Collection (ATCC, Manassas VA, USA). The ER negative BT 20 was derived from a 74 year old caucasian female with mammary adenocarcinoma. The ER negative MDA-MB-231 was isolated from the pleural effusion of a 51 year old caucasian female with poorly differentiated adenocarcinoma. The ER positive ZR75-1 cell line was established from a malignant ascitic effusion of a 63 year old caucasian female with infiltrating ductal carcinoma. The ER positive MCF-7 was isolated from the pleural effusion of a 69 year old caucasian female who relapsed 3 years after radical mastectomy. All cancer cell lines were cultured in complete RPMI supplemented with 5% FBS in a 5% CO_2 humidified atmosphere at 37°C.

3.2.3 Derivation of primary fibroblast cultures from breast tissues

Breast tissues for the establishment of primary fibroblast cultures were obtained with written consent and the approval of the Research Ethics Committee at Flinders Medical Centre from patients undergoing surgery for breast cancer. After surgical removal, breast tissue from normal and malignant areas was provided at diagnostic pathology cut up. Tissues were washed 3 times with CMF-Hank's balanced salt solution in a sterile dish. Approximately one third of the tissue was fixed in 10% phosphate buffered formalin and processed to paraffin wax for histological examination. The remaining tissue was cut into

small fragments and transferred to a sterile centrifuge tube containing 10 ml of complete RPMI supplemented with 0.1% collagenase, 0.1% hyaluronidase, and 10% FBS. After digestion overnight at 37°C with gentle agitation, the cell suspension was centrifuged for 5 min at 2000 rpm in a bench top centrifuge. The cell pellets were resuspended in 5 ml of complete RPMI supplemented with 10% FBS. The cells were cultured in 25 cm^2 tissue culture flasks previously coated with FBS about 1 hour before using. The flasks were maintained at 37°C in a humidified 5 % CO_2 and 95% air incubator. Confluent cell monolayers were observed after 10 days of culture. At passage number 3 or 4, the cells were trypsinized (0.05% trypsin/0.02% EDTA) for 3 min at 37°C and centrifuged at 2000 rpm for 5 min and resuspended in complete RPMI supplemented with 10% FBS and 10% dimethyl sulphoxide (DMSO). They were cryopreserved by freezing overnight at -70°C in 1.5 ml aliquots. The aliquots were stored in liquid nitrogen.

3.2.4 Culture of mammary fibroblasts on glass coverslips

Cultured fibroblasts (at passage 2 or 3 before storage in liquid nitrogen) were trypsinized and approximately $1x10^4$ cells (suspended in 1 ml of complete RPMI supplemented with 10% FBS) were plated onto tissue culture grade coverslips in the wells of a 24 well plate. After 48-72 hours, the coverslips were removed from the wells and the bottom face glued onto glass microscope slides using UV light-activated adhesive. The glue was cured by exposing the slides to UV light for 10 min. The cells were fixed in 10% phosphate buffered formalin for 15 min at room temperature and subsequently washed with phosphate buffered saline (PBS). The cells were permeabilised by immersion in methanol and acetone at -20°C for 3 min and 1 min, respectively. After washing with PBS, the slides were stored in aqueous sucrose/glycerol medium at -20°C for upto 2-4 weeks.

3.2.5 Immunocytochemical characterisation of cytoskeletal markers on cultured mammary fibroblasts

Mammary fibroblasts cultured on coverslips and control dewaxed tissue sections of the breast cancers from which the fibroblasts were derived were washed in PBS prior to immunostaining. The antigenicity of cytokeratins (AE1/AE3), desmin (clone D33), and vimentin (clone V9) is masked by formalin fixation and paraffin embedding, and microwave pretreatment is required to retrieve antigenicity. The slides were placed in 10 mM citrate buffer pH 6.0 and heated until boiling at the high power setting (ie 100%) of microwave oven, followed by 15 min at low power (ie 50%). The slides were allowed to cool down to room temperature and washed in PBS. All slides were treated with 10% normal goat serum for 20 min at room temperature to block non-specific binding sites. Diluted monoclonal mouse antibodies to: cytokeratin (1:150), vimentin (1:200), and desmin (1:200) were applied to the slides and incubated overnight at 4°C. Subsequently, the slides were rinsed in PBS, incubated sequentially with biotinylated goat anti-mouse secondary antibody (1:400) and peroxidase-conjugated streptavidin (1:500) for 30 min. All incubation steps were followed by two washes of 5 min in PBS. Immunostaining was visualized using DAB (0.03% in 50 mM Tris-HCl pH 7.6, 6 min). Following washing with tap water, the samples were counterstained with weak haematoxylin, dehydrated, cleared, and mounted in depex.

3.2.6 Collection of serum-free conditioned medium (CM) from breast cancer cell lines

The human breast cancer cell lines BT 20, MCF-7, MDA-MB-231, and ZR75-1 were grown in 80 cm^2 culture flasks in complete RPMI with 5% FBS . When the monolayers were 80% confluent, the culture medium was changed to complete RPMI supplemented with 0.5% FBS for 24 h and then replaced with serum-free medium (complete RPMI plus

ITS). After 72 h, the CM was collected and stored at -70°C. Additional flasks of the ER positive cells, MCF-7 and ZR75-1, were grown in complete RPMI+ITS medium in presence of 1 nM oestradiol (E_2). Control medium was obtained from tissue culture flasks containing no cells.

3.2.7 Treatment of mammary fibroblast cultures with breast cancer cell CM

Primary fibroblast cultures at passage 6-7 were harvested with 0.05% trypsin/0.02% EDTA solution. The cells were re-plated at a density of $1x10^4$ cells/cm^2 into 80 cm^2 flasks containing 10 ml complete RPMI plus 5% FBS. After 4 days of culture, the medium was replaced with complete RPMI plus 0.5% FBS for 24 h. CM and control medium from breast cancer cell lines were thawed and filtered through 0.22 μm membranes. The media were diluted 1:1 in complete RPMI+ITS medium and added to the fibroblast cultures. The fibroblast medium and cell pellets were collected at 24, 48, and 72 h of culture. A cocktail of protease inhibitors (0.5M EDTA, 2% NaN_3, and 0.1M PMSF) was added to the medium in order to inhibit proteolytic degradation of versican. Fibroblast culture medium was stored at -70°C for analysis of versican expression by immunoblot. Cell pellets were stored at -70° C for analysis of versican mRNA expression by RT-PCR.

3.2.8 Treatment of mammary fibroblast cultures with recombinant growth factors and specific growth factor antibodies

Primary breast fibroblasts at passage 6-7 were plated into 12 well plates (10^5 cells/well) and maintained in complete RPMI plus 5% FBS. At confluence, cells were induced to become quiescent by culture in 0.1% FBS for 24 h. The cells were then incubated for 48 h in serum-free medium containing recombinant growth factors with or without addition of specific neutralizing antibody. The following growth factors were used: 10 ng/ml rhTGF-β1, 10 ng/ml rhPDGF-AB, and 1ng/ml rhbFGF. The following antibodies were incubated with the recombinant growth factors (for 1h at room temperature) prior to addition to the

cell cultures; 20 μg/ml anti- TGF-β1 (raised in chicken), 20 μg/ml anti PDGF (raised in rabbit), and 18 μg/ml anti bFGF (raised in rabbit). The same neutralizing antibodies were incubated with the CM from breast cancer cell lines for 1 h at room temperature before addition to the primary fibroblast cultures. The harvested fibroblast media in presence of complete protease inhibitor cocktail tablets were stored at -70°C until analysed by immunoblot. The number of cells in each well was counted after trypsinization using a haemocytometer.

3.2.9 RT-PCR detection of versican mRNA expression by fibroblasts and breast cancer cell lines

Total cellular RNA was extracted from cultured primary fibroblasts and breast cancer cell lines using RNeasy mini kit (QIAGEN), according to the manufacturer's protocol. Total RNA (1 μg) was reverse transcribed using SuperscriptTM II and random oligo (dT) primers in a total volume of 20 μl as recommended by the manufacturer (Invitrogen). Controls included were RNA without enzyme (RNA-RT), and no RNA with enzyme (no RNA+RT). PCR amplificaftion was performed in a 50 μl of total volume containing 2 μl of cDNA, 0.4 units Taq polymerase, 5x PCR buffer, 25 mM $MgCl_2$, 10 mM dNTP, 50 ng of sense and antisense primers, H_2O, and covered with 30 μl of mineral oil. The following specific primers used were: for versican V1 isoform (375 bp, product), sense 5'-CGGGATCCGGGGTGAGAACCCTGTATCG-3' (1227-1243, exon 6) and antisense 5'-ACTCTAGAGGCCACGCCTAGCTTCTGCAGC-3' (4563-4541, exon 8): for versican V0 isoform (436 bp, product), sense 5'-ACAAGCTTACACAGCCAACAAGACCA-3' (4128-4145, exon7) and the same antisense primer used to amplified V1. The PCR reaction was amplified with initial denaturation at 95°C for 3 min, followed by 30 cycles of 1 min denaturation at 95°C, 1 min annealing at 65°C, and 1 min extension at 72°C, with a final

extension of 10 min at 72°C. To determine that all samples originally contained amounts of cellular RNA, the samples were coamplified for the presence of an internal standard, glyceraldehyde 3-phosphate dehydrogenase (GAPDH). The primers for GAPDH (452 bp, product) were sense 5'-ACCACAGTCCATGCCATCAC-3' and antisense 5'-TCCACCACCCTGTTGCTGTA-3'. The PCR reaction conditions for GAPDH included an initial denaturation at 94°C for 3 min, followed by 35 cycles of 30 sec denaturation at 94°C, 45 sec annealing at 60°C, and 1 min extension at 72°C, with a final extension of 10 min at 72°C. All amplifications included controls with RNA-RT, no RNA+RT, and no cDNA template. The PCR products were run on a 1.5% agarose gel and stained with ethidium bromide for size verification.

3.2.10 Western blot analysis

The protein concentration of media harvested from mammary fibroblasts cultured in breast cancer cell CM was determined using Bradford assay. The assay was performed in duplicate on the samples. 10 µl of sample was added to 2 ml of Bradford dye (diluted 1:4 in deionised water) and absorbance measured at 595 nm using a spectrophotometer. To allow electrophoretic migration of the versican molecule (~900kDa) through polyacrylamide gel, the CS side chains were cleaved using chondroitinase ABC to yield the core protein (~400 kDa). Samples were digested in the following reaction: 40 µl of each sample solution; 8 µl of buffer (50 mM Tris-HCl/50 mM NaCl pH 8.0); 3 µl of chondroitinase ABC, and the trypsin inhibitor ovomucoid. Incubation was for 3 h at 37°C. 60 µl of sample buffer (1 M Tris-HCl pH 6.8, 10%SDS, 10% glycerol, 0.1% bromophenol blue, and 5% β-mercaptoethanol) was added to the sample, which was then heated at 95°C for 5 min. Samples treated with neutralizing antibody to PDGF and bFGF were performed as mentioned above, except for incubation with sample buffer without 5% β-

mercaptoethanol. An equal volume of each sample (20µl) was loaded onto gradient polyacrylamide gels (4-9%) together with 5 µl of SeeBlue plus2 pre-stained protein standard as a marker (Ricciardelli et al, 2002). The protein was electrophoresed in SDS-PAGE running buffer for 45 min at 200 V and transferred to Hybond ECL nitrocellulose membrane by electrophoresis at 33 V overnight in transfer buffer. The samples treated with neutralizing antibody to PDGF and bFGF were electrophoresed on gel under non-reducing conditions and proteins were transferred to nitrocellulose membrane at 4°C for 15-18 h at a constant of 150 mA. The membranes were blocked for 1 h in a solution of 3% w/v skim milk power in 1M Tris-buffered saline pH 7.4, containing 0.1% Tween-20 (TBS-T) and rinsed twice in TBS-T. Rabbit anti-versican (1:1000 in TBS-T), mouse anti-versican (2-B-1, 1: 500 in TBS-T), and rabbit anti-transferrin (1:5000 in TBS-T) were added to the membranes for 2 h and subsequently incubated with peroxidase-conjugated sheep anti-rabbit IgG (1:1000) and peroxidase-conjugated goat anti-mouse IgG (1:1000) for 45 min. After each antibody incubation, the membranes were washed 3 times with TBS-T for 10 min. Immunoreactive protein was detected using the enhanced chemiluminescence (ECL) system according to the manufacturer's instructions. After the membranes were exposed to X-ray film for 1s-2 min, the intensities of the versican bands were measured using ImageQuant TM software (Molecular Dynamics, USA). Transferrin from the ITS supplement was used as an internal control to confirm equal sample loading.

3.2.11 Cell proliferation assays

Primary mammary fibroblasts were seeded into 96 well plates at a density of 4,000 cell/well. The cells were grown in complete RPMI supplemented with 5% FBS at 37°C in 5% CO_2 atmosphere. After 4 days, the culture medium was changed to complete RPMI supplemented with 0.5% FBS for 24 h. Thereafter, cells were cultured in complete RPMI containing ITS. Control or conditioned media from breast cancer cell lines (sterilised

using 0.22 μm filters and diluted 1:1 in complete RPMI supplemented with ITS) was added to the fibroblast cell culture. At 24, 48, and 72 h, 10 μl of 5 mg/ml aqueous MTT was applied to each well and incubated for 4 h at 37°C . Subsequently, 100 μl of 20% SDS in 0.02 M HCl was added and left overnight at room temperature in the dark. The plates were measured at dual wavelengths of 570 nm and 655 nm using a microplate reader (BioRad 450). Six duplicate samples were analyzed at each timepoint.

3.3 Results

3.3.1 Derivation and characterisation of primary fibroblast cultures from breast tissues

Primary cultures of human mammary fibroblasts were derived from 2 patients undergoing surgery for breast cancer. Both normal and malignant tissue were processed to isolate stromal fibroblasts. Two cell types were observed to initially attach to the culture flask. The majority of cells were elongate and bipolar in shape, consistent with the phenotype of stromal cells. A minority of cells formed clusters of round, epithelial-like cells. After the first passage, only the elongated stromal-like cells continued to grow in the culture. All of the primary cell cultures were free from mycoplasma contamination as determined by PCR analysis. Histopathological examination of tissue sections taken from the tissue fragment adjacent to that used for establishment of the primary cell cultures confirmed two as breast cancers, one as normal breast tissue and one as normal breast tissue with associated fibrosis.

To characterise the stromal cells derived from breast tissue, monolayer cells were grown on tissue culture coverslips (at passage 3 or 4) and stained using specific monoclonal antibodies to the cytoskeletal markers cytokeratin, vimentin, and desmin. The anti-human cytokeratin labels epithelial cells. The anti-human desmin labels cells of myogenic origin, ie both striated and smooth muscle cells. The anti-human vimentin labels cells of mesenchymal origin including fibroblasts, smooth muscle cells, endothelial cells, and lymphoid cells. The monolayer cell cultures were stained in parallel with breast and prostate tissue sections used as positive controls. The anti-vimentin stained only the peritumoral stroma of invasive ductal carcinoma tissue (Figure 3.1A). Cytokeratin was strongly expressed in malignant epithelial glands of breast cancer tissue (Figure 3.1C), while desmin staining was localized to the smooth muscle cells of the prostate gland

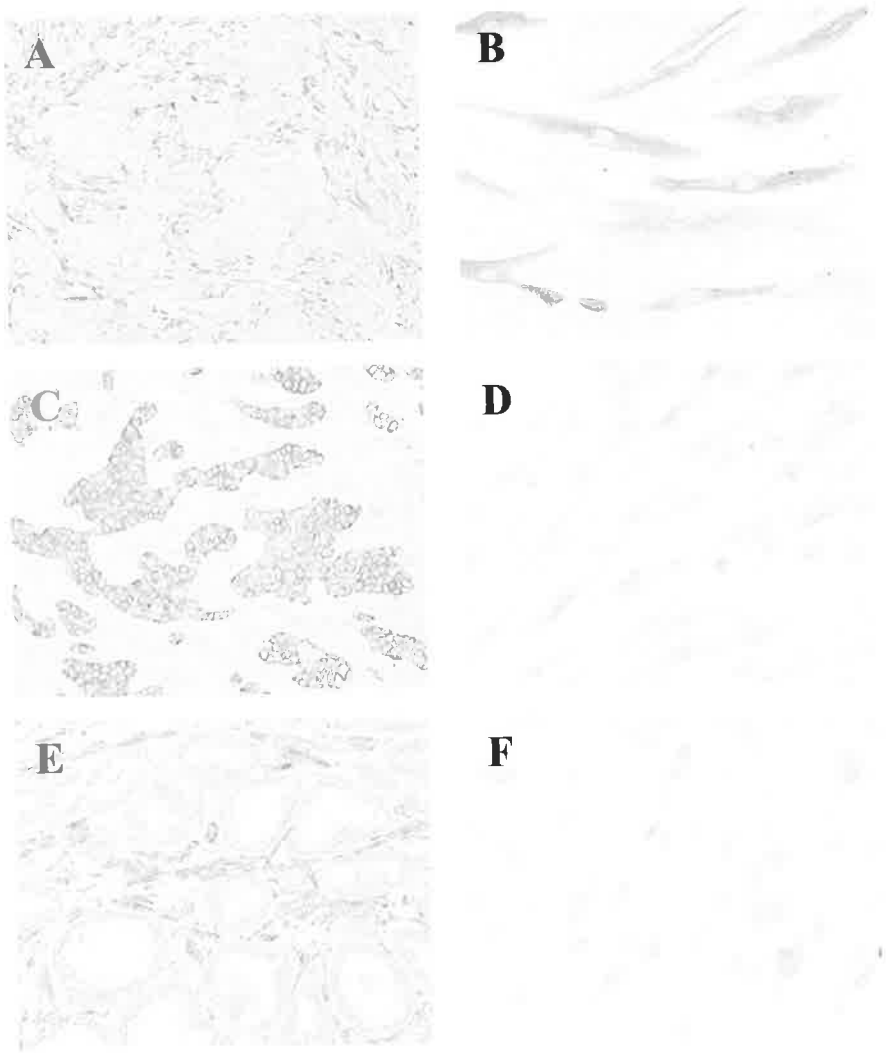

Figure 3.1. Immunostaining for cytoskeletal markers: vimentin, cytokeratin and desmin. Vimentin staining is present in tumor stroma of invasive ductal breast carcinomas (A) (x 100) and is also seen in cytoplasm of primary cultures of human mammary fibroblasts (B) (x 200). Cytokeratin staining is strongly expressed in malignant cells of breast cancer tissue (C) (x 100), whereas staining of cytokeratin is not detectable in cytoplasm of primary cultures of human mammary fibroblasts (D) (x 200). Desmin staining of prostatic carcinoma tissue is localized in smooth muscle cells of peritumoral stroma (E) (x 100), while desmin staining is absent from primary cultures of human mammary fibroblasts (F) (x 200)

(Figure 3.1E). All of the primary mammary stromal cells were strongly positive for vimentin (Figure 3.1B) but none showed positive immunostaining for cytokeratin (Figure 3.1D) or desmin staining (Figure 3.1F). These results indicated that the primary cell cultures were of mesenchymal and not of epithelial origin. Furthermore, negative staining for desmin confirmed the absence of smooth muscle cells. Thus, the primary stromal cell cultures were consistent with fibroblasts.

Immunostaining for versican performed on sections of the breast tissue fragment adjacent to that used for isolation of the primary stromal cell cultures demonstrated the presence of versican in stromal cells and stromal matrix surrounding tumor cell nests, but not in the cancer cells (Figure 3.2A). Immunoreactivity for versican was also observed in cytoplasm of all breast fibroblast cultures (Figure 3.2C). Negative control without versican antibody, demonstrated absence of staining in breast tissue section (Figure 3.2B) and in fibroblast cell culture (Figure 3.2D). There was no difference in morphology or immunocytochemical staining for versican between fibroblasts derived from breast cancer tissue and non-malignant mammary tissue fibroblasts.

3.3.2 RT-PCR of versican mRNA in fibroblast and breast cancer cell cultures

Primary cultures of mammary fibroblasts expressed two isoforms of versican mRNA: V0 (436 bp) and V1 (375 bp), whereas none of the breast cancer cell lines demonstrated versican mRNA expression (Figure 3.3A and B). GAPDH was used as an internal positive control for the RNA and a PCR product (452 bp) detected for all samples (Figure 3.3C). No bands were observed in the control lanes containing no RNA + RT and no DNA (Figure 3.3A, B, and C).

3.3.3 Immunoblot analysis of versican in fibroblast cultures

Immunoblot analysis detected two bands (approximately 450 kDa and 400 kDa) for versican isoforms V0 and V1 in mammary fibroblast culture medium (Figure 3.4),

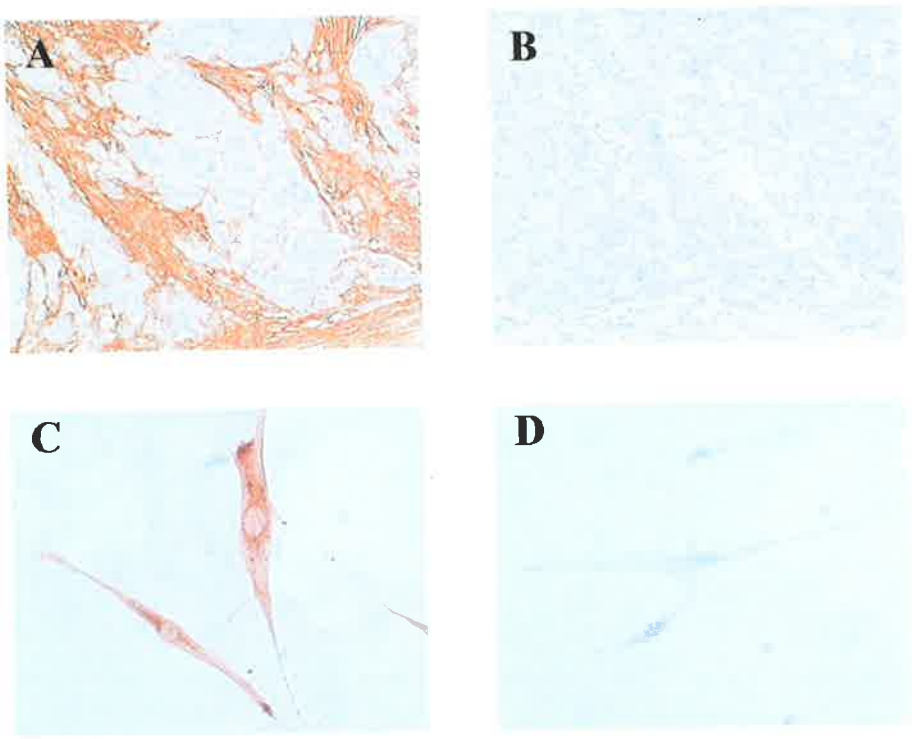

Figure 3.2. Immunostaining for versican in breast tissue sections and primary cultures of mammary fibroblasts derived from breast cancer tissue. Versican expression is located in stromal cells and stroma surrounding tumor cell nests (A) (x 100). Immunoreactivity of versican is noted in cytoplasm of fibroblasts (C) (x 200). Negative controls, incubation without versican antibody for breast cancer tissue section (B) (x 100) and fibroblast cell culture (D) (x 200).

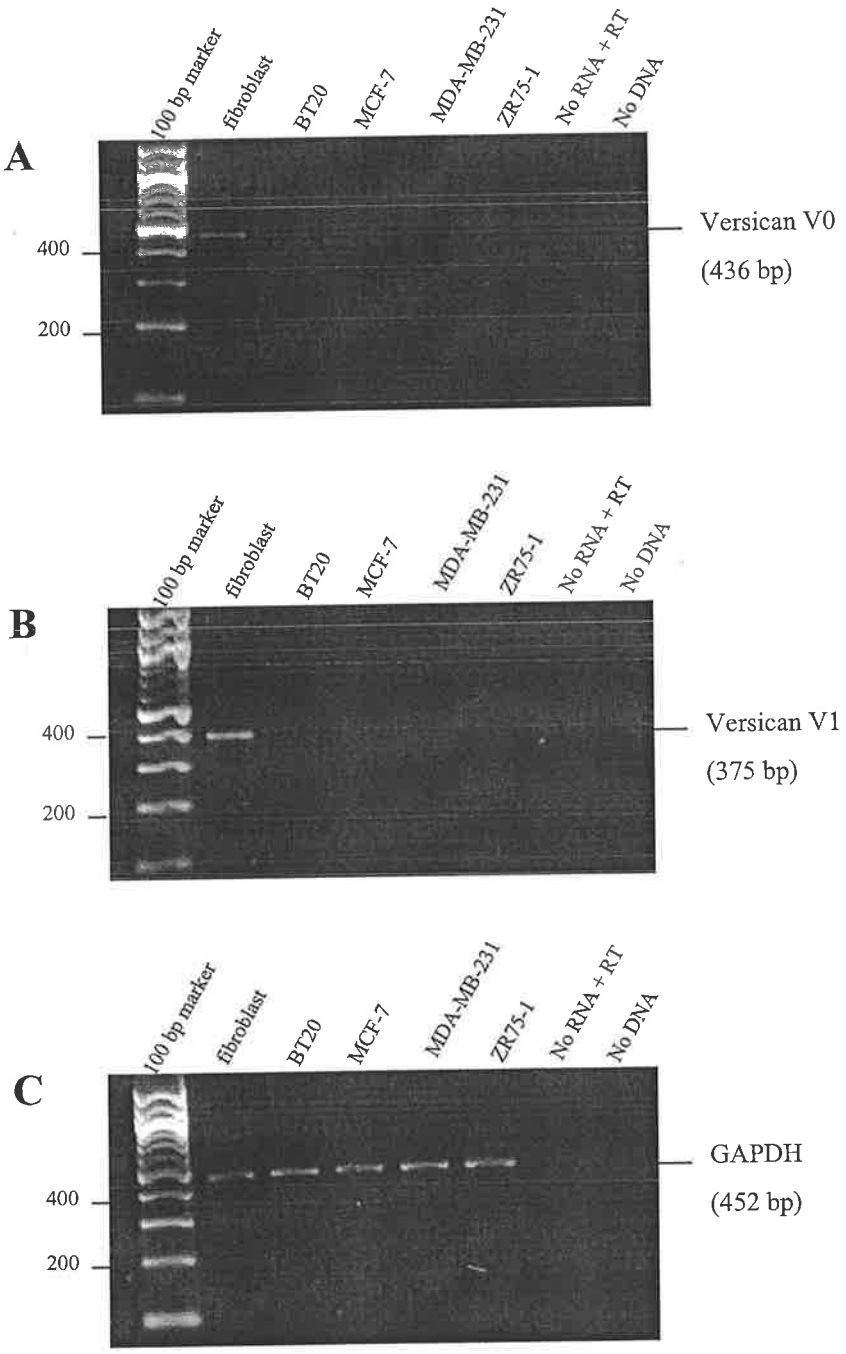

Figure 3.3. RT-PCR showing amplified mRNA of (A) versican isoform V0, (B) V1, and (C) GAPDH. Primary cultures of mammary fibroblasts derived from breast cancer tissue expressed amplified product of both versican V0 (436 bp) and V1 (375 bp), whereas no versican isoform was detected for any of the human breast cancer cell lines: BT20, MCF-7, MDA-MB-231, and ZR75-1. Expression of GAPDH was found in all samples, except negative controls (water substituted for RNA and DNA).

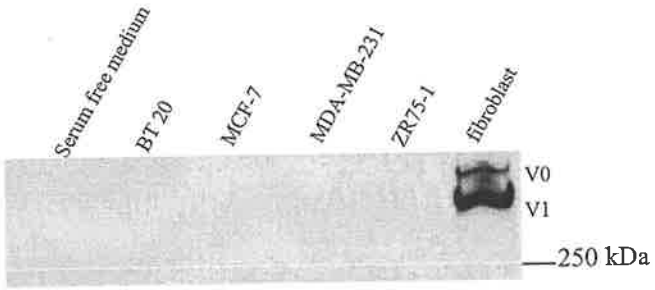

Figure 3.4. Immunoblot analysis for versican confirmed that versican (V0 and V1) was secreted by mammary fibroblast derived from breast cancer tissue and not by BT 20, MDA-MB-231, MCF-7, and ZR75-1 breast cancer cell lines.

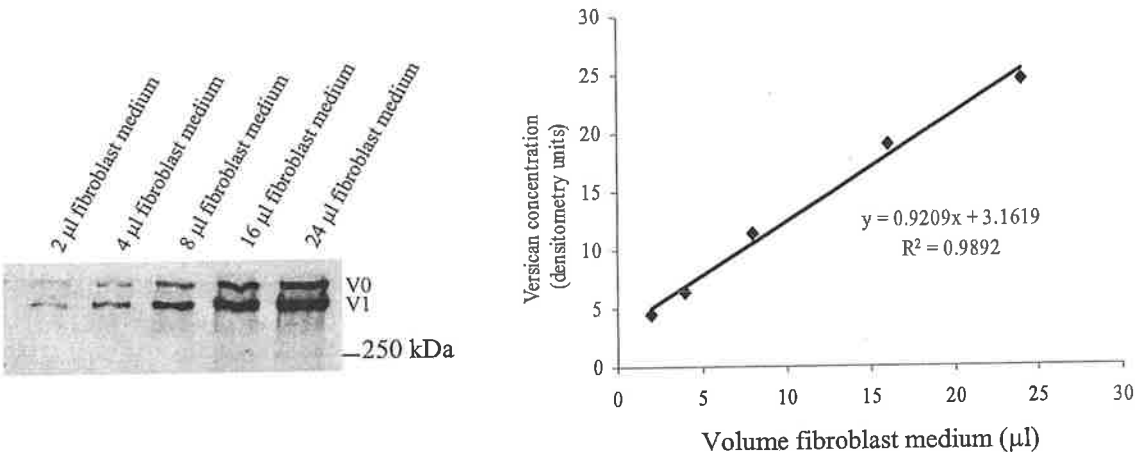

Figure 3.5. Linear detection of versican by immunoblot analysis. The culture medium of mammary fibroblasts derived from breast cancer tissue (concentrated 15-fold) was loaded onto western gels in increasing volumes, ranging from 2 to 24 µl. The concentration plot for versican was linear confirming that versican secretion into fibroblast culture medium could be accurately measured by immunoblotting.

indicating that versican is a product of fibroblasts and not breast cancer cells: BT 20, MDA-MB-231, MCF-7, and ZR75-1. This data is in agreement with the RT-PCR data presented in Figure 3.3. Figure 3.5 is a plot of versican concentration measured by immunoblotting for increasing volumes of fibroblast culture medium. The plot was linear, indicating accurate measurement could be achieved by immunoblotting and enhanced chemiluminescence. Immunoblot analysis of serum-free media harvested from mammary fibroblasts (at passage 6 or 7) demonstrated increased levels of versican after 24 h, 48 h, and 72 h treatment with CM from breast cancer cell lines, in comparison with control fibroblast medium (Table 3.1). CM from BT 20 breast cancer cell lines stimulated versican synthesis in non malignant mammary tissue fibroblasts up to 2.3-fold and in mammary fibroblasts derived from breast cancer tissue up to 2-fold. CM from MDA-MB-231 breast cancer cell lines increased versican synthesis by non malignant mammary fibroblasts and mammary fibroblasts derived from breast cancer tissue to a level of 3.3-fold and 2.7-fold of control, respectively. CM from MCF-7 and ZR75-1 stimulated versican synthesis by non malignant mammary fibroblasts up to 4.2-fold, and approximately 2.7-fold by fibroblasts from cancer tissue. The inclusion of estradiol during culture of MCF-7 and ZR75-1 breast cancer cell lines, and carry over of its presence into CM, lead to negligible differences in versican production compared to mammary fibroblasts treated with CM obtained from cells cultured in the absence of estradiol. Statistical analysis of the changes in versican levels was not performed. Typical immunoblots and scanning densitometric analysis illustrating the effect of CM from breast cancer cells on versican synthesis by non malignant mammary tissue fibroblasts and by mammary fibroblasts derived from breast cancer tissue are shown in Figure 3.6 and Figure 3.7, respectively.

Table 3.1. Summary of immunoblot analysis of versican accumulation in culture medium of isolates of mammary fibroblasts from two non-malignant breast tissues (NF1,2) and two breast cancer tissues (TF1,2). Each fibroblast culture was stimulated with CM from BT 20, MDA-MB-231, MCF-7, MCF-7+E_2, ZR75-1, and ZR75-1+E_2 breast cancer cell lines. Data is represented as a percentage of control, mean ± SD of four determinations from two independent experiments. Immunoblots were detected using ECL and scanning densitometry.

Source of CM	Breast fibroblast	Versican concentration (percent of control)		
		24 h	48 h	72 h
BT 20	NF1	161 ± 29	193 ± 38	218 ± 13
	TF1	150 ± 13	209 ± 29	169 ± 11
	NF2	128 ± 5	234 ± 28	96 ± 4
	TF2	101 ± 1	115 ± 2	144 ± 2
MDA-MB-231	NF1	240 ± 57	338 ± 69	305 ± 40
	TF1	170 ± 26	270 ± 32	219 ± 10
	NF2	131 ± 2	241 ± 12	116 ± 3
	TF2	181 ± 4	243 ± 10	196 ± 3
MCF-7	NF1	206 ± 39	211 ± 32	206 ± 19
	TF1	175 ± 18	273 ± 35	197 ± 32
	NF2	313 ± 22	421 ± 41	100 ± 4
	TF2	119 ± 1	187 ± 11	140 ± 2
MCF+E_2	NF1	227 ± 21	165 ± 8	154 ± 19
	TF1	200 ± 44	232 ± 86	163 ± 30
	NF2	301 ± 16	297 ± 79	89 ± 6
	TF2	172 ± 15	193 ± 10	101 ± 1
ZR75-1	NF1	155 ± 7	131 ± 9	166 ± 29
	TF1	155 ± 11	272 ± 15	199 ± 17
	NF2	320 ± 30	420 ± 41	129 ± 2
	TF2	143 ± 10	180 ± 2	104 ± 3
ZR75-1+E_2	NF1	222 ± 29	160 ± 21	153 ± 20
	TF1	192 ± 65	209 ± 42	151 ± 28
	NF2	236 ± 17	319± 32	115 ± 1
	TF2	165 ± 12	196 ± 11	119 ± 14

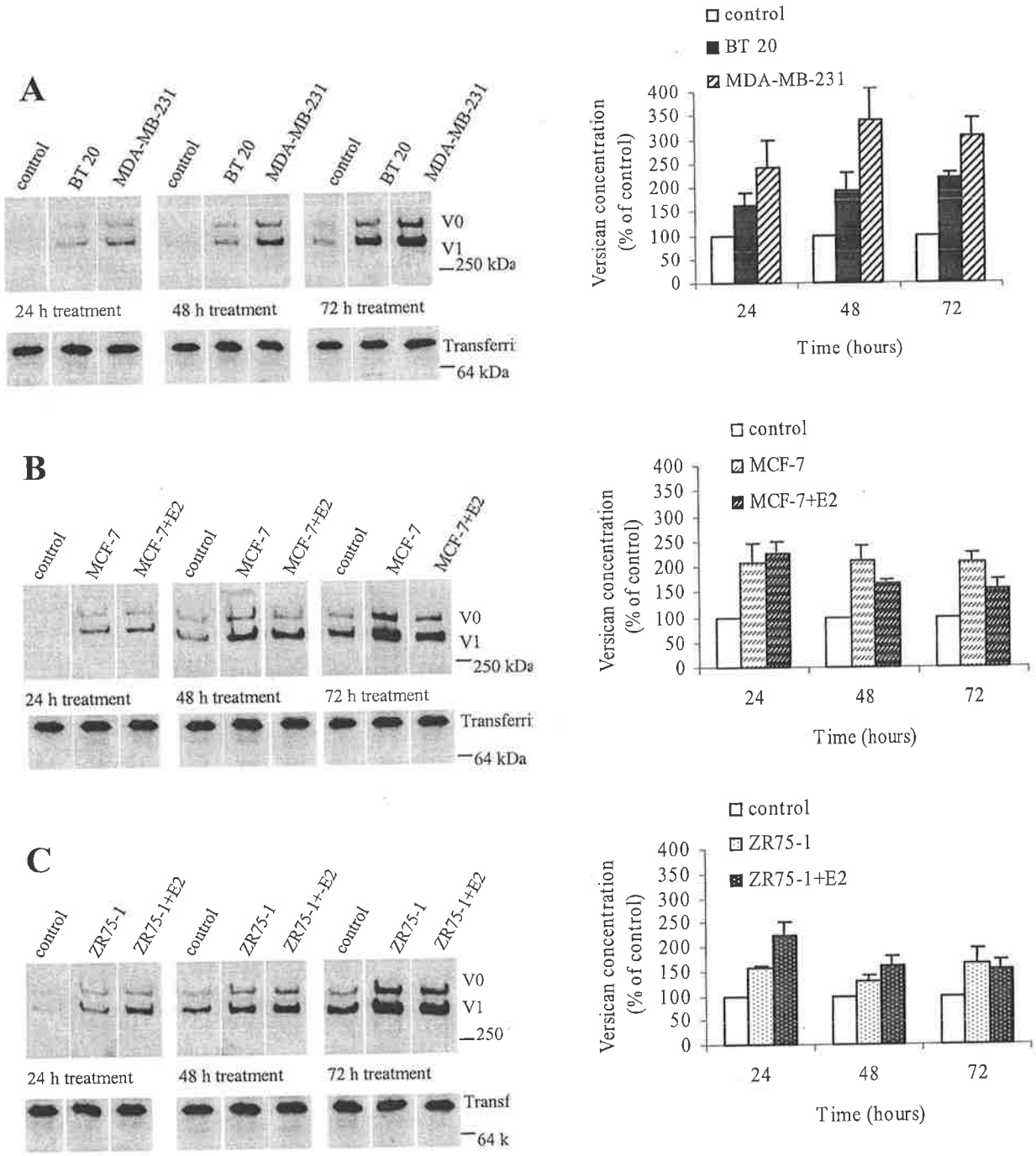

Figure 3.6. Immunoblot analysis of versican accumulation in the culture medium of non malignant mammary fibroblasts stimulated with CM from BT 20 and MDA-MB-231 (A), MCF-7 and MCF-7+E2 (B), and ZR75-1 and ZR75-1+E2 (C). Two isoforms of versican, V0 & V1 were measured in culture medium. Transferrin immunoblotting was performed on all gels. Immunoblots were detected using ECL and scanning densitometry. Graphs to the right of each immunoblot summarise the mean ± SD of four determinations from two independent experiments. Statistical analyses were not performed.

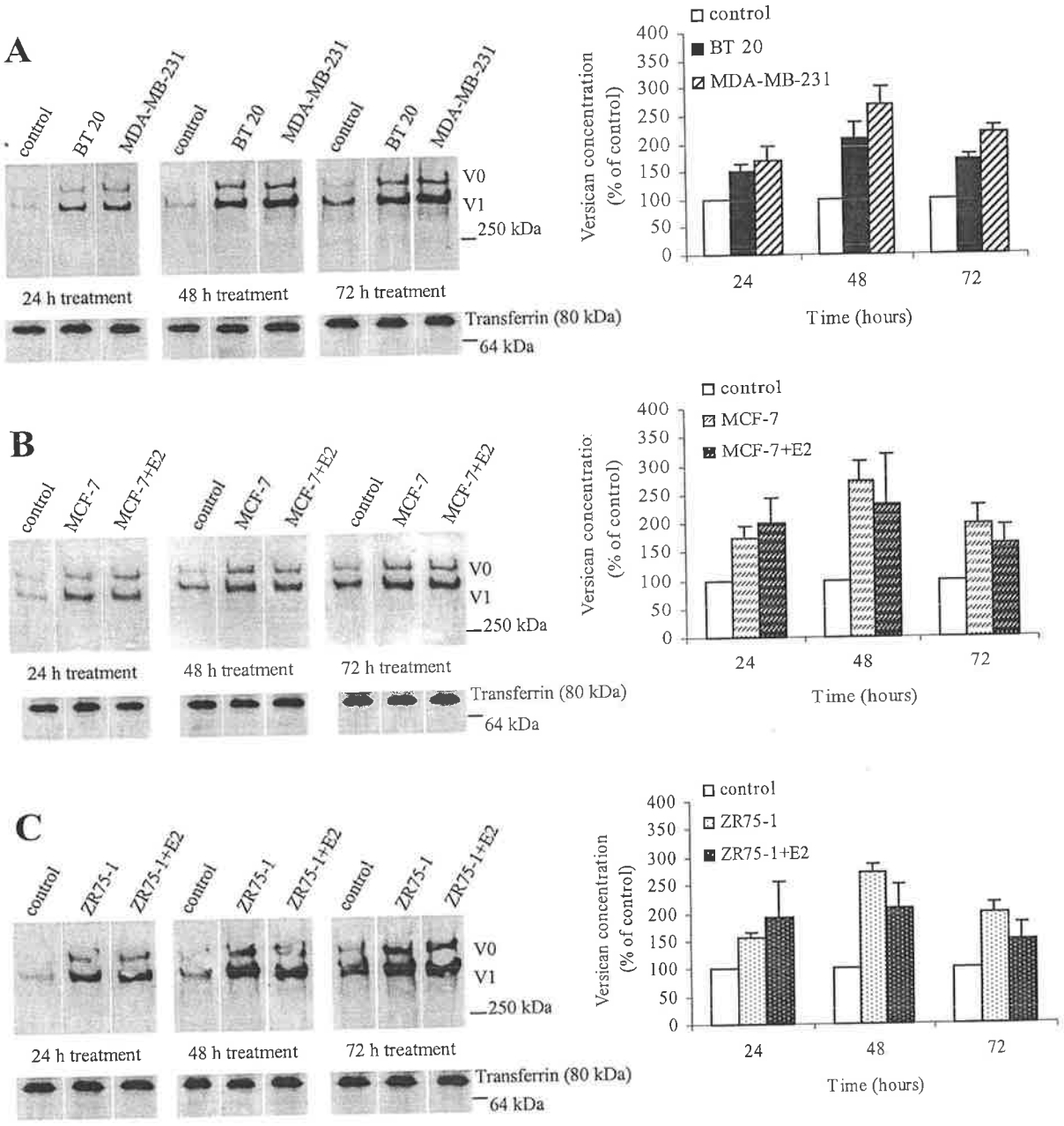

Figure 3.7. Immunoblot analysis of versican accumulation in culture medium of mammary fibroblasts derived from breast cancer tissue stimulated with CM from BT 20 and MDA-MB-231 (A), MCF-7 and MCF-7+E2 (B), ZR75-1 and ZR75-1+E2 (C). Two isoforms V0 & V1 were measured. Transferrin immunoblotting was performed on all gels. Immunoblots were detected using ECL and scanning densitometry. Graphs to the right of each immunoblot summarise the mean ± SD of four determinations from two independent experiments. Statistical analyses were not performed.

3.3.4 Effect of breast cancer cell conditioned medium on fibroblast proliferation

To determine whether the increased versican accumulation in mammary fibroblast culture medium was due to increased rate of secretion or cell proliferation, cultured mammary fibroblasts were measured using MTT assay and the number of cells derived from a standard plot of known cell number (Figure 3.8A and 3.9A). Treatment with CM from all breast cancer cell lines lead to an increased proliferation rate of non malignant mammary fibroblasts when compared to fibroblasts cultured in control medium (Figure 3.8). Proliferation of mammary fibroblasts derived from breast cancer tissue was again increased following culture in CM from all breast cancer cell lines, excepting BT 20 where a decrease was observed, when compared with the proliferation rate of mammary fibroblasts cultured in control medium (Figure 3.9).

A comparison of versican synthetic rate relative to cell proliferation was achieved through the use of the ratio of increases in versican accumulation and cell number over control levels for each timepoint. Considerable variability was observed in this ratio between treatments (Table 3.2) However, the change in the ratio of versican accumulation to cell proliferation with time of treatment could be grouped into 5 patterns (Figure 3.10A-E). The majority (63%, 15/24) of trends with time fell into pattern A, ie the ratio of versican accumulation / proliferation was increased at 24 and 48 h, and then decreased at 72 h (Figure 3.10A). The peak ratio at 48 h (ratio >2) suggested that increased versican accumulation was not associated with fibroblast proliferation. The minority trends demonstrated either a decreasing ratio at 24 and 48 h, then increasing at 72 h (Figure 3.10B), a progressively decreasing ratio from 24 , 48, to 72 h (Figure 3.10C), a progressively increasing ratio from 24 , 48, to 72 h (Figure 3.10D), or a ratio which changed little between 24 and 72 h (Figure 3.10E).

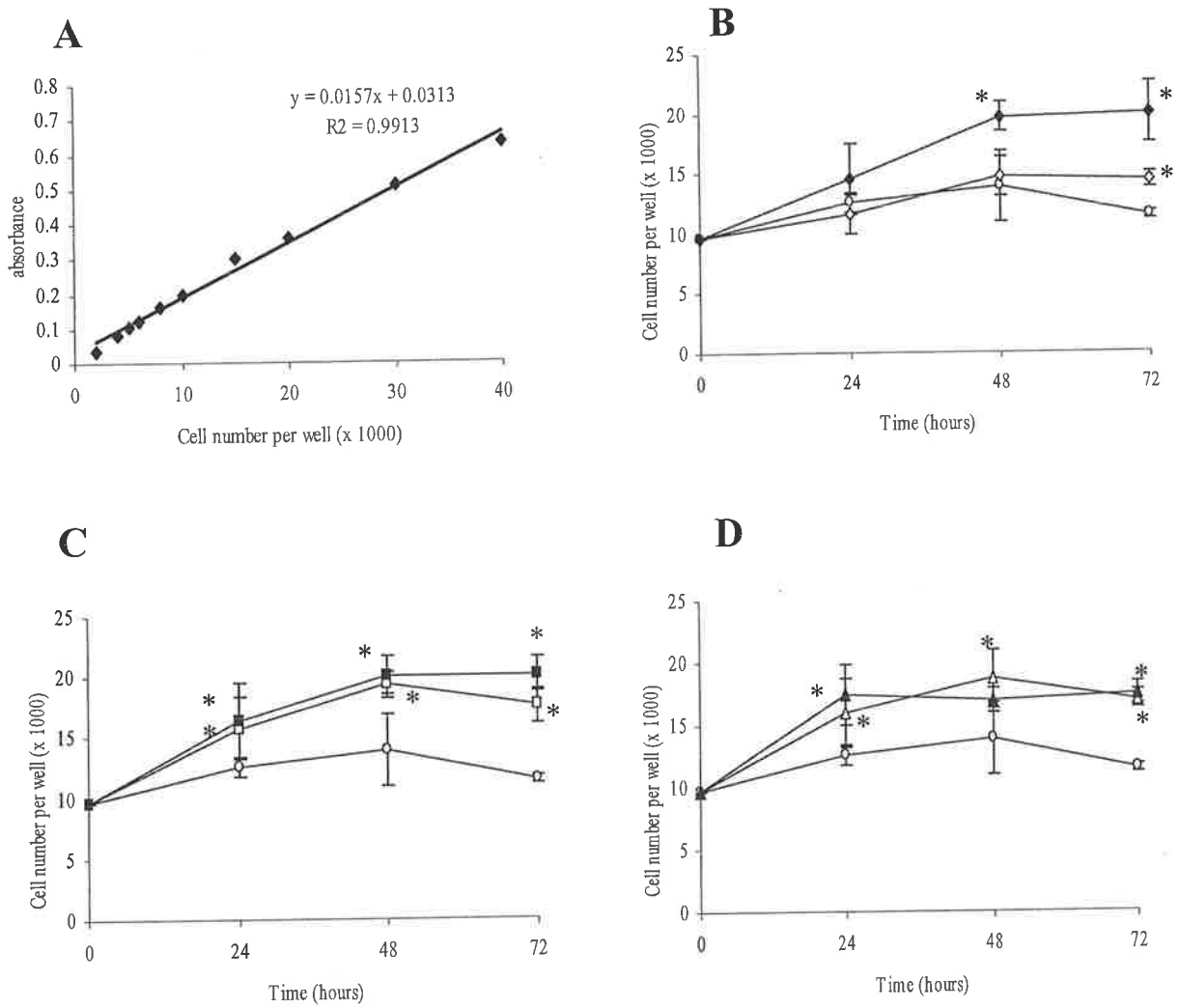

Figure 3.8. Proliferation rates of non malignant mammary fibroblasts following treatment with CM from breast cancer cell lines or control medium (RPMI + ITS). (A). Standard plot of absorbance to cell number used to calculate the number of fibroblasts. Effects on fibroblast proliferation of (B) CM from BT 20 (◇) and MDA-MB-231 (◆), (C) CM from MCF-7 (□) and MCF-7+ E_2 (■), (D) CM from ZR75-1 (△) and ZR75-1+E_2 (▲). Comparison was made in each figure with control medium (●). Data were expressed as mean values ± SD of six replicate wells for treatments of 24, 48, and 72 h. * indicates significant difference between CM from each breast cancer cell line and control medium at $P < 0.05$ (Mann-Whitney U Test). MTT assay was used to measure cell number.

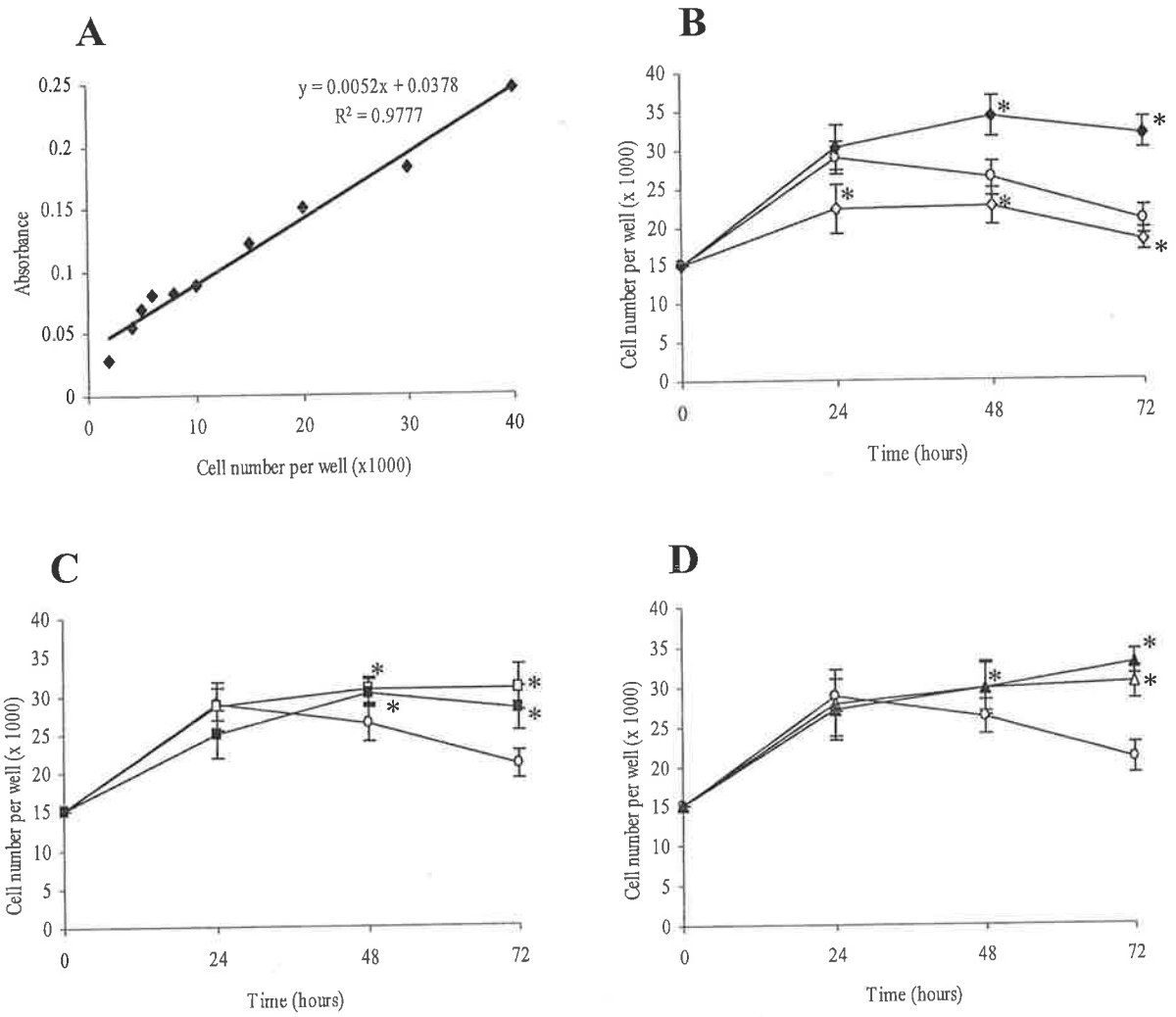

Figure 3.9. Proliferation rates of fibroblasts derived from breast cancer tissue following treatment with CM from breast cancer cell lines or control medium (RPMI + ITS). (A). Standard plot of absorbance to cell number used to calculate the number of fibroblasts. Effect on fibroblast proliferation of (B) CM from BT 20 (◇) and MDA-MB-231(◆), (C) CM from MCF-7 (□), and MCF-7-E_2 ■), (D) CM form ZR75-1 (△) and ZR75-1-E_2 (▲). Comparison was made in each figure with control medium (○). Data were expressed as mean ± SD of six replicate wells for treatment of 24, 48, 72 h. * indicates significant difference between CM from each breast cancer cell line and control medium at $P < 0.05$ (Mann-Whitney U Test). MTT assay was used to measure cell number.

Table 3.2. Summary of immunoblot analysis of versican accumulation in culture medium of two isolates of mammary fibroblasts from non-malignant breast tissues (NF1,2) and two breast cancer tissues (TF1,2) as a function of fibroblast proliferation. Each fibroblast culture was stimulated with CM from BT 20, MDA-MB-231, MCF-7, MCF-7+E_2, ZR75-1, and ZR75-1+E_2 breast cancer cell lines.

Source of CM	Breast fibroblast	Versican concentration / cell proliferation		
		24 h	48 h	72 h
BT 20	NF1	1.7	1.8	1.8
	TF1	1.8	2.3	1.9
	NF2	1.2	2.6	1.1
	TF2	1.1	1.2	1.5
MDA-MB-231	NF1	2.1	2.5	1.9
	TF1	1.7	2.2	1.6
	NF2	1.2	2.4	1.2
	TF2	1.8	2.3	1.9
MCF-7	NF1	1.7	1.6	1.4
	TF1	1.8	2.4	1.5
	NF2	2.6	4.0	1.0
	TF2	1.2	1.9	1.4
MCF+E_2	NF1	1.8	1.2	0.9
	TF1	2.3	2.1	1.3
	NF2	2.6	2.9	1.0
	TF2	1.7	1.9	1.0
ZR75-1	NF1	1.3	1.0	1.2
	TF1	1.6	2.5	1.5
	NF2	2.5	3.8	1.2
	TF2	1.5	1.7	1.0
ZR75-1+E_2	NF1	1.7	1.3	1.1
	TF1	2.0	1.9	1.1
	NF2	2.1	3.0	1.2
	TF2	1.5	1.8	1.1

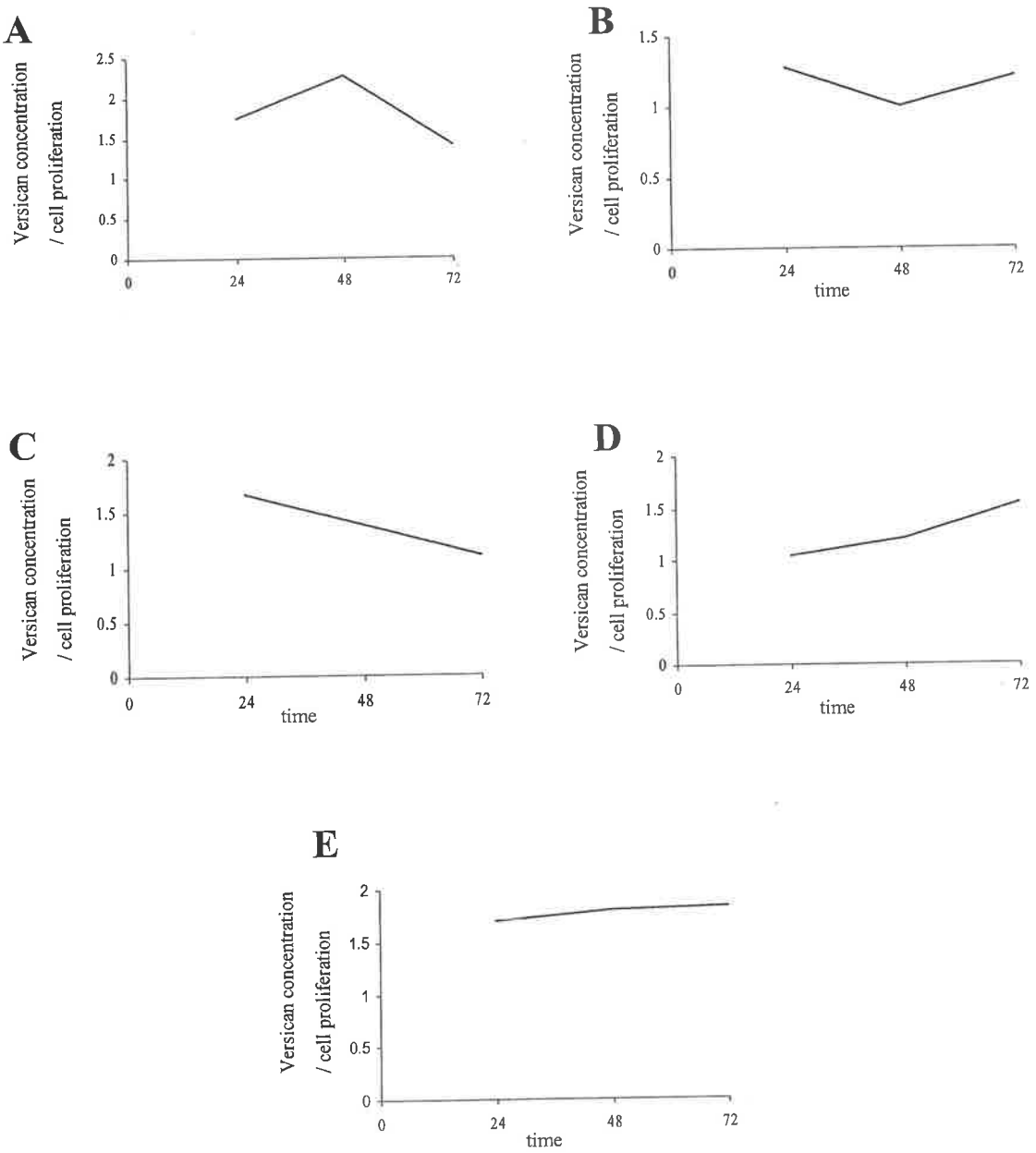

Figure 3.10. Ratio of increases in versican accumulation to cell proliferation for mammary fibroblasts cultured in cancer cell CM over control levels after treatment at 24, 48, and 72 h was grouped into five patterns (A-E). Percentage (proportion) of experimental treatments falling into each pattern: A, 63% (15/24), B 4% (1/24), C 17% (4/24), D 8% (2/24), E 8% (2/24). Data derived from Table 3.2.

3.3.5 Effect of growth factors and their specific neutralising antibodies on versican accumulation in mammary fibroblast cultures

Mammary fibroblasts derived from breast cancer tissue were used to study growth factors modulating versican expression. Addition of TGF-β1, PDGF-AB, and bFGF to the mammary fibroblasts induced increases in versican accumulation in culture medium of 1.4-fold, 2.4-fold, and 1.7-fold, respectively compared to control medium-treated mammary fibroblasts (Figure 3.11, 3.12, and 3.13, respectively). Addition of neutralising antibody against TGF-β1 (20 μg/ml) reduced the increase in versican accumulation induced by exogenous TGF-β1 and MCF-7 CM, but had no apparent effect on CM from BT 20, MDA-MB-231, and ZR75-1 breast cancer cell lines (Figure 3.11). The neutralising antibody against PDGF (20 μg/ml) and bFGF (18 μg/ml) neutralized the increase in versican accumulation induced by exogenous PDGF, bFGF, and CM from BT 20, MDA-MB-231, MCF-7 and ZR75-1 breast cancer cell lines (Figure 3.12 and 3.13, respectively).

3.3.6 Effect of growth factors and their specific neutralising antibodies on mammary fibroblast proliferation

To examine whether the increased versican accumulation in mammary fibroblast culture medium was due to cell proliferation in presence of growth factors, the number of mammary fibroblasts were counted after 48 h treatment using a haemocytometer. Compared to control medium-treated mammary fibroblasts, mammary fibroblast proliferation in the presence of PDGF-AB increased 1.2-fold, whereas in the presence of TGF-β1 and bFGF mammary fibroblast proliferation decreased 1.8-fold and 1.1-fold, respectively (Figure 3.11-3.13). Addition of the specific neutralising antibody had little if any effect on proliferation of mammary fibroblast induced by the corresponding exogenous growth factors. Addition of the neutralising antibody against TGF-β1 had no

Figure 3.11. Immunoblot analysis of the effect of TGF-β1 and anti- TGF-β1 neutralizing antibody on versican accumulation in culture medium of mammary fibroblasts derived from cancer tissue after treatment with CM from breast cancer cell lines. Addition of 10 ng/ml of TGF-β1 to mammary fibroblast culture increased versican accumulation in culture medium 1.4-fold compared with control medium-treated fibroblasts (A, lane 2 versus 1). Addition of 15 μg/ml neutralizing antibody to TGF-β1 reduced versican accumulation induced by either exogenous TGF-β1 (A, lane 3 versus 2) or CM from MCF-7 cells (A, lane 9 versus 8), but not by CM from BT 20, MDA-MD-231, and ZR75-1 cells (A, lane 5, 7, 11 versus 4, 6, 10, respectively). Immunoblots were detected using ECL and quantitated using imageQuant software. Each data point represents mean ± SD from two determinations (B). Mammary fibroblasts proliferation in the presence of exogenous TGF-β1 or breast cancer cell CM treated with or without neutralizing antibody to TGF-β1 (C). Each data point represents mean ± SD of two determinations from one experiment.
Statistical analyses were not performed.

A

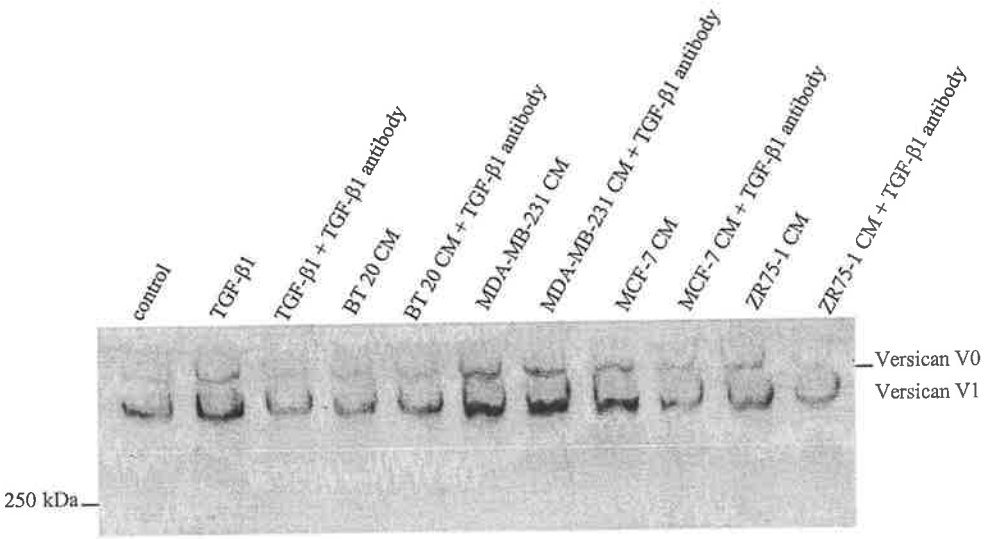
control
TGF-β1
TGF-β1 + TGF-β1 antibody
BT 20 CM
BT 20 CM + TGF-β1 antibody
MDA-MB-231 CM
MDA-MB-231 CM + TGF-β1 antibody
MCF-7 CM
MCF-7 CM + TGF-β1 antibody
ZR75-1 CM
ZR75-1 CM + TGF-β1 antibody
Versican V0
Versican V1
250 kDa

B

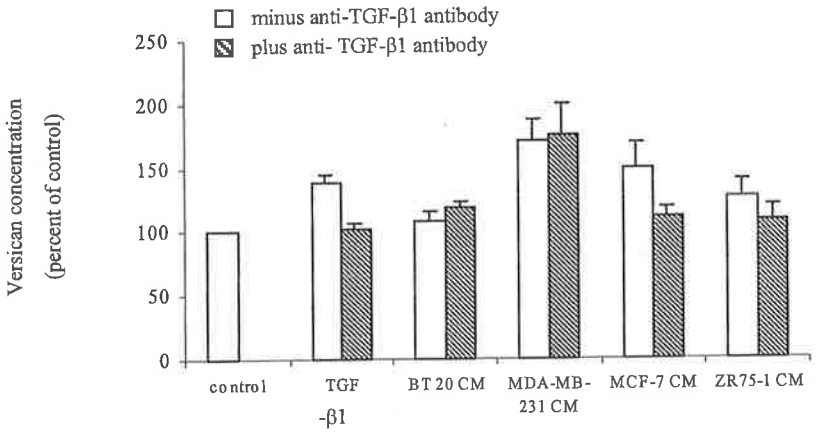
minus anti-TGF-β1 antibody
plus anti- TGF-β1 antibody
Versican concentration (percent of control)
250
200
150
100
50
0
control
TGF -β1
BT 20 CM
MDA-MB-231 CM
MCF-7 CM
ZR75-1 CM

C

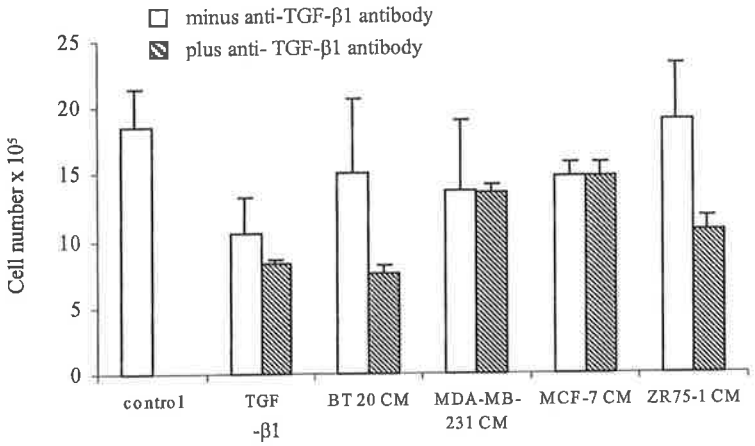
minus anti-TGF-β1 antibody
plus anti- TGF-β1 antibody
Cell number x 10⁵
25
20
15
10
5
0
control
TGF -β1
BT 20 CM
MDA-MB-231 CM
MCF-7 CM
ZR75-1 CM

Figure 3.12. Immunoblot analysis of the effect of PDGF-AB and anti-PDGF neutralizing antibody on versican accumulation in culture medium of mammary fibroblasts derived from cancer tissue after treatment with CM from breast cancer cell lines. Addition of 10 ng/ml of PDGF-AB to mammary fibroblast culture increased versican accumulation in culture medium 2.4-fold compared with control medium-treated fibroblasts (A, lane 2 versus 1). Addition of 20 μg/ml neutralizing antibody to PDGF reduced versican accumulation induced by either exogenous PDGF-AB (A, lane 3 versus 2) or CM from BT 20, MDA-MD-231, MCF-7, and ZR75-1 cells (A, lane 5, 7, 9, 11 versus 4, 6, 8, 10, respectively). Immunoblots were detected using ECL and quantitated using imageQuant software. Each data point represents mean ± SD from two determinations (B). Mammary fibroblasts proliferation in the presence of exogenous PDGF-AB or breast cancer cell CM treated with or without neutralizing antibody to PDGF (C). Each data point represents mean ± SD of two determinations from one experiment.

Statistical analyses were not performed.

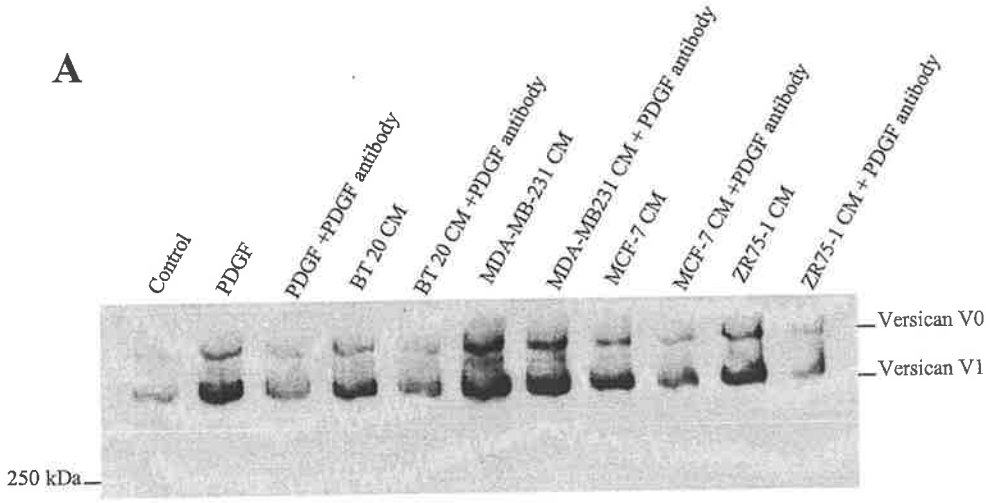
A
Control
PDGF
PDGF +PDGF antibody
BT 20 CM
BT 20 CM +PDGF antibody
MDA-MB-231 CM
MDA-MB231 CM + PDGF antibody
MCF-7 CM
MCF-7 CM +PDGF antibody
ZR75-1 CM
ZR75-1 CM + PDGF antibody
Versican V0
Versican V1
250 kDa

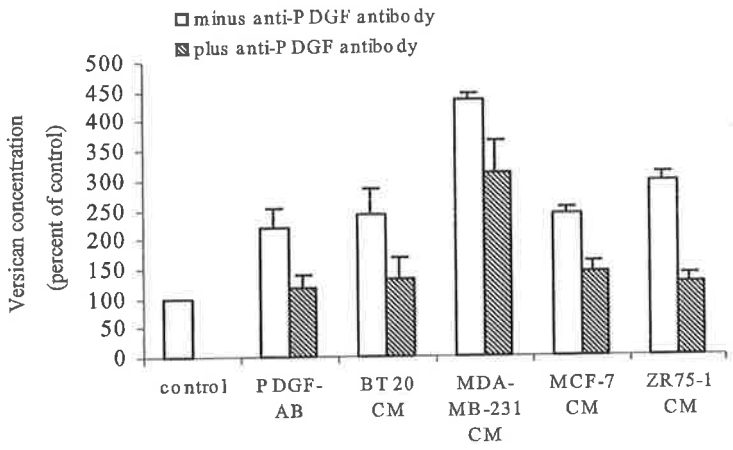
B
minus anti-PDGF antibody
plus anti-PDGF antibody
Versican concentration (percent of control)
500
450
400
350
300
250
200
150
100
50
0
control
PDGF-AB
BT 20 CM
MDA-MB-231 CM
MCF-7 CM
ZR75-1 CM

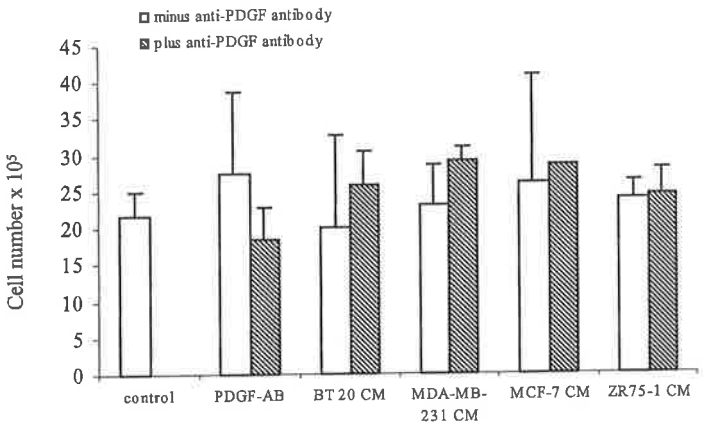
C
minus anti-PDGF antibody
plus anti-PDGF antibody
Cell number x 10⁵
45
40
35
30
25
20
15
10
5
0
control
PDGF-AB
BT 20 CM
MDA-MB-231 CM
MCF-7 CM
ZR75-1 CM

Figure 3.13. Immunoblot analysis of the effect of bFGF and anti-bFGF neutralizing antibody on versican accumulation in culture medium of mammary fibroblasts derived from cancer tissue after treatment with CM from breast cancer cell lines. Addition of 1 ng/ml of bFGF to mammary fibroblast culture increased versican accumulation in culture medium 1.7-fold compared with control medium-treated fibroblasts (A, lane 2 versus 1). Addition of 18 μg/ml neutralizing antibody to bFGF reduced versican accumulation induced by either exogenous bFGF (A, lane 3 versus 2) or CM from BT 20, MDA-MD-231, MCF-7, and ZR75-1 cells (A, lane 5, 7, 9, 11 versus 4, 6, 8, 10, respectively). Immunoblots were detected using ECL and quantitated using imageQuant software. Each data point represents mean ± SD from two determinations (B). Mammary fibroblasts proliferation in the presence of exogenous bFGF or breast cancer cell CM treated with or without neutralizing antibody to bFGF (C). Each data point represents mean ± SD of two determinations from one experiment.
Statistical analyses were not performed.

A

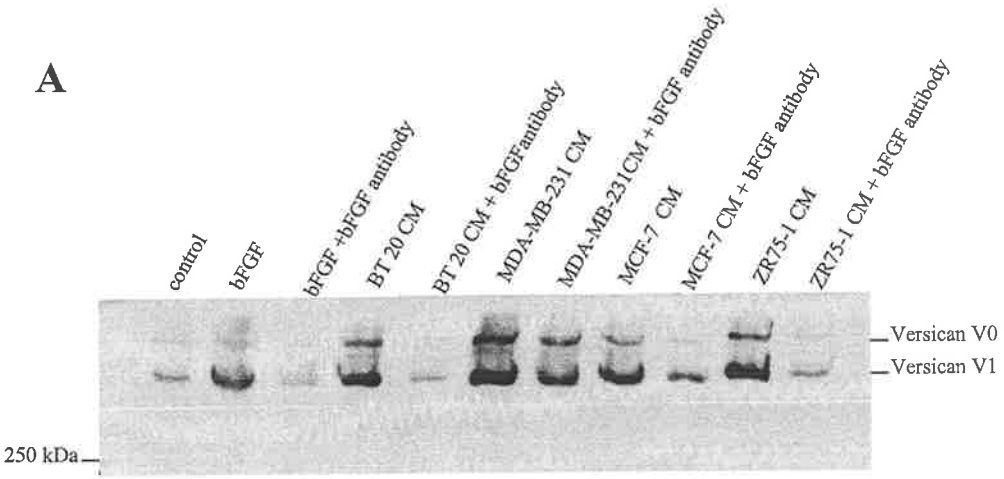
control
bFGF
bFGF +bFGF antibody
BT 20 CM
BT 20 CM + bFGFantibody
MDA-MB-231 CM
MDA-MB-231CM + bFGF antibody
MCF-7 CM
MCF-7 CM + bFGF antibody
ZR75-1 CM
ZR75-1 CM + bFGF antibody
Versican V0
Versican V1
250 kDa

B

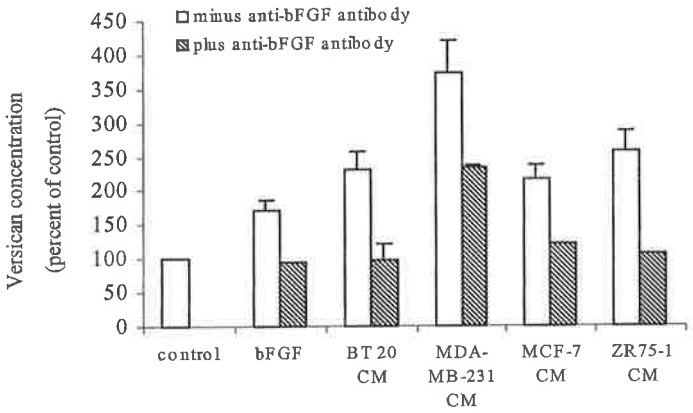
minus anti-bFGF antibody
plus anti-bFGF antibody
Versican concentration (percent of control)
450
400
350
300
250
200
150
100
50
0
control
bFGF
BT 20 CM
MDA-MB-231 CM
MCF-7 CM
ZR75-1 CM

C

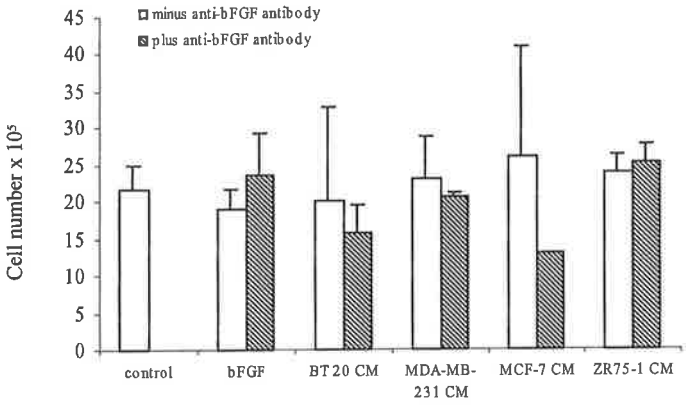
minus anti-bFGF antibody
plus anti-bFGF antibody
Cell number x 10⁵
45
40
35
30
25
20
15
10
5
0
control
bFGF
BT 20 CM
MDA-MB-231 CM
MCF-7 CM
ZR75-1 CM

effect on mammary fibroblast proliferation induced by CM from MDA-MB-231 and MCF-7 , but decreased the proliferation induced by CM from BT 20 and ZR75-1 cells. Addition of the neutralising antibody against PDGF appeared to have little effect on the proliferation of mammary fibroblast induced by CM from BT 20, MDA-MB-231, MCF-7, ZR75-1 cells. Addition of the neutralising antibody against bFGF appeared to decreased proliferation of mammary fibroblasts induced by MCF-7 CM, but there was little difference apparent for CM from BT20, MDA-MB-231, and ZR75-1 cells.

Discussion

Changes to the stromal compartment of an organ are a recognized characteristic of pathologic lesions, ie benign hyperplastic, premalignant and malignant tissues. The immunohistochemical studies in the previous chapter indicated increased versican expression was present in the stromal tissue surrounding breast tumors and was associated with disease outcome in women with node-negative breast cancer. Epithelial-stromal cell interactions during normal and pathological development are mediated by various growth factors via paracrine mechanisms. Increased levels of versican in peritumoral breast stroma may result from paracrine activation of stromal cells by soluble mediators secreted by tumor cells. In this chapter, CM from breast cancer cell lines stimulated increased accumulation of versican V0 and V1 isoforms in the medium of cultured mammary fibroblasts. The CM from estrogen receptor positive-cell lines (MCF-7 and ZR75-1 cells) stimulated an increase of approximately 200% in versican accumulation in the medium of cultured mammary fibroblasts. The CM from estrogen receptor negative-cell lines (BT 20 and MDA-MB-231 cells) induced an increase of approximately 200% and 300%, respectively, in versican accumulation in the medium of cultured mammary fibroblasts. However, there was no discernable difference between the level of versican accumulation in mammary fibroblast cultures induced by the CM from estrogen recepter positive-cell lines cultured in estradiol compared to culture without estradiol. A recent report indicates that versican mRNA expression by the granulosa cells of mouse and rat ovaries was not significantly altered by estradiol or FSH treatment (Russell et al., 2003). This supports our observations that versican expression in breast cancer tissues is not mediated by estradiol. The fact that versican mRNA and protein for isoform V0 and V1 were expressed by mammary fibroblasts, but not by the breast cancer cell lines BT 20, MDA-MB-231, MCF-7, and ZR75-1, suggests that versican expression in breast cancer is achieved by the ability

of breast cancer cells to secrete factors which stimulate increased expression of versican by mammary fibroblasts in the peritumoral stroma.

Studies in this chapter suggest that the increases in versican accumulation in fibroblast culture media *in vitro* result from an increased rate of secretion, rather than as a result of increased cell proliferation. The ratio of versican accumulation to change in cell number with time being greater than unity confirmed this tenet. However, the fall in the ratio with time was unexpected. Plotting of the raw versican accumulation data for both CM- and control-treated fibroblast cultures (Figure 3.14), rather than expressing the data as a percentage of control values (eg Figure 3.6 and 3.7), provided an explanation of the falling ratios. Three patterns describing versican accumulation in cultured mammary fibroblasts are illustrated in Figure 3.14A-C. The majority of the patterns were similar to the curves shown in Figure 3.14A, where the amount of versican in culture medium of fibroblasts treated with CM at 24 and 48 h had increased much more than that of fibroblasts treated with control ITS medium, whereas the amount of versican in culture medium of fibroblast treated with CM at 72 h was only slightly greater than that of fibroblasts treated with control ITS. Therefore, the amount of versican represented as a percentage of control was maximal at 48 h, suggesting that soluble factors from cancer cells may be more effective at stimulating fibroblasts to produce increases in versican secretion at earlier time points. A minority of the patterns demonstrated that the amount of versican accumulation progressively increased to a greater degree in CM-treated compared to controls for all time points (Figure 3.14B). In the third pattern, (Figure 3.14C) the difference in versican accumulation between CM- and control medium-treated fibroblasts was maximal at 24 h, and then decreased at 48 and 72 h. The difference between the individual values for the CM- and the control medium-treated cultures illustrated in Figure 3.14A-C parallel the ratios of versican accumulation to cell proliferation depicted in Figure 3.10A, D and C,

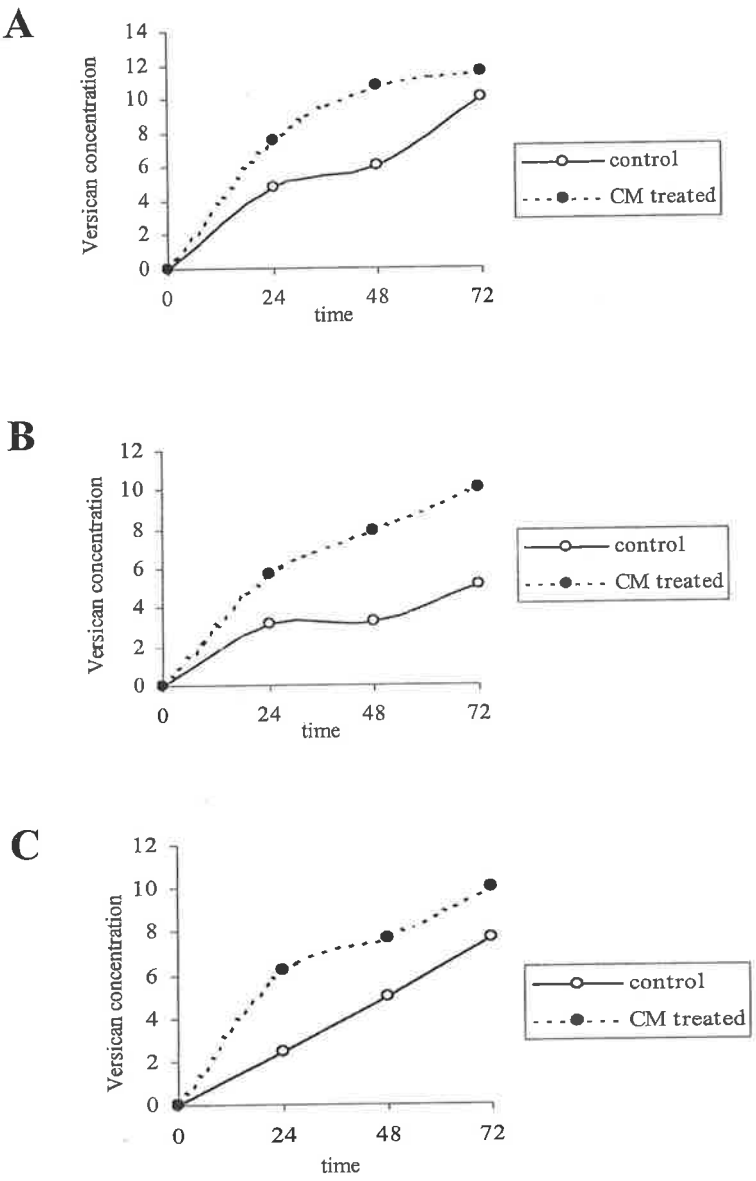

Figure 3.14. Three patterns illustrate versican accumulation in cultured mammary fibroblasts treated with CM from breast cancer cell lines and control ITS.

respectively. The variation in versican secretion between fibroblast isolates observed in this chapter might be explained by differences in the responsiveness of the mammary fibroblasts to soluble factors present in the CM. It has been reported that structural and functional differences exist between stromal fibroblasts from normal breast and breast cancer with respect to the responsiveness to soluble factors present in CM from MCF-7 cells (Valenti et al., 2001), however, no clear differences between isolates from malignant and non-malignant breast tissue were detected in this study.

A number of different polypeptide growth factors have been described as secreted products of breast tumor cells. PDGF has been described as secreted by the human breast cancer cell lines MDA-MB-231, MCF-7, and ZR75-1 (Bronzert et al., 1987, Mobus et al., 1998). *In vivo*, elevated PDGF levels in the circulation and increased expression by tumor cells correlated with increased metastasis, shortened survival, and a lower response to chemotherapy in patients with breast cancer (Ariad et al., 1991, Seymour and Bezwoda, 1994). It has also been reported that PDGF induced increased versican mRNA expression in monkey smooth muscle cells and cultured human gingival and peridontal ligament fibroblasts (Schonherr et al., 1991, Haase et al., 1998). In this chapter, PDGF increased versican levels in the culture medium of human mammary fibroblasts. Neutralizing antibody to PDGF inhibited the stimulatory effect on versican accumulation of the exogenous recombinant PDGF, and of the CM from all breast cancer cell lines tested, suggesting that PDGF secreted by breast cancer cells was at least partially responsible for stimulating mammary fibroblasts to increase versican secretion.

The FGFs are a family of angiogenic factors and related GAG-binding molecules (Penc et al., 1998). bFGF reportedly upregulates the expression of the decorin gene by cultured normal and keloid skin fibroblasts, but the mRNA level for versican remained unchanged (Tan et al., 1993). In this chapter, exogenous bFGF was able to stimulate mammary

fibroblasts to increase versican secretion. The addition of bFGF neutralizing antibody to the cultures inhibited the action of exogenous bFGF, and also inhibited the action of CM from the breast cancer cell lines by reducing versican levels secreted by mammary fibroblasts to background level. This suggests that bFGF might also be partially responsible for the stimulatory action of breast cancer CM on mammary fibroblast production of versican. bFGF is known to be expressed by both epithelial and stromal cell compartments of breast tissue (de Jong et al., 1998). However, an earlier study reported little or no expression of bFGF by ZR75-1, MCF-7, and MDA-MB-231 cell lines using PCR (Luqmani et al., 1992). An explanation for our finding that bFGF contributes to the inductive activity of CM from these breast cancer cell lines for versican secretion by mammary fibroblasts might be that a cancer cell factor stimulates mammary fibroblasts to produce bFGF which acts in an autocrine manner.

Numerous studies utilising cultured fibroblasts derived from various sources have indicated that exogenous TGF-β1 up regulates versican gene expression. Specifically, cultured human skin and gingival fibroblasts (Kahari et al., 1991), vascular smooth muscle cells (Evanko et al., 1998), and prostate fibroblasts (Sakko et al., 2001) have been used. In addition, neutralising antibody to TGF-β1 inhibited the secreted mediator(s) in CM from prostate cancer cell lines, which induced increases in versican secretion in prostate fibroblast culture (Sakko et al., 2001). TGF-β1 has been reported to be secreted by breast tumors, and MDA-MB 231, MCF-7, and ZR75-1 breast cancer cell lines (Lei et al., 2002, Chiquet-Ehrismann et al., 1989, Mobus et al., 1998). An elevated expression of TGF-β is associated with disease progression in breast cancer (Dalal et al., 1993, Walker and Dearing, 1992, Gorsch et al., 1992). In this chapter, exogenous recombinant TGF-β1 incrcased versican accumulation 1.4 fold in mammary fibroblast culture. Neutralizing

antibody to TGF-β1 inhibited the ability of MCF-7 CM to stimulate versican accumulation, but did not inhibit the corresponding ability of MDA-MB-231 CM. In this series of experiments, the response of mammary fibroblasts to BT 20 and ZR75-1 CM with respect to versican synthesis varied from 100-250% of control medium level. In the experiments specifically investigated the role of TGF-β1, the level of versican accumulation following treatment with BT 20 and ZR75-1 CM was not different from control, it was therefore not possible to determine unequivocally whether the neutralizing antibody to TGF-β1 had any effect on the CM from these cell lines. Overall, the data in this chapter suggest that PDGF and potentially TGF-β1 may play a role as cancer cell secreted mediators regulating versican production by mammary fibroblasts.

Future potential experimentation in this area should include studies to improve the reproducibility of cell quantitation. The study in this chapter investigating the effect of recombinant growth factors and the corresponding neutralizing antibodies on cell proliferation measured cell number by haemocytometer counting, using two determinations from one experiment. Reproducibility of counting could be improved by increasing the number of determinations made using the MTT assay, and without the necessity for trypsinization of the cell monolayers, and the consequent potential for cell loss. A second area for further study would be to further examine the role of TGF-β1, as a candidate mediator in cancer cell CM.

Chapter 4

Effect of Fibroblast Conditioned Medium on Breast Cancer Cell Adhesion, Invasion, and Migration *in vitro*

4.1 Introduction

Tumour invasion and metastasis are complex cascades of events resulting from alterations in the interaction between cancer cells and stroma. The sequential events involved in invasion and metastasis result from altered cancer cell attachment to the components of basement membrane or interstitial ECM, digestion of the ECM components by enzyme secreted by cancer cells or host stromal cells (such as fibroblasts) induced to elaborate proteolytic enzyme, and cancer cell migration through the degraded basement membrane and areas of matrix proteolysis to ultimately enter blood or lymphatic vessels, where they are carried to distant sites (Liotta and Kohn, 1990). The invasive potential of a cancer cell has been shown experimentally to relate directly to its ability to modulate its attachment to ECM components (Bartsch et al., 2003, Gui et al., 1995). A prime function of CSPGs in ECM is to modulate adhesion of cells to various ECM components and thereby promote proliferation, differentiation, cell migration, and angiogenesis (Lochter and Bissell, 1995). Versican, a prominent member of the CSPG family, acts as an anti-adhesive molecule by interfering with the attachment of embryonic fibroblasts to matrix proteins: laminin, fibronectin and collagen type I (Yamagata et al., 1989). This CSPG was found in the subcellular space of cultured fibroblasts, but was specifically excluded from focal adhesion contact with the substratum, where fibronectin, vinculin and integrins were localized (Yamagata et al., 1993). Studies of cultured human osteosarcoma MG63 cells, which produce a large amount of versican, indicated that the ability of versican to reduce cell-

substratum adhesion could be repressed by transfection with versican specific antisense RNA (Yamagata and Kimata, 1994). Furthermore, it has been demonstrated that the G1 domain of versican reduces astrocytoma cell adhesion and enhances astrocytoma cell migration (Ang et al., 1999). More recently, purified versican has been shown to inhibit melanoma cell adhesion to fibronectin and collagen type I substrates (Touab et al., 2002).

Nara et al. (1997) reported that versican was localized to the proliferating mesenchymal cells at the peripheral invasive areas of infiltrative breast cancer and in the vascular and perivascular elastic tissues associated with tumour invasion. Previous studies from our laboratory reported that increased levels of versican in the peritumoral stroma of prostate cancer patients was associated with prostate-specific antigen relapse (Ricciardelli et al., 1998). The studies outlined in Chapter 2 now indicate that elevated expression of CS versican localized in the peritumoral stroma of breast cancer tissue is related to relapse in patients with node negative disease (Ricciardelli 2002, Suwiwat 2003 submitted). Recently, we have shown that versican purified from CM of cultured human prostatic fibroblast has anti-adhesive activity, reducing prostate cancer cell attachment to fibronectin. This biological effect depends on the structural integrity of the CS side chains and the ability of versican to bind the RGD peptide sequence of fibronectin (Sakko et al., 2003).

Studies outlined in Chapter 3 indicated that mammary fibroblasts derived from breast cancer tissue secreted versican into culture medium *in vitro*, but the ability of this molecule to modulate breast cancer cell-substratum adhesion and cell migration is unknown. Thus, the aim of this chapter is to determine whether versican isolated from mammary fibroblast CM has the capacity to modulate breast cancer cell-substratum attachment, migration and invasion *in vitro*.

4.2 Materials and Methods

4.2.1 Materials

Fibronectin, laminin, collagen type I, RGD (Arg-Gly-Asp) peptide, ITS, MTT, BSA, chondroitinase ABC, anti-mouse IgG peroxidase conjugated were from Sigma Chemical Co (St Louis, MO, USA). Polycarbonate filters, PVP free of 12 μm pore size were from Osmonics (Livermore, CA, USA). Protease inhibitor cocktail tablets were from Roche (Mannheim, Germany). Diff-Quik fixative and stains were from LabAids Pty Ltd (Narrabeen, NSW, Australia). RPMI 1640, trypsin, L-glutamine solution, and Penicillin Streptomycin solution were from JRH Biosciences (Lenexa, KS, USA). Foetal Bovine Serum was purchased from Trace Scientific Ltd (Melbourne, NSW, Australia). Anti-rabbit IgG peroxidase conjugated was from Amrad Biotech (Boronia, Victoria, Australia). Mouse monoclonal anti-1B5 (anti-C-0-S) and 6B6 (anti-decorin) were from Seikagaku Corporation (Tokyo, Japan). Mouse monoclonal anti-2B6 (anti-C-4-S) and 3B3 (anti-C-6-S) were from ICN Biochemicals (Aurora, OH, USA). Polyclonal antibody to human versican was supplied by Dr R LeBaron, University of Texas, San Antonio, USA. Nitrocellulose membrane and ECL detection reagent were from Amersham (Buckinghamshire, England). SeeBlue pre-stained protein standard molecular weight markers were from Novex, Invitrogen (Carlsbad, CA, USA). Acrylamide was from BioRad Laboratories (Hercules, CA, USA). Q-Sepharose and Sephacryl S400 were purchased from Amersham Pharmacia (Uppsala, Sweden). Centriprep centrifugal filters were from Amicon Bioseparations Millipore (Bedford MA). Nanosep microconcentrators were from Pall Gelman laboratory (Ann Arbor, MI). All inorganic salts and solvents were from either Sigma Chemical Co or Ajax Chemicals (Sydney, Australia).

4.2.2 Cell lines

MCF-7, MDA-MB-231, and Hs578T breast cancer cell lines were obtained from the American Type Culture Collection (ATCC, Manassas, VA, USA) to be used for cell adhesion and invasion assays. These cells were grown routinely in RPMI 1640 supplemented with 5% FBS. The proportion of invasive cells within these cell lines was reported as MCF-7 20-40%, MDA-MB-231 and Hs578T >80% (Thompson et al., 1992). The Hs578T cell line appears unique in that it produces versican due to an epithelial-mesenchymal transition (refer to versican immunoblot, Figure 5.3).

4.2.3 Collection of mammary fibroblast conditioned medium

Conditioned medium (CM) was harvested from confluent primary mammary fibroblasts derived from breast cancer tissue. Fibroblast CM was collected after incubation 72 h with serum-free medium (RPMI plus ITS). For cell adhesion assay, the harvested fibroblast CM was treated with protease inhibitor to reduce proteolytic degradation of bioactive molecules. Fibroblast CM harvested for use in cell migration and invasion experiments was not treated with protease inhibitor to ensure that proteases associated with cancer cell invasion through the matrix coated membrane remained active. The harvested fibroblast CM was concentrated 25-fold for adhesion assay and 15-fold for migration and invasion assays using Centriprep centrifugal filters (cut off 50 kDa), and Nanosep microconcentrators (cut off 300 kDa) at 4°C.

4.2.4 Versican purification

CM was collected from mammary fibroblasts (originally derived from breast cancer tissue) cultured in RPMI supplemented with 5% FBS. Versican was isolated from the serum-enriched medium by sequential ion-exchange and gel chromatography. The CM (1000 ml) was batch-adsorbed to Q-Sepharose (10 ml/liter of medium) overnight at 4°C on a rotator. After washing with PBS, the pellet was packed in a BioRad disposable column and

adsorbed versican was batch-eluted with 2M NaCl in PBS. The versican-containing eluate, in presence of protease inhibitors, was purified by gel chromatography on Sephacryl S400 (1.6 x 84 cm column) equilibrated with PBS (pH 7.4) at a rate of 5 ml/10 min. After the first 50 ml of elution was discarded, sequential 5 ml fractions were collected in presence of protease inhibitors and assayed by immunoblot for versican. The fractions containing versican were concentrated 20-fold using Centriprep centrifugal filters (cut off 50 kDa) and Nanosep microconcentrators (cut off 300 kDa) at 4°C.

4.2.5 Immunoblot analysis of fibroblast conditioned medium

To verify the presence of versican and determine whether other CS proteoglycans contaminated the preparation, concentrated fibroblast CM (starting material) and eluted fractions were analyzed by immunoblotting. The concentrated fibroblast CM and eluted fractions were digested with chondroitinase ABC to cleave the CS side chains covalently linked to the core protein in order to permit electrophoresis on gradient polyacrylamide gels (4-9%). Electrophoresis, immunoblot, and immunostaining protocols were described in section 3.2.10. For immunostaining, the membranes were incubated with rabbit anti-versican antibodies (1:500) 2 h at room temperature and or mouse monoclonal anti-CS epitopes 1B5, 2B6, 3B3, or anti-decorin (6B6) (1:500, each) at 4°C overnight. Visualization and measurement were assessed using enhanced chemiluminescence (ECL) and scanning densitometry.

4.2.6 Adhesion assay

Adhesion of MCF-7, MDA-MB-231, and Hs578T human breast cancer cell lines was investigated using an established protocol (Current Protocols in Cell Biology, 2000.) 96-well tissue culture microtiter plates (Costar) were coated with fibronectin or laminin (10 μg/ml in PBS pH 7.4, 100 μl/well, overnight at 4°C). After washing with PBS, the plates were blocked for nonspecific binding using 150 μl of 10 mg/ml heat-denatured BSA

solution (diluted in PBS, incubated at 85°C for 10 min and cooled at room temperature prior to use) for 30 min at room temperature. Negative control wells were coated only with the heat-denatured BSA solution. After removing the BSA solution, the plates were washed 3 times with PBS. Twenty five µl of serum-free medium (RPMI plus ITS) or concentrated fibroblast CM or purified versican were added to each well. In some experiments, cell attachment to fibronectin was performed using versican pretreated with 50 µg/ml synthetic peptide RGD (Arg-Gly-Asp) or 2 units/ml chondroitinase ABC (ChABC) for 2 h at 37°C. The plate was then left at room temperature for 30 min during preparation of cell suspensions. The breast cancer cells were harvested using 0.05% trypsin/0.02% EDTA solution and resuspended in serum-free medium (RPMI plus ITS) containing 1 mg/ml BSA at density of 2×10^5, 4×10^5, and 8×10^5 cells/ml. Fifty µl of the cell suspensions were plated to the pretreated wells and incubated at 37°C in a 5% CO_2 incubator with the microtiter plate lid off (to allow the pH of the medium to equilibrate quickly). After 30 min, non-adherent cells were removed by aspiration with a micropipette and adherant cells washed 3 times with PBS. 100 µl of RPMI plus ITS were added to the adherent cells, followed by 10 µl of 5 mg/ml aqueous MTT, then incubated for 4 h at 37°C. Subsequently, the cells were lysed with 20% SDS in 0.02 M HCl overnight at room temperature in the dark. The absorbance was determined in a microtiter plate reader at 570 and 655 nm (BioRad 450).

4.2.7 Cell migration and invasion assays

Migration and invasion ability of MCF-7, MDA-MB-231 and Hs 578T cells was studied using a modified Boyden chamber as previously described (Albini et al., 1987). Briefly, polycarbonate membrane filters (13 mm diameter, 12 µm pore size, PVP free) were coated with various concentrations of collagen type I and fibronectin, dried in a cell culture hood,

then stored at 4°C. For invasion assay, the filters were coated with 10 μg/filter of collagen type I plus 1 or 0.25 μg/filter of fibronectin. To determine whether fibroblast CM affected cell invasion, 15μl of 15-fold concentrated fibroblast CM (without protease inhibitors) was added to the collagen type I and fibronectin mixture. For haptotactic migration assay, the filters were coated with 0.5 μg/filter of collagen type I plus 0.05 μg/filter of fibronectin. In some motility experiments, the filters were coated with 15 μl of concentrated fibroblast CM (without protease inhibitors) plus collagen type I and fibronectin. Lower chambers were filled with 165 μl of 15-fold concentrated fibroblast CM (without protease inhibitors) or 5% FBS containing 1 mg/ml BSA as a chemoattractant and RPMI plus ITS containing 1 mg/ml BSA as a control. The coated filters ,matrix coating upwards, were placed over the lower wells containing the chemoattractant solution, then the upper compartments were screwed tightly into the chamber. Cells were trypsinized (0.05% trypsin/0.02% EDTA), washed, and resuspended in RPMI plus ITS containing 1 mg/ml BSA. The cell suspensions (10^6cells/ml of MCF-7, 5 x 10^5 cells/ml of MDA-MB-231 and Hs578T) 150 μl/well were added to the upper chamber of assembled Boyden chamber and incubated at 37°C in a 5% CO_2 incubator for 3, 5, 6, and 24 h. After flicking off excess medium, the chambers were disassembled and the filters were removed. The filters (coated surface face down) were pinned to a solidified layer of paraffin wax in a petri dish. The invasive cells on the surface of the filters were fixed by immersion in Diff-Quik fixative and stained using Diff-Quik stain according to the manufacturer's directions. The filters were inverted and transferred to a microscopic slide. The non-invasive cells on the top surface of the filter were removed with cotton buds and mounted in DePex mounting solution. The invasive cells were counted under a microscope in 30 predetermined fields of 3-4 wells at a magnification of 200X.

4.2.8 Statistical analysis

The Mann-Whitney U test was performed to determine statistical differences between control and treated groups using the SPSS 10.0 for Windows software (SPSS Inc., Chicago, IL). Differences were considered statistically significant at $P < 0.05$.

4.3 Results

4.3.1 Adhesion of breast cancer cells to fibronectin and laminin

As shown in Figure 4.1, adhesion of breast cancer cells to fibronectin and laminin increased with increasing number of cells. The maximum cell adhesion for fibronectin, attained using 4 x 10^4 MCF-7 cells/well, was approximately 5-fold higher than for laminin. MDA-MB-231 and Hs578T cells were able to bind to fibronectin and laminin with equal efficiencies. Binding of cells to negative control BSA-coated wells was essentially zero.

4.3.2 Characterization and effect on breast cancer cell adhesion of fibroblast CM

By immunoblotting, two isoforms of versican (M_r ~ 400,000) were identified in 25-fold concentrated CM from mammary fibroblasts (derived from breast cancer tissue), and collected in RPMI plus ITS (Figure 4.2A). Specific epitopes of chondroitin sulfate (CS) side chain stubs (following chondroitin ABC digestion) were recognized using antibodies to 2B6 (4-sulfated chondroitin, Figure 4.2B), 3B3 (6-sulfated chondroitin, Figure 4.2C), and 1B5 (unsulfated chondroitin, Figure 4.2D). The sizes of the molecules bearing CS chains in fibroblast CM were in each case consistent with the sizes of the versican isoforms detected with anti-versican, indicating that the CS chain stubs were linked to the versican core protein.

A single band for decorin was detected in concentrated fibroblast CM using monoclonal antibody 6B6. The molecular size of decorin (M_r ~40,000) was consistent with that reported in a previous study (Theocharis et al., 2003). Fraction 11 containing 2 isoforms of decorin from versican purification (Fig 4.4B) was used as control.

Concentrated fibroblast CM had a significant inhibitory effect on the attachment of MCF-7 cells to fibronectin, but not on the attachment of MDA-MB-231 or Hs578T, when compared to control serum free-medium (Figure 4.3A). At the maximum concentration of

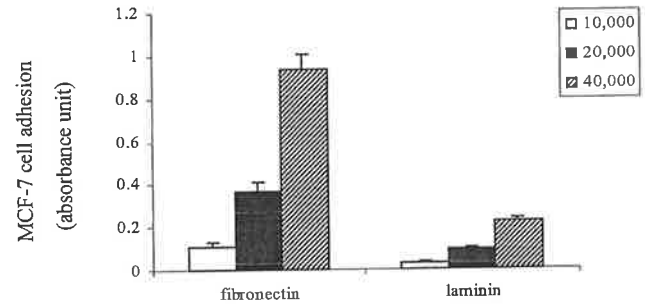

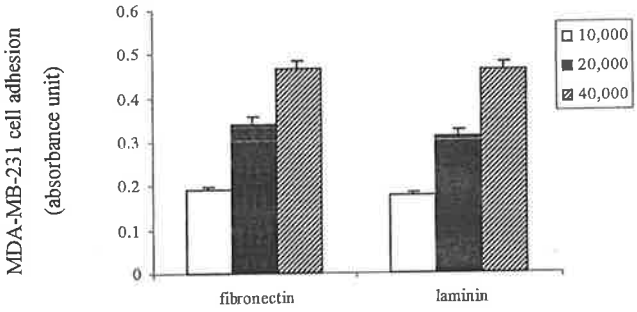

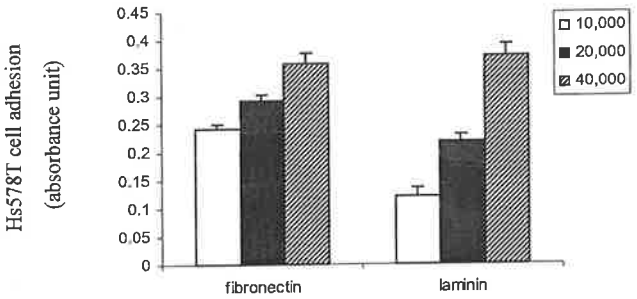

Figure 4.1. Adhesion of breast cancer cell lines : MCF-7, MDA-MB-231, and Hs578T to multiwell plates coated with matrix proteins : fibronectin and laminin at concentration 10 μg/ml. The breast cancer cell lines were plated at 1 x 10^4, 2 x 10^4, and 4 x 10^4 cells/well in serum-free medium. Each data point is expressed as the number of attached cells (absorbance unit) and represents the mean ± SD of 8 replicates from two independent experiments.

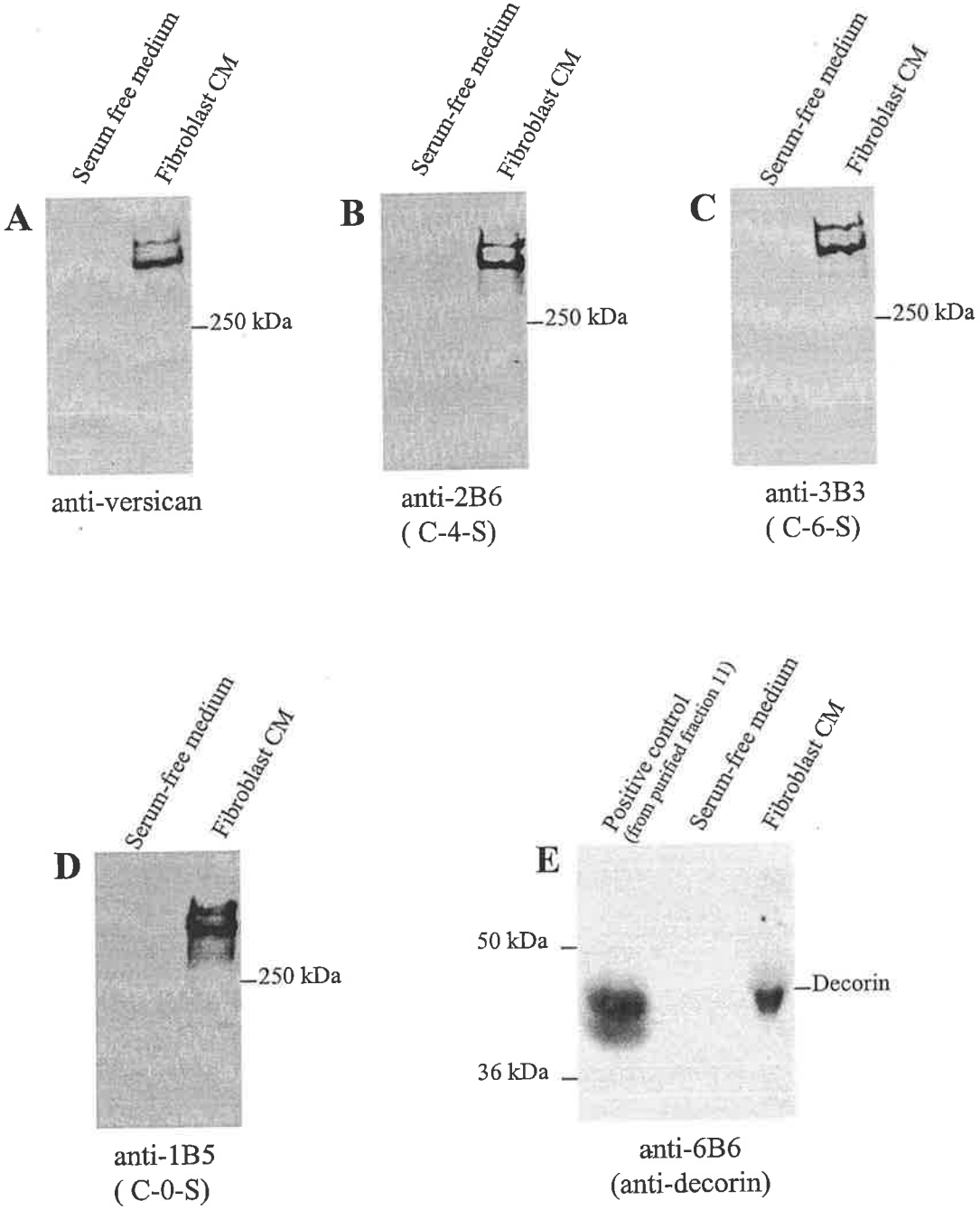

Figure 4.2. Characterization of concentrated fibroblast CM by immunoblotting. Concentrated CM (25-fold) from mammary fibroblasts (derived from breast cancer tissue) contained bands of versican (A), chondroitin-4-sulfate (B), chondroitin-6-sulfate (C), chondroitin-unsulfate (D), and decorin (E). No versican, chondroitin sulfate chains, or decorin were detected in serum-free medium. Fraction 11 from versican purification, Fig 4.4B, was used as positive control for decorin isoforms.

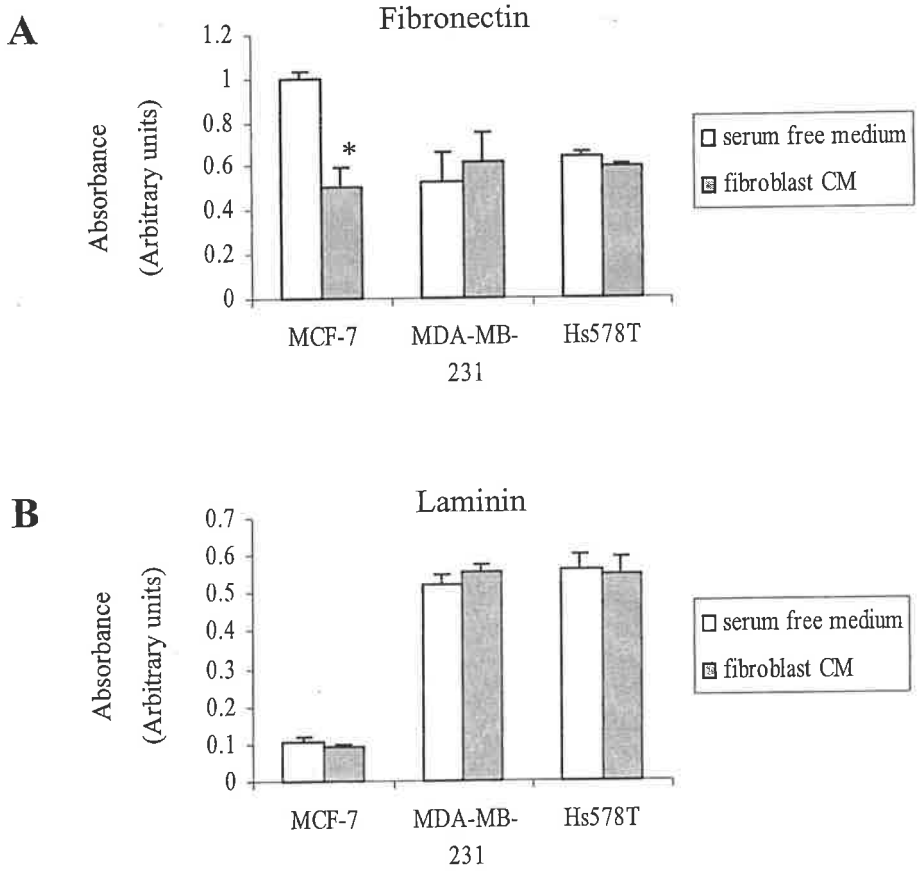

Figure 4.3. Effect of mammary fibroblast CM on the adhesion of breast cancer cells to plates coated with fibronectin (A) and laminin (B). The breast cancer cell lines were plated at 4 x 10^4 cells/well. The number of MCF-7 cells attached to fibronectin was significantly decreased after treatment of the fibronectin coating with concentrated CM from mammary fibroblasts when compared to treatment with serum-free medium. The effect of concentrated CM from mammary fibroblasts on the adhesion of MDA-MB-231 and Hs578T cells to fibronectin was not significantly altered (A). There was no significant difference in the number of breast cancer cell : MCF-7, MDA-MB-231, and Hs578T cells attached to laminin after treatment of the laminin coating with concentrated CM from mammary fibroblasts, when compared to treatment with serum-free medium (B). Each data points represent the mean ± SD of 8 replicates from two independent experiments. *, $P < 0.05$ (Mann-Whitney U Test).

the MCF-7 cells tested (4 x 10^4 cells/well), 50% inhibition in attachment was observed. The concentrated fibroblast CM had no detectable effect on attachment to laminin for any of the breast cancer cell lines, when compared to control serum free-medium (Figure 4.3B).

4.3.3 Characterization and inhibitory effect of purified versican fractions on MCF-7 cell attachment

In order to purify a sufficient amount of versican, 1000 ml fibroblast CM was collected from mammary fibroblasts (derived from breast cancer tissue) cultured in RPMI plus 5%FBS instead of RPMI plus ITS, and processed for purification. As shown in Figure 4.4A, versican was identified by immunoblotting using rabbit antibody to recombinant human versican. The V0 and V1 isoform of versican were detectable in unconcentrated CM from fibroblasts cultured in medium containing FBS. Similarly, the sequential fractions 6-13 eluted from the Sephacryl S400 gel chromatography column contained the two versican isoforms. In addition, antibody against decorin was used to test all of the eluted fractions (Figure 4.4B). Two isoforms of decorin were detectable after gel chromatography in fractions 9-13. The presence of decorin was not detected in the unconcentrated CM from fibroblasts cultured in medium containing FBS, nor in fractions 6-8. Fraction 6 and the pooled fractions 7+8 contained the greater proportion of versican and were concentrated 20-fold for characterization and for testing of its functional properties.

Immunoblotting was performed on the concentrated purified versican fraction 6 and 7+8, using monoclonal antibody 2B6 reactive for C-4-S (Figure 4.5). Two bands were detected of molecular size M_r ~400,000, in agreement with the sizes of versican core protein isoforms. Another band was observed with apparent M_r of ~180,000. The identity of this band is unknown. ECL measurement indicated that the amount of versican in fractions 7+8

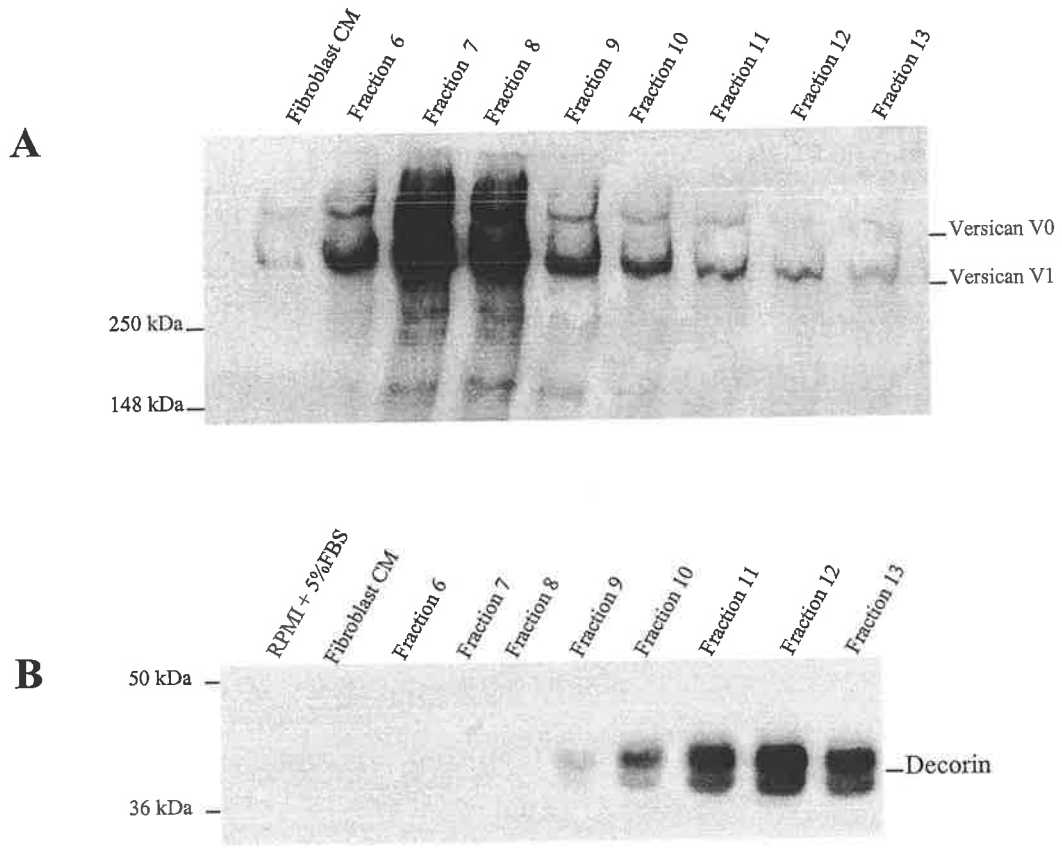

Figure 4.4. Characterization of chromatographically purified versican in CM from mammary fibroblasts derived from breast cancer tissue.

A. Immunoblot of fractions isolated during purification of versican using antibody to recombinant human versican. Unconcentrated CM from mammary fibroblasts cultured in RPMI plus 5% FBS (lane 1, loaded 15 µl), and fraction 6-13 from Sephacel S400 chromatography (lane 2-9, loaded 15 µl) all contain V0 and V1 isoforms of versican.

B. Immunoblot of fractions isolated during purification of versican using antibody to decorin. Decorin is not detectable in CM (unconcentrated) from mammary fibroblasts (lane 2, loaded 15 µl) nor in fractions 6-8 (lanes 3-5, loaded 15 µl), but was present in fractions 9-13 (lane 6-10, loaded 15 µl).

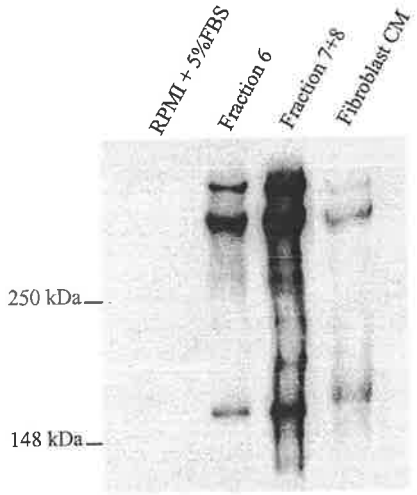

Figure 4.5. Immunoblot of fractions isolated during purification of versican using antibody to C-4-S. Fraction 6 (lane 2, loaded 3 μl of 20-fold concentrated), pooled fraction 7+8 (lane 3, loaded 3 ul of 20-fold concentrated), and CM from mammary fibroblasts (lane 4, loaded 5 ul of 25-fold concentrated) contain two core proteins with CS stubs (M_r ~ 400,000 and 180,000). The bands of M_r ~ 400,000 are consistent with versican. The other band of M_r ~ 180,000 is of unknown identity.

was 2.2-fold greater than that in fraction 6, while the difference in amount of the M_r ~180,000 CS proteoglycan between the fractions was 4-fold. Purified versican fraction 6 and 7+8 inhibited MCF-7 cell adhesion to fibronectin in a dose dependent manner. The inhibition was reduced corresponding with increasing dilution of both fractions (Figure 4.6). The relative amount of inhibitory activity of versican in fractions 7+8 is about 2.2-fold higher than that in fraction 6.

To demonstrate the specificity of inhibition of the purified versican fractions on attachment of MCF-7 cells to fibronectin, the attachment assays were performed using the purified versican fraction 7+8 treated either with RGD peptide (50 μg/ml) or ChABC (2U/ml). The addition of RGD peptide (ie the minimal essential component of fibronectin for attachment of various cell types) reversed significantly the inhibition of MCF-7 cell attachment (Figure 4.7). A similar reversal in MCF-7 attachment, but of a lesser magnitude, was observed when the versican was treated with ChABC to degrade the CS side chains. There was no significant difference in the inhibition of MCF-7 cell attachment produced by the RGD or ChABC treatment of the control serum-free medium, when compared to the control serum-free medium without treatment.

4.3.4 Effect of serum-containing media and fibroblast CM on the ability of breast cancer cells to penetrate coated filters during *in vitro* motility and invasion assays

The only distinction between the Boyden chamber models of cell motility and invasion is in the thickness of the matrix coating over the perforated membrane. Invasion involves both cell motility and ability to digest matrix coating. To determine the conditions for rapid but discriminating assays for cell migration and invasion in these assay systems, the time allowed for transmigration or penetration were varied for each of the breast cancer cell lines.

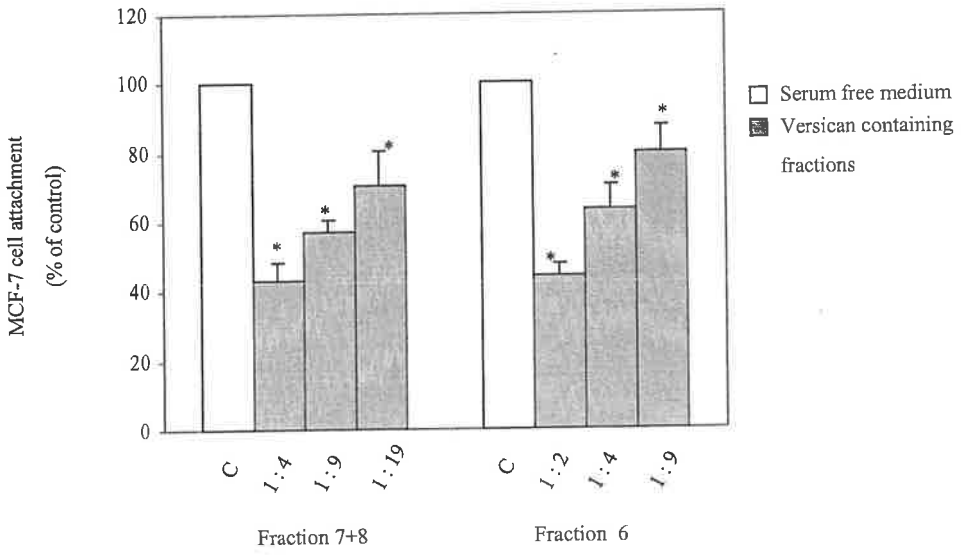

Figure 4.6. Effect of versican-containing fraction 7+8 and fraction 6 isolated during versican purification from CM of mammary fibroblasts on MCF-7 cell (5 x 10^4 cells/well) attachment to fibronectin. The number of MCF-7 cells attached to fibronectin was decreased significantly in a dose dependent manner with decreasing dilution of 20-fold concentrate fractions 7+8 and 6 (closed bar), in comparison to fibronectin coated substrate treated with control serum-free medium (open bar). Each data point is expressed as a percentage of control and represents mean ± SD of 6 replicates from two experiments. * $P < 0.05$ (Mann-Whitney U test)

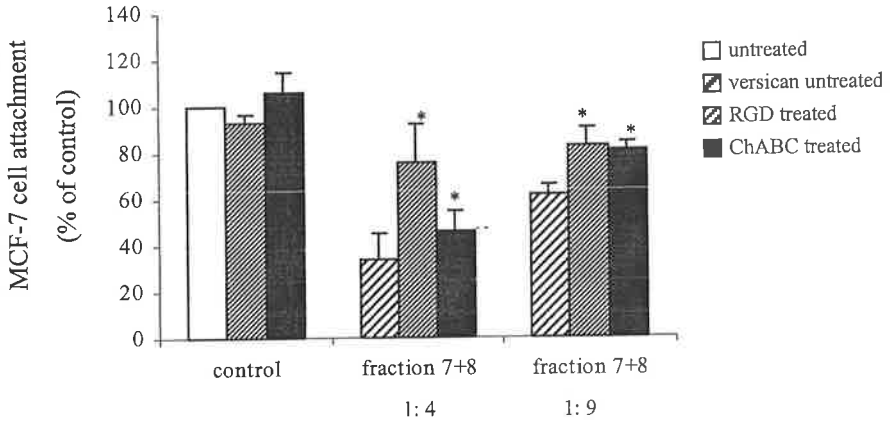

Figure 4.7. Effect of RGD peptide and enzyme chondroitinase ABC (ChABC) treatment of versican- containing fraction 7+8 on the attachment of MCF-7 cells to fibronectin. MCF-7 cells plated at 5 x 10^4 cells/well demonstrated significant decrease in attachment to fibronectin, after treatment of the fibronectin coating with versican-containing fraction 7+8 compared with control serum-free medium. This effect was reversed when the fraction 7+8 was treated with RGD peptide or ChABC before assay. Each data point is expressed as a percentage of control and represents mean ± SD of quadruplicates from one experiment. *, $P < 0.05$ comparing treated to versican untreated.

Significant numbers of MCF-7 cells migrated through thin filter coatings of collagen type I (0.5 μg) plus fibronectin (0.05 μg) after 24 h, and significant numbers invaded through thick filter coatings of collagen type I (10 μg) plus fibronectin (1 μg) was also observed after 24 h. Minimal migration of MCF-7 cells was observed through coated filters in the absence of chemoattractant (ie control RPMI culture medium). Migration of the cells increased significantly when concentrated fibroblast CM and 5% FBS were used as chemoattractants (Figure 4.8). When serum-containing medium was used as chemoattractant, and concentrated fibroblast CM was included in the filter coating matrix with collagen type I and fibronectin, a significant increase in chemotactic response of MCF-7 cell migration was observed in comparison with a similar system lacking addition of concentrated fibroblast CM to the filter coating of matrix.

The ability of MCF-7 cells to invade through the coated filters increased significantly when concentrated fibroblast CM and 5% FBS were used as chemoattractants, in comparison with control culture medium (Figure 4.9). Using serum-containing medium as chemoattractant, the number of MCF-7 cells which invaded through filters coated with collagen type I and fibronectin incorporating concentrated fibroblast CM was lower, but not significantly different from the number observed with filter coatings of collagen type I and fibronectin lacking concentrated fibroblast CM.

MDA-MB-231 migrated through thin filter coatings of collagen type I (0.5 μg) plus fibronectin (0.05 μg) after 3 h., while the cells invaded through thick filter coatings of collagen type I (10 μg) plus fibronectin (0.25μg) after 5 h. A significant increase in migration of MDA-MB-231 cells was observed when concentrated fibroblast CM and 5% FBS were used as chemoattractant (Figure 4.10). Similar to the finding for MCF-7 cells, migration of MDA-MB-231 cells through a filter coating of collagen type I and

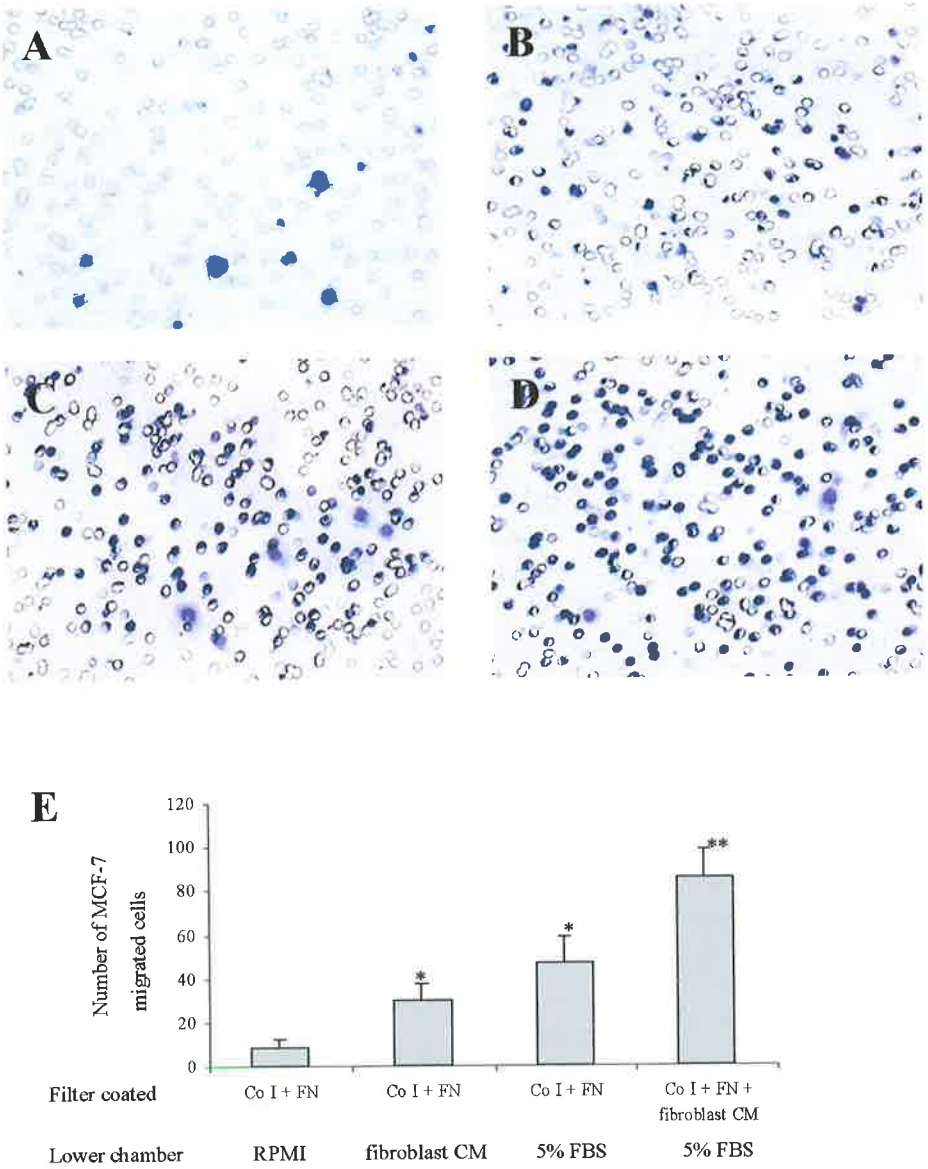

Figure 4.8. Boyden chamber migration assay. Migration of MCF-7 cells (24 h) through membrane coated with either collagen type I (0.5 µg/filter) plus FN (0.05 µg/filter) towards lower chamber filled with RPMI (A), concentrated fibroblast CM (B), or 5% FBS (C). Incorporation into filter matrix coating of concentrated fibroblast CM (15-fold, 15 µl/filter), MCF-7 cell migration towards lower chamber filled with 5% FBS (D). Photographs were taken using a microscope at magnification of 100X. The number of migrated cells were counted under a microscope in 30 fields of two experiments at a magnification of 200 X (E). The data points shown represent mean ± SD. *, $P < 0.05$ comparing fibroblast CM and 5%FBS to RPMI. **, $P < 0.05$ comparing filter coated with collagen type I plus FN to collagen type I plus FN plus fibroblast CM in chemoattractant: 5% FBS.

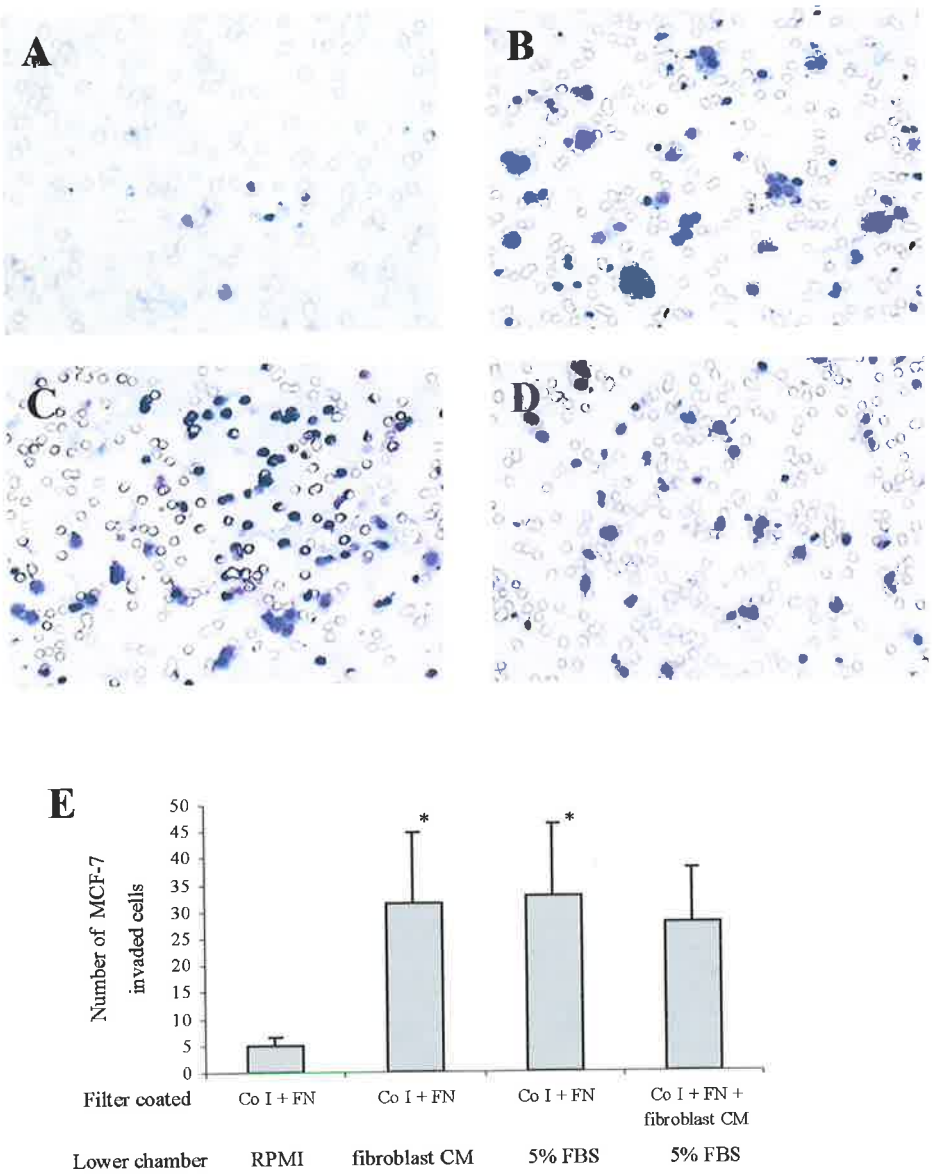

Figure 4.9. Boyden chamber invasion assay. Invasion of MCF-7 cells (24 h) through membrane coated with either collagen type I (10 µg/filter) plus FN (1 µg/filter) towards lower chamber filled with RPMI (A), concentrated fibroblast CM (B), or 5% FBS (C). Incorporation into filter matrix coating of concentrated fibroblast CM (15-fold, 15 µl/filter), MCF-7 cell invasion towards lower chamber filled with 5% FBS (D). Photographs were taken using a microscope at magnification of 100X. The number of invaded cells were counted under a microscope in 30 fields of two experiments at a magnification of 200 X (E). The data points shown represent mean ± SD. *, $P < 0.05$ comparing fibroblast CM and 5% FBS to RPMI.

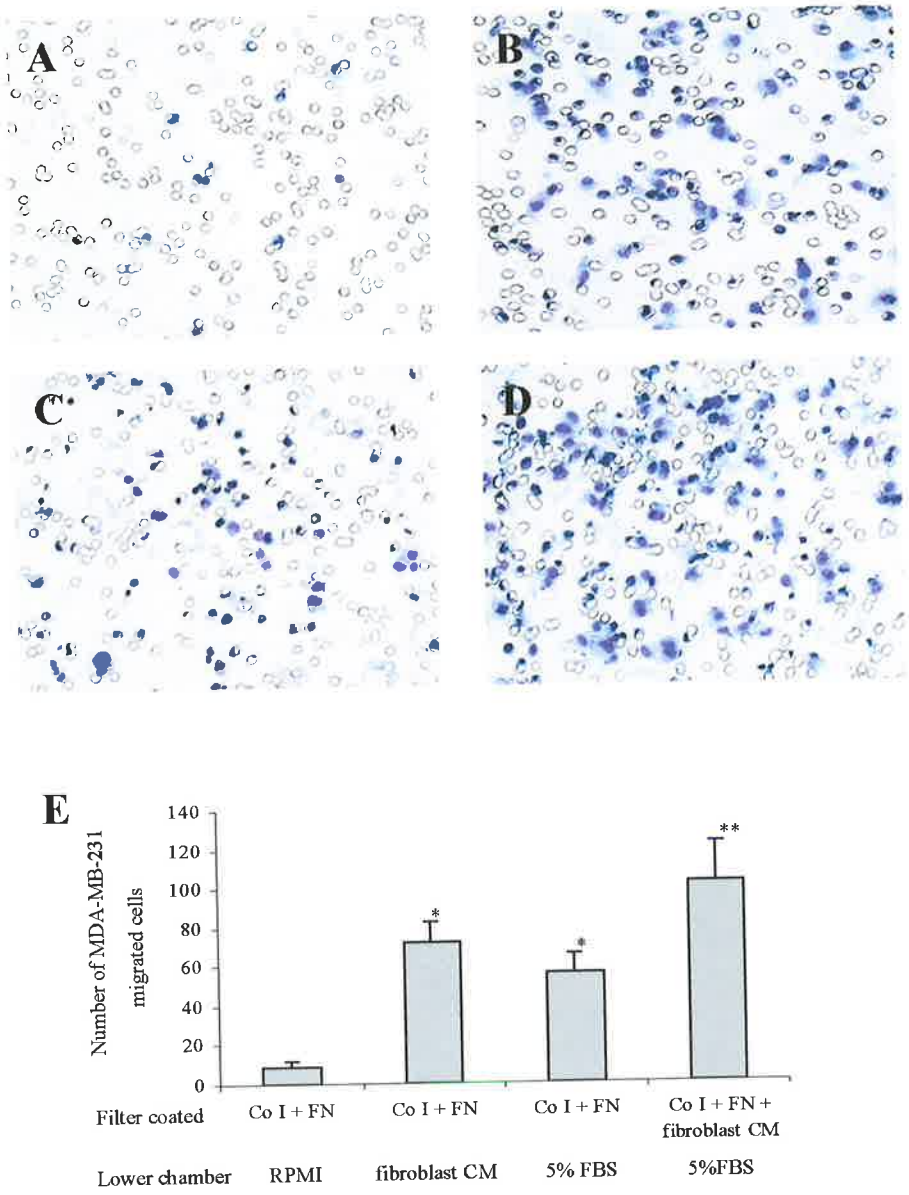

Figure 4.10. Boyden chamber migration assay. Migration of MDA-MB-231 cells (3 h) through membrane coated with either collagen type I (0.5 µg/filter) plus FN (0.05 µg/filter) towards lower chamber filled with RPMI (A), concentrated fibroblast CM (B), or 5%FBS (C). Incorporation into filter matrix coating of concentrated fibroblast CM (15-fold, 15 µl/filter), MDA-MB-231 migration towards lower chamber filled with 5% FBS (D). Photographs were taken using a microscope at magnification of 100X. The number of migrated cells were counted under a microscope in 30 fields of two experiments at a magnification 200X (E). The data points shown represent mean ± SD. *, $P < 0.05$ comparing fibroblast CM and 5% FBS to RPMI. ** , $P < 0.05$ comparing filter coated with collagen type I plus FN to collagen type I plus FN plus fibroblast CM in chemoattractant: 5% FBS.

fibronectin, incorporating concentrated fibroblast CM was significantly higher than that through filter coatings of collagen type I and fibronectin without concentrated fibroblast CM.

MDA-MB231 cells were able to invade through the matrix coated filter with concentrated fibroblast CM and serum-containing medium as chemoattractants to a greater extent than with serum-free control medium (Figure 4.11). Incorporation of concentrated fibroblast CM into the matrix coating of collagen type I and fibronectin significantly decreased invasion by MDA-MB-231 cells, when compared to matrix coated filters lacking concentrated fibroblast CM.

Hs578T cells migrated through thin filter coatings of collagen type I (0.5 μg) plus fibronectin (0.05 μg) after 4 h, while the cells invaded through thick filter coatings of collagen type I (10 μg) plus fibronectin (1 μg) after 6 h. The results of the migration and invasion assays using Hs578T cells were similar. Significant increases in the rate of cell migration and invasion were observed in the presence of chemoattractants compared with control culture medium (Figure 4.12 and 4.13). Using serum-containing medium as chemoattractant, the ability of Hs578T cells to migrate and invade through the filters coated with collagen type I and fibronectin, incorporating concentrated fibroblast CM decreased significantly when compared with filters coated only with collagen type I and fibronectin (Figure 4.12 and 4.13).

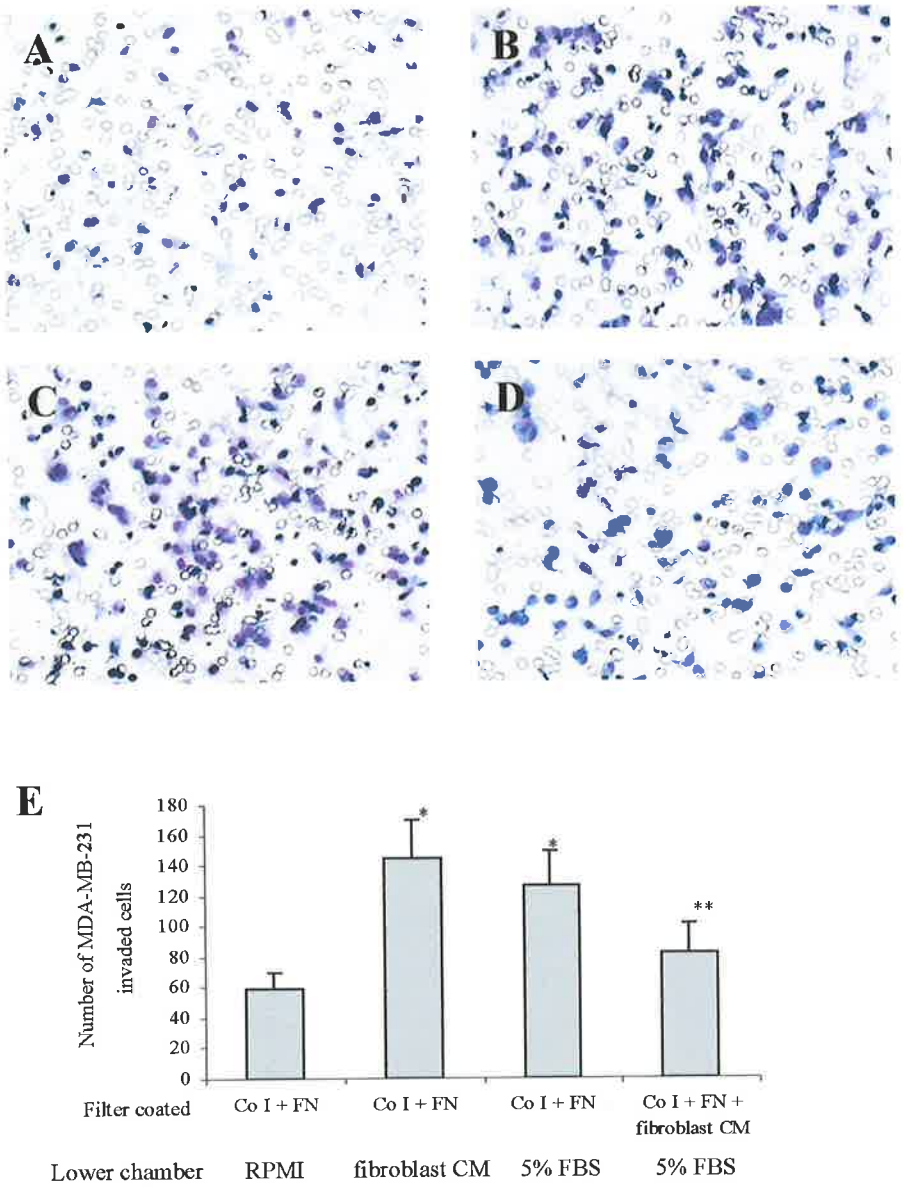

Figure 4.11. Boyden chamber invasion assay. Invasion of MDA-MB-231 cells (5 h) through membrane coated with either collagen type I (10 µg/filter) plus FN (0.25 µg/filter) towards lower chamber filled with RPMI (A), concentrated fibroblast CM (B), or 5%FBS (C). Incorporation into filter matrix coating of concentrated fibroblast CM (15-fold, 15 µl/filter), MDA-MB-231 cell invasion towards lower chamber filled with 5% FBS (D). Photographs were taken using a microscope at magnification of 100X. The number of invaded cells were counted under a microscope in 30 fields of two experiments at a magnification 200X (E). The data points shown represent mean ± SD. * , $P < 0.05$ comparing fibroblast CM and 5% FBS to RPMI. **, $P < 0.05$ comparing filter coated with collagen type I plus FN to collagen type I plus FN plus fibroblast CM in chemoattractant: 5% FBS.

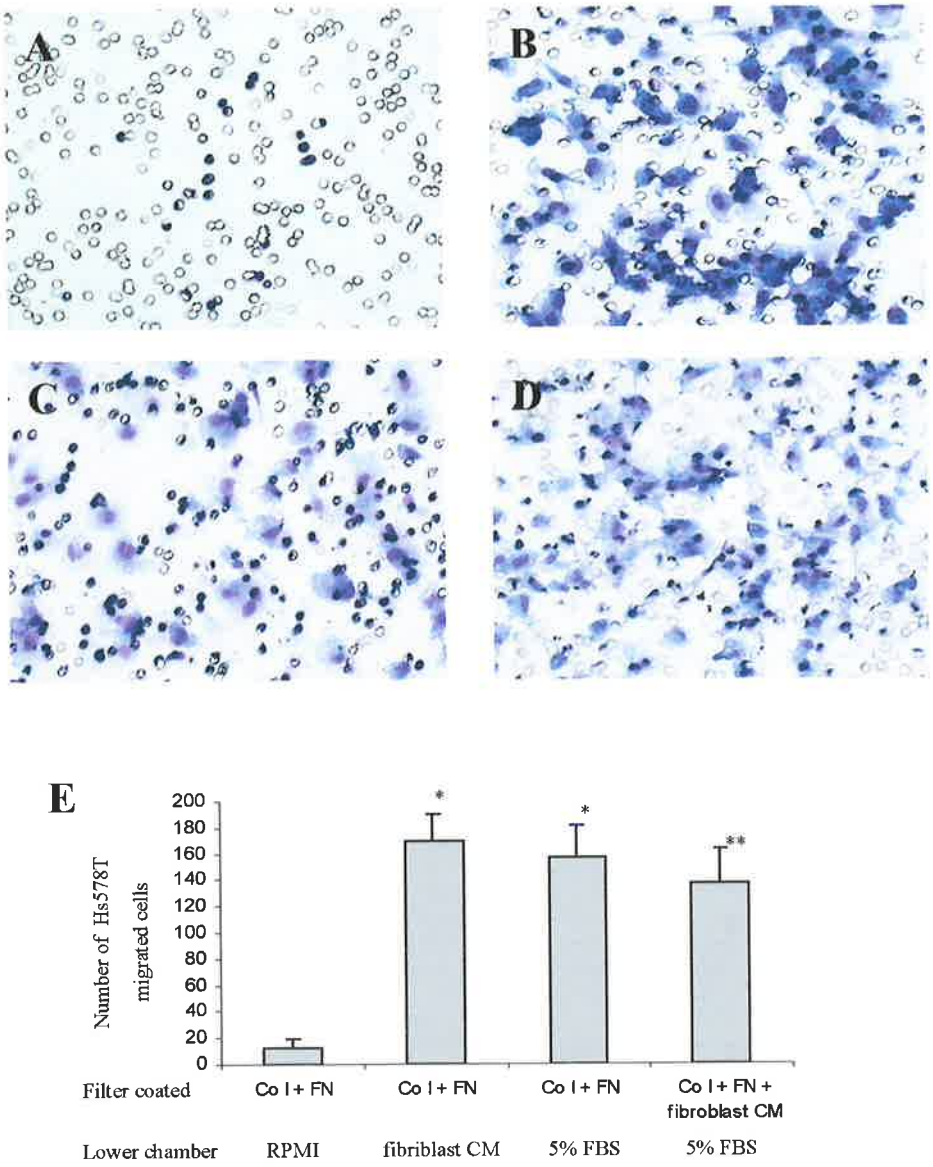

Figure 4.12. Boyden chamber migration assay. Migration of Hs578T cells (4 h) through membrane coated with either collagen type I (0.5 μg/filter) plus FN (0.05 μg/filter) towards lower chamber filled with RPMI (A), concentrated fibroblast CM (B), or 5% FBS (C). Incorporation into filter matrix coating of concentrated fibroblast CM (15-fold, 15 μl/filter), Hs578T cell migration towards lower chamber filled with 5% FBS (D). Photographs were taken using a microscope at magnification of 100X. The number of migrated cells were counted under a microscope in 30 fields of two experiments at a magnification of 200X (E). The data points shown represent mean ± SD. *, $P < 0.05$ comparing fibroblast CM and 5%FBS to RPMI. ** , $P < 0.05$ comparing filter coated with collagen type I plus FN to collagen type I plus FN plus fibroblast CM in chemoattractant: 5% FBS.

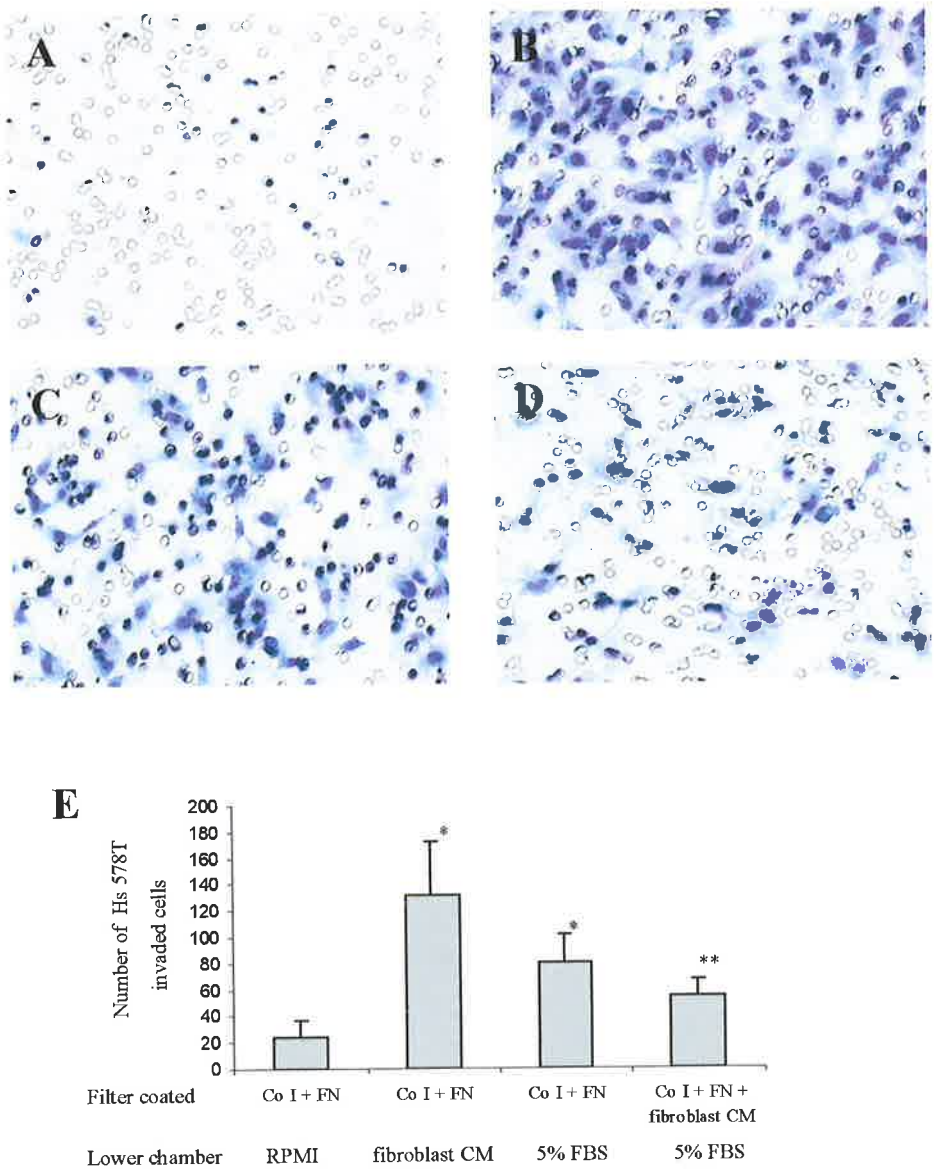

Figure 4.13. Boyden chamber invasion assay. Invasion of Hs578T cells (6 h) through membrane coated with either collagen type I (10 μg/filter) plus FN (1 μg/filter) towards lower chamber filled with RPMI (A), concentrated fibroblast CM (B), or 5% FBS (C). Incorporation into filter matrix coating of concentrated fibroblast CM (15-fold, 15 μl/filter), Hs578T cell invasion towards lower chamber filled with 5% FBS (D). Photographs were taken using a microscope at magnification of 100X. The number of invaded cells were counted under a microscope in 30 fields of two experiments at a magnification of 200X (E). The data points shown represent mean ± SD. *, $P < 0.05$ comparing fibroblast CM and 5% FBS to RPMI. **, $P < 0.05$ comparing filter coated with collagen type I plus FN to collagen type I plus FN plus fibroblast CM in chemoattractant: 5%FBS.

4.4 Discussion

This study demonstrated that CM from cancer-associated mammary fibroblast cultures, which contains secreted versican, selectively inhibited breast cancer cell attachment to matrix. The binding of MCF-7 cells to fibronectin, but not the binding of MDA-MB-231 or Hs578T cells, was inhibited by CM. Cell binding to laminin was not inhibited by CM for any of the three breast cancer cell lines. Versican was confirmed as the active inhibitory molecule in mammary fibroblast CM by chromatographic purification. This finding is in agreement with the recently published observation that versican isolated from the CM of cultured prostatic fibroblasts inhibited prostate cancer cell adhesion to fibronectin, but not to laminin (Sakko et al., 2003). There is an extensive literature outlining the inhibitory properties of versican for cell binding to various matrix components. Melanoma cell adhesion to fibronectin and collagen type I is inhibited by versican (Touab et al., 2002). Moreover, versican extracted from chick embryonic fibroblasts binds directly to fibronectin and collagen type I but not to laminin and collagen type IV (Yamagata et al., 1986). Whereas there is agreement regarding the inability of versican to bind collagen type IV, controversy exists about whether versican inhibits cell binding to collagen type I and laminin (Yamagata et al., 1989, Braunewell et al., 1995). Overall, the suggestion is that versican may reduce cell adhesion to components of the interstitial matrix rather than of the basement membrane.

The fact that versican-containing CM from mammary fibroblast cultures was unable to inhibit adhesion of MDA-MB-231 and Hs578T cells to fibronectin suggests that substrate binding by these cell lines involves alternative adhesion mechanisms eg. different integrins (matrix receptors) or CD44 (HA receptor). In support, these cell lines have been shown to adhere to fibronectin via multiple integrin types present on the cell surface (Bartsch et al., 2003, Gui et al., 1995). In addition, high level expression of CD44 has been reported in

Hs578T cells, and moderate levels of expression in MDA-MB-231 cells (Culty et al., 1994). CD44 has binding affinity not only for HA, but also for fibronectin, collagen, growth factors and cytokines (Jalkanen and Jalkanen, 1992, Ehnis et al., 1996, Wolff et al., 1999).

The inhibitory effect of purified versican fractions from mammary fibroblasts on the adhesion of MCF-7 cells to fibronectin was found to be partially reversed by treatment of the fibronectin-coated substrate with RGD peptide. This peptide contains the minimal sequence capable of inhibiting cell binding to fibronectin, and represents a candidate cell binding site. This provides evidence that versican inhibitory action may target cell binding to fibronectin via the RGD sequence. However, similar to the situation reported for versican action in reducing LNCaP prostate cancer cell attachment (Sakko et al., 2003), addition of RGD peptide itself (ie in the absence of versican) has no effect on MCF-7 cell attachment to fibronectin. This suggests that the mechanism of versican inhibitory action on cell attachment and its reversal by RGD peptide might be explained by the ability of versican to bind the RGD sequence in fibronectin and the RGD peptide. Although the binding sites for MCF-7 breast cancer and LNCaP prostate cancer cells within fibronectin appear independent of the RGD sequence (as denoted by the insensitivity of cell binding to RGD peptide), the adjacent cell binding site is masked by versican binding of the fibronectin RGD sequence (Sakko et al., 2003). Although integrin $\alpha5\beta1$ fibronectin receptors which interact with the RGD sequence are expressed by MCF-7 cells, other integrin receptors are also exhibited by this cell line and might dominate cell attachment to fibronectin via an RGD-independent binding mechanism.

Digestion of the CS side chains from the purified versican fraction using ChABC resulted in partial reversal of the inhibitory effect of versican on MCF-7 cell adhesion. This finding

is in agreement with previous studies describing partial losses of anti-adhesive activity for both prostate cancer cell attachment to fibronectin and melanoma cell attachment to fibronectin and collagen type I, following ChABC digestion of versican from prostate fibroblasts (Sakko et al., 2003) and astrocytoma cells (Touab et al., 2002), respectively. The reversal of versican inhibitory activity by both RGD peptide and ChABC indicates the importance of both the protein core and the presence of CS chains for modulation of cell attachment to matrix-coated substrate.

The purity of the versican sample was illustrated by the presence of no stained bands other than of versican by "Stains-all" protein stain (not shown). Characterization of the mammary fibroblast CM by immunoblotting detected the presence of CS proteoglycans in addition to versican and decorin. Antibodies to the CS epitopes (C-0-S, C-4-S, C-6-S) detected two bands with M_r ~400,000, which likely correspond to the V0 and V1 isoforms of versican detected using rabbit polyclonal antibody. This indicates that these epitopes are expressed in the CS stubs remaining on the versican core protein after ChABC digestion. There was no indication from the original CM used to purify versican in this study, that three other CSPGs (M_r 180,000, 210,000, and 260,000) found in prostate fibroblast CM were secreted by breast cancer fibroblasts (Sakko et al., 2003). However, after chromatographic purification and concentration of versican from both mammary and prostatic fibroblast CM, a contaminant CS proteoglycan with M_r ~180,000 was detectable. Thus a putative CS proteoglycan was potentially in common to the purification of versican from breast and prostate fibroblasts. It seems unlikely that the band at M_r ~180,000 is a glycosylated breakdown product of versican, since no band of this size was detected by the polyclonal antibody to versican. It is also unlikely that the inhibitory activity in the purified fractions could be attributed to this contaminating proteoglycan, because whereas the difference in versican concentration and the inhibitory activity between purified fractions 6

and 7+8 for MCF-7 cell attachment to fibronectin were 2.2-fold, the concentration difference between the fractions for the band at $M_r \sim$ 180,000 was 4-fold.

Because our findings and previous studies suggested that versican interacted preferentially with components of interstitial matrix (eg. fibronectin, collagen type I, HA) rather than basement membrane (eg. laminin, collagen type IV), we used modified Boyden Chamber assays incorporating filters coated with fibronectin and collagen type I as *in vitro* models to study the effect of mammary fibroblast CM containing versican on breast cancer cell migration and invasion. Preliminary data indicated that serum-containing medium and concentrated mammary fibroblast CM containing versican but no protease inhibitors, enhanced the ability of the three breast cancer cell lines to migrate and invade through matrix-coated filters by acting as chemoattractants. A similar result was observed in a previous study which showed that fibroblast CM from MRC-5 human embryo fibroblasts and serum-containing media increased motility and invasion of the breast cancer cell lines MDA-MB-231, MCF7/6 and MCF-7/AZ (Heylen et al., 1998). Chemotactic factors are considered to be important in the metastatic process of malignant cell movement into a target organ. The complex mixture of factors in fibroblast CM, which may impact on the process of cell metastasis has been documented. For example, various cytokines, such as IGF-I, HGF, TGF-β1, PDGF, and EGF produced by fibroblasts, effected migration and invasion of breast cancer cells (Doerr and Jones, 1996, Yamashita et al., 1994, Walker et al., 1994, Ikeda et al., 2001). In particular, an invasion-stimulating factor, a 77 kDa protein isolated from skin fibroblasts of patient with breast cancer, has been reported to stimulate the invasive capability of breast cancer cells (Ikeda et al., 2001). In addition, members of the matrix metalloprotease (MMP) family of collagenases and gelatinases secreted by fibroblasts have been implicated in the degradation of ECM, with consequent promotion of cell migration and invasion.

In this study, the chemotactic motility response to 5% FBS differed between the MCF-7, MDA-MB-231 and Hs578T cell lines when concentrated mammary fibroblast CM containing versican was added to the membrane coating of collagen type I and fibronectin. The rate of cell migration of MCF-7 and MDA-MB-231 was increased by the presence of fibroblast CM in the filter matrix coating, but the rate of cell migration of Hs578T was reduced. Because versican inhibits MCF-7 cell attachment to fibronectin, inclusion of versican-containing fibroblast CM in the filter coating could potentially have promoted increased migration of the MCF-7 cells. Alternatively, it is possible that the fibroblast CM contained sufficient proteolytic enzyme to degrade the filter coating of matrix to permit migration of additional MCF-7 cells. Since versican had no impact on attachment of MDA-MB-231 cells to fibronectin, the fact that fibroblast CM increased cell motility may indicate the presence of some other factor which may impact on cell attachment and motility. MDA-MB-231 cells express significantly higher CD44 levels than MCF-7 cells. Increased plasma levels of CD44 are frequently associated with malignant disease, suggesting that malignant transformation may promote the release of soluble CD44 (Cichy et al., 2002). Soluble CD44 has been shown to bind directly to immobilized HA (Kawashima et al., 2000). The possibility exists therefore, that soluble CD44 released by MDA-MB-231 cells binds to the immobilized HA component of fibroblast CM leading to reduced cell attachment to the substrate. This may induce increased tumor cell motility. Conversely, Hs578T cells respond to the addition of fibroblast CM to filter coating of matrix by decreased chemotactic migration toward the serum-containing chamber. Hs578T cells display a different profile of motility-related factors from MCF-7 and MDA-MB-231 cells, in that the Hs578T cells express versican, in addition to HA and CD44, possibly due to an epithelial-mesenchymal cell transition (Lippman et al., 1988). These three molecules bind each other to form a cell motility-modulating complex, the mechanism underlying this

event being currently under investigation. Versican and HA are recognized by multiple link module sites of CD44 (Kawashima et al., 2000). Competition for binding between the versican and HA molecules produced by Hs578T cells and the same components within fibroblast CM immobilized to the filter coating may result in decreased movement by the cells. In support, recent studies have shown that CD44-HA interactions inhibited osteoclast-like FLG 29.1 cell migration toward fibronectin by down regulating the production of the locomotion-associated protease MMP-9 (Spessotto et al., 2002).

In the *in vitro* invasion assay, addition of the fibroblast CM to the filter matrix coating, where the concentration of matrix proteins was several times greater than for the migration assay, chemotaxis-induced invasion towards the 5% FBS source was decreased for all the breast cancer cell lines. The capacity of the tumor cells to invade the physical matrix barrier depends on both motility and secreted proteolytic enzymes. The differences observed in our study in invasive behavior between the individual breast cancer cell lines could be due to quantitative and qualitative differences in secreted proteolytic enzymes. The concentration of ECM coating may also be an important factor influencing cell invasion. The high concentration of collagen type I and fibronectin used to coat the filters in the invasion assays of this study might have provided an increased density and number of cell binding sites, which the versican and HA within fibroblast CM could not inhibit, thereby resulting in a decreased capacity for cell invasion.

In conclusion, this chapter has shown that versican purified from mammary fibroblast culture has the capacity to inhibit attachment of MCF-7 breast cancer cells to fibronectin (Figure 4.14). This modulation of cell attachment by versican was then reflected by an increased motility of MCF-7 cells in the *in vitro* haptotactic assay of cell motility, when the perforated membrane filter was coated with matrix components, fibronectin, collagen type I, and versican-containing fibroblast CM. However, unexpectedly, the presence of

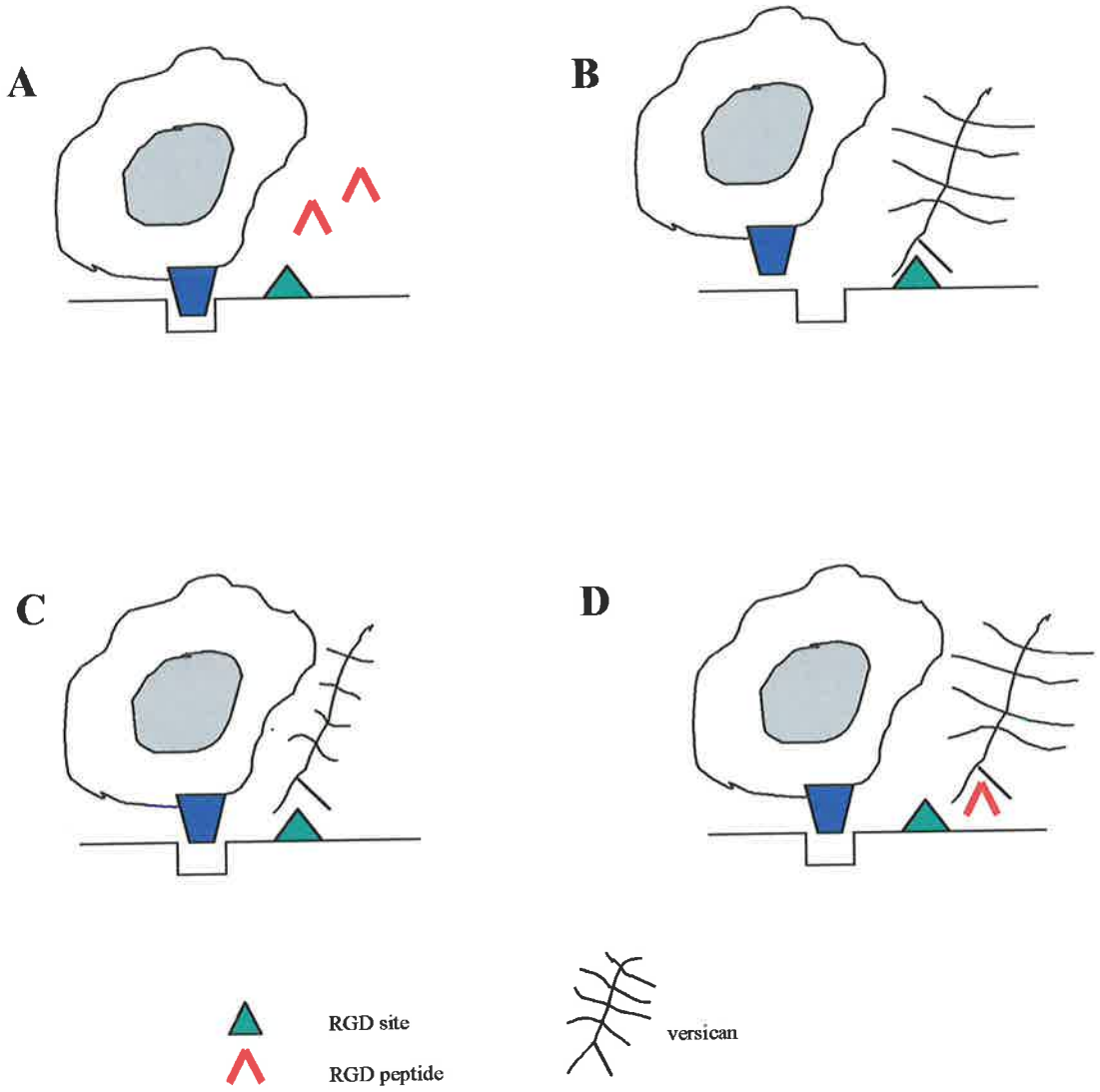

Figure 4.14. Schematic representation of hypothesised mechanisms to explain versican inhibiting activity on MCF-7 cell binding to fibronectin. A. No treatment or RPMI plus RGD peptide: MCF-7 cell binds to fibronectin at site adjacent to RGD site. B. Plus versican: Versican binds to fibronectin via RGD site and interferes with cell adhesion to adjacent site. C. Plus versican digested with ChABC: Inhibition of cell adhesion reduced, suggesting that presence of CS side chains of versican is responsible for cell adhesion. D. Plus versican treated with RGD peptide: RGD peptide competitively binds to versican reducing the capacity of versican to inhibit cell adhesion.

versican-containing fibroblast CM in the invasion assay lead to decreased invasive capacity, which may have been due to the increased concentration of matrix binding sites in the system. Future studies would need to determine whether this is indeed the case including using purified versican.

Chapter 5

Effect of Fibroblast Conditioned Medium on Formation of Pericellular Matrix by Breast Cancer Cell Lines

5.1 Introduction

Various cell types including fibroblasts, chondrocytes, smooth muscle cells, and certain tumor cell lines surround themselves in culture by pericellular matrices or sheaths rich in hyaluronan (HA) (Clarris and Fraser, 1968, Knudson et al., 1996, Blom et al., 1995, Evanko et al., 2001). The sheaths can be visualized by exclusion of particles (eg. red blood cells) resulting in a clear zone surrounding the cells. The assembly of sheath is believed to depend on a minimum of three components: HA, a matrix hyaladherin, and attachment of HA to the cell via either interaction with HA receptor on the outer cell membrane (eg. CD44) or transmembrane interaction with HA synthase (Knudson et al., 1993, Heldin and Pertoft, 1993).

The presence of a pericellular sheath of matrix may provide a favorable milieu for cell motility, proliferation, differentiation, and may participate in cellular-extracellular matrix interactions. The assembly of sheath, rich in HA and the proteoglycan versican, has been shown to be a prerequisite for proliferation and migration *in vitro* of vascular smooth muscle cells (Evanko et al., 1999). Removal of this sheath by competitive HA oligosaccharides that block the binding of HA to the cell surface prevents formation of pericellular sheath and inhibits cell division and migration. It has been also suggested that the matrix sheath may protect cells directly from viral infections as well as from cytotoxic effects of lymphocytes (Patterson et al., 1975, McBride and Bard, 1979). Additionally, the

retention of native pericellular matrix stimulates matrix production and assembly in chondrocytes (Larson et al., 2002).

It is not known whether pericellular matrix sheaths exist *in vivo* in the form in which they do *in vitro*. However, Knudson and Toole (1985) demonstrated that the expression of pericellular matrix around chondrocytes *in vitro* correlated well with degree of extracellular matrix surrounding chondrocytes *in vivo*. These data support the suggestion that these structures do in fact exist *in vivo*. It has been reported that certain cell types (eg. human urinary bladder carcinoma cell lines, HCV-29T and HU-456, SV-3T3, and endothelial cells) express HA receptor, but lack the capacity to assemble sheath (Knudson and Knudson, 1991). Following addition of exogenous HA in combination with cartilage proteoglycan, all of these cells exhibited significant sheath assembly. If these components were added separately or the components were added in the presence of HA hexasaccharides, a competitive inhibitor for binding of HA to cell surface HA receptor, no sheath was detectable. Non–invasive human urinary bladder papilloma, RT-4 cell line and B-16 mouse melanoma cell line which demonstrated a lack of binding of HA to their cell surface also lacked the capacity to assemble sheath under similar conditions (Knudson and Knudson, 1991). In support of the role of HA receptor in sheath assembly, transfection into COS cells of CD44, facilitated sheath assembly in the presence of exogenously added HA and proteoglycan (Knudson et al., 1993).

Expression of the individual matrix components of sheath have been reported in tumor tissue and in some cases have been statistically associated with disease outcome. Specifically, spread of disease and survival from breast cancer have been related to expression of HA in the peritumoral stroma and in the cancer cells (Auvinen et al., 2000). In addition, not only has versican been described as being located at the peripheral invasive area of breast cancer, which contains high levels of HA (Nara et al., 1997), but elevated

levels of versican in peritumoral stroma have now been associated with increased risk and rate of relapse in women with node-negative breast cancer (chapter 2; Suwiwat et al, submitted for publication; Ricciardelli et al., 2002). A panel of human breast cancer cell lines showed expression of variants in the CD44 HA receptor (Culty et al., 1994). Expression of these CD44 isoforms was associated with early stage of breast carcinogenesis and also related to motility and invasion by tumor cells (Bankfalvi et al., 1998, Herrera-Gayol and Jothy, 1999).

In this chapter, we investigated whether breast cancer cell lines exhibiting cell surface HA receptor CD44 had the capacity to assemble pericellular matrix sheath, when cultured either alone in control medium, in CM containing versican and HA secreted by mammary fibroblasts, or with purified versican and HA.

5.2 Materials and methods

5.2.1 Materials

Hyaluronic acid (from human umbilical cord), 3,3',5,5 tetramethyl benzidine (TMB), *Streptomyces* hyalurolyticus (hyaluronidase), ITS, goat serum, and DAB were purchased from Sigma Chemical Co (St Louis, MO, USA). RPMI1640, FBS, trypsin/EDTA, streptomycin, superscript ™ II RNase H⁻reverse transcriptase were purchased from Life Technologies (NY, USA). Monoclonal antibody to CD44s (clone 156-3C11) was from NeoMarkers (Fremont, CA, USA). Biotinylated hyaluronic acid binding protein (bHABP) was from Seikagaku Corporation (Tokyo, Japan). Biotinylated goat anti-mouse secondary antibody was from Dako (Sydney, NSW, Australia). Avidin-biotin-peroxidase complex was from Vector Laboratories (Irvine, CA). Random hexamers and GAPDH primers were from Bresatec (Adelaide, Australia). HAS primer was from Geneworks. 100 bp DNA Ladder was from New England Biolabs Inc (Beverly, MA, USA). RNeasy mini kit was from Qiagen (Hilden, Germany). Taq DNA polymerase was from Perkin Elmer (Norwalk, CT). Revercell (pooled red cells) was from CSL (Parkville,Victoria, Australia). All organic salts and solvents were from either Sigma Chemical Co or Ajax Chemicals (Sydney, NSW, Australia).

5.2.2 Cell lines and fibroblast conditioned medium

MCF-7, MDA-MB-231, and Hs578T breast cancer cell lines and primary mammary fibroblasts were maintained in complete RPMI containing 5%FBS. For measurement of HA secretion, breast cancer cell lines and mammary fibroblasts derived from breast cancer tissue were seeded into 24 well plates at density of $1x10^4$ cells/well. After culture for 24 h, the medium was changed from complete RPMI containing 5% FBS to complete RPMI containing 0.5% FBS for 24 h. The cells were grown in complete RPMI plus ITS for 48 h. The media were collected for analysis of HA levels and the cells were trypsinized and

counted. Fibroblast CM was collected from confluent primary fibroblasts grown in complete RPMI containing ITS for 72 h.

5.2.3 ELISA assay for measurement of hyaluronan levels in culture medium

The amount of HA in culture medium was measured using a competitive ELISA-like assay as described by Fosang et al., 1990. For assay, 96 well plates were coated with 25 μg/ml HA in 50 mM sodium carbonate buffer pH 9.5 overnight at room temperature. After removing the coating buffer, the plates were blocked with 1% BSA in PBS at 37°C for 90 min and washed with 0.05% Tween-PBS. Standard concentrations of HA (0.1-12.5 μg/ml) or medium samples were applied to the plates, followed by 1 μg/ml biotinylated HABP (bHABP) diluted in 0.05% Tween-PBS, then mixed and incubated overnight at room temperature. Blank wells contained 0.05% Tween-PBS in place of bHABP. Subsequently, the plates were incubated with horseradish peroxidase-streptavidin at 1 μg/ml for 30 min at 37°C, rinsed in 0.05%Tween-PBS, and 100 μl/well substrate solution TMB added for 15-30 min at room temperature. Absorbance was read at 655 nm. Four duplicates were analyzed for each sample. The amount of HA in each test sample was calculated from the plot of absorbance versus standard HA concentration.

5.2.4 RT-PCR detection of hyaluronan synthase (HAS) expression by fibroblasts and breast cancer cell lines

Total cellular RNA were extracted from primary cultured fibroblast and breast cancer cell lines as described in section 3.2.9. The primer sequences were: HAS1, sense 5' TACTGGGTAGCCTTCAATGTGGA-3', antisense5'-TACTTGGTAGCATAACCCAT-3';HAS2,sense 5'-GAAAGGGCCTGTCAGTCTTATTT-3', antisense 5'-TTCGTGAGAT GCCTGTCATCACC-3'; HAS3, sense 5'-GAGCGGGCCTGCCAGTCCTACTT-3', and antisense 5'-AGCCAAGGCTCAGGACTCGGTT-3' (Konttinen et al., 2001). cDNA was

amplified with initial denaturation at 95° C 5 min, followed by forty cycles of 1 min at 95° C, 1 min at 57° C, 1 min at 72° C and a final extension of 10 min at 72° C. To determine that all samples originally contained cellular RNA, the samples were coamplified for the presence of an internal standard, GAPDH, as per section 3.2.9.

5.2.5 Immunoblot analysis of breast cancer cell lines and fibroblast cultures

To determine the presence of versican in culture medium from breast cancer cell lines: MCF-7, MDA-MB-231, and Hs578T and mammary fibroblasts, culture medium of these cells were harvested and analyzed using immunoblot as described in section 3.2.10.

5.2.6 Immunocytochemical staining of cell monolayers for CD44 and hyaluronan

Breast cancer cell lines and mammary fibroblasts grown on coverslips in 24 well plates were fixed in 10% phosphate buffered formalin for 15 min, followed by methanol and acetone for 3 min and 1 min respectively, and washed with PBS. To detect CD44, the cells were incubated with monoclonal antibody specific for CD44s (clone 156-3C11, diluted 1:200) overnight at 4°C. Subsequently, biotinylated goat anti-mouse IgG and avidin-biotin peroxidase complex were applied to the samples. To detect HA, the cells were blocked for non-specific binding with 1% bovine serum albumin in PBS and incubated with 2 μg/ml bHABP overnight at 4°C, followed by addition of avidin-biotin-peroxidase complex. The staining specificity for HA was determined by predigesting cell samples with *Streptomyces* hyaluronidase (4 unit/ml 0.1M sodium acetate buffer pH 5.0) for 1 h at 37°C before incubation with bHABP. Visualization of the immunoreaction was developed with DAB/ 0.03% hydrogen peroxide in 50mM Tris-HCl, pH 7.6 for 6 min. Finally, the cell monolayers were washed in water, counterstained with haematoxylin, dehydrated through graded alcohol, cleared in xylene, and mounted using DPX.

The intensity of CD44 and HA staining was graded as 'weak' when 5-40% cells were stained, 'moderate' when 41-70% cells were stained, and 'strong' when 71-100% cells were stained.

5.2.7 Particle exclusion assay for pericellular matrix

Breast cancer cell lines and mammary fibroblasts were added to 24 well plates at density of $1x10^4$ cells/well and cultured for 24 h at 37°C in a humidified incubator supplied with 5% CO_2. The medium was then changed from complete RPMI containing 5% FBS to complete RPMI containing 0.5% FBS for 24 h. The cells were treated with serum free complete RPMI medium containing ITS or FB-CM for 24 h. The medium was then removed and 300 µl human erythrocytes (approximately 10^8 cells/ml) were added and allowed to settle for 15 min at room temperature. Pericellular sheath was observed as a clear halo surrounding the cancer cells or fibroblasts from which erythrocytes were excluded. Representative cells were photographed using a Nikon inverted phase-contrast microscope at 200x magnification. Sheath formation was quantitated from digital photographs using the Video Pro image analysis system (Leading Edge P/L, Marion, South Australia). The area delimited by red blood cells and the area delimited by the cell membrane yield the coat to cell ratio. A ratio of one indicates no matrix. Cells with a ratio of 2.0 or greater were determined to have pericellular matrix. To confirm the dependence of pericellular matrix on HA, cells were treated with *Streptomyces* hyaluronidase (5 unit/ml) at 37°C for 30 min.

5.3 Results

5.3.1 Measurement of HA levels in culture medium

The secretion of HA by breast cancer cell lines and mammary fibroblasts derived from breast cancer tissue was measured in 48 h cell culture medium using the competitive ELISA assay (Figure 5.1). MCF-7 and MDA-MB-231 cells secreted only small amounts of HA. The level of HA secretion by Hs578T was approximately 3-fold higher than MCF-7 and MDA-MB-231. The greatest level of HA was released by mammary fibroblasts. The following values expressed in $\mu g/10^5$ cells were recorded for HA secreted over 48 h of culture: MCF-7 0.12 μg, MDA-MB-231 0.14 μg, Hs578T 0.42 μg, and mammary fibroblasts 11.74 μg.

5.3.2 RT-PCR of HAS mRNA expression in cultured cells

HAS2 and HAS3 (158 bp and 178 bp, respectively) were the predominant isoforms detected in the breast cancer cell lines: MCF-7, MDA-MB231, and Hs578T. A minor amount of HAS1 (212bp) expression was detected in MDA-MB231 cells. In mammary fibroblasts, all three HAS isoforms were detected. GAPDH mRNA was detected in all samples (Figure 5.2).

5.3.3 Immunoblot analysis of versican in breast cancer cells and fibroblast cultures

Two versican isoforms (V0 and V1) were secreted by mammary fibroblasts grown in both control ITS medium and medium supplemented with 5% FBS and by Hs578T breast cancer cells (Figure 5.3). Versican expression was not detected in the culture medium of MCF-7 and MDA-MB-231 cells.

5.3.4 HA and CD44 staining

Each of the breast cancer cell lines and the mammary fibroblasts demonstrated positive staining for HA (Figure 5.4). Staining of cell monolayers localized HA over the cytoplasmic membrane. MDA-MB-231, Hs578T, and mammary fibroblasts showed strong

A

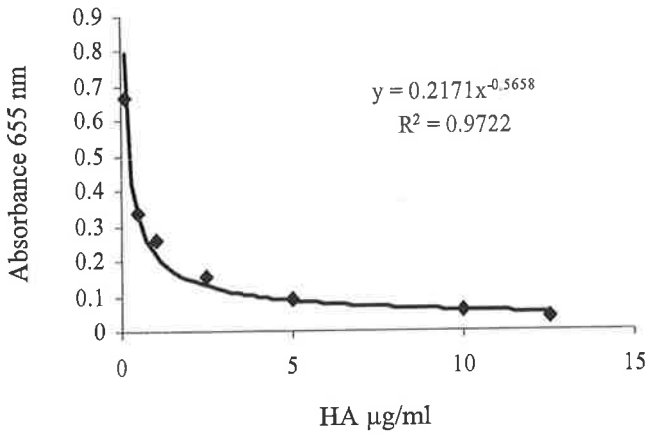

B

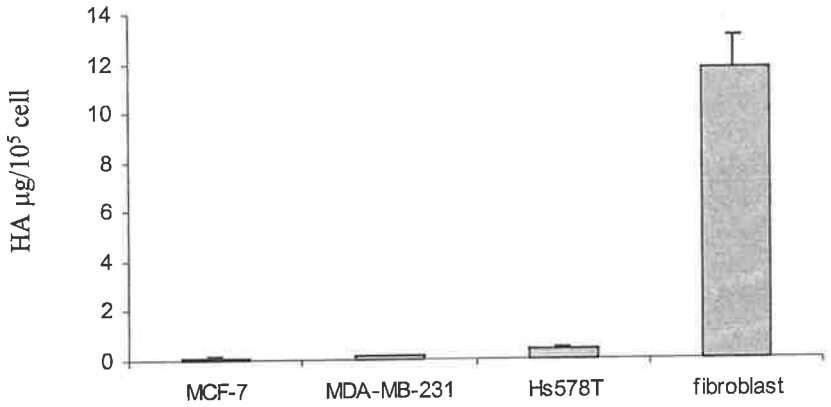

Figure 5.1. A. Competition ELISA assay, curve was generated by use of standard HA concentrations 0.1-12.5 µg/ml. Detection was achieved using TMB substrate and the absorbance was read at 655 nm. B. HA levels were measured in samples of culture medium from MCF-7, MDA-MB-231, Hs578T, and mammary fibroblasts derived from breast cancer tissue. Data were expressed as mean ± SD µg/10^5 cells of four replicate wells.

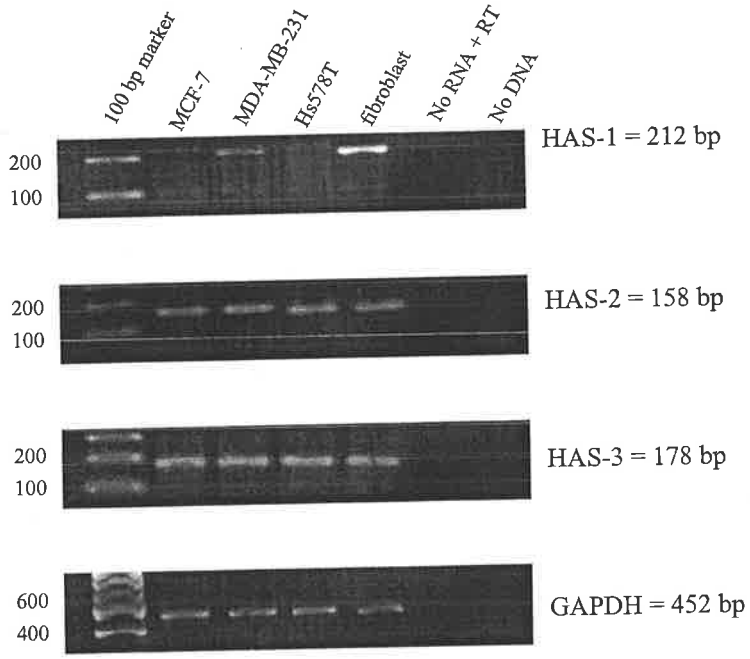

Figure 5.2. HA synthase expression in breast cancer cell lines and mammary fibroblasts. Total RNA was extracted from cell cultures of MCF-7, MDA-MB-231, Hs578T, and mammary fibroblasts derived from breast cancer tissue. RT-PCR was performed to determine the expression of mRNA for HAS-1 (212bp), HAS-2 (158 bp), HAS-3 (178 bp), and GAPDH (452 bp). Negative controls (water substituted for RNA and DNA) were included all reactions.

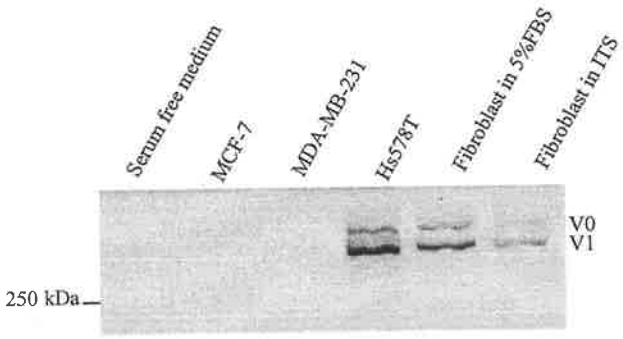

Figure 5.3. Immunoblot analysis for versican confirmed that two versican isoforms (V0 and V1) were secreted by mammary fibroblasts derived from breast cancer tissue and by Hs578T cells. No detectable versican expression was observed for MCF-7 and MDA-MB-231 cells.

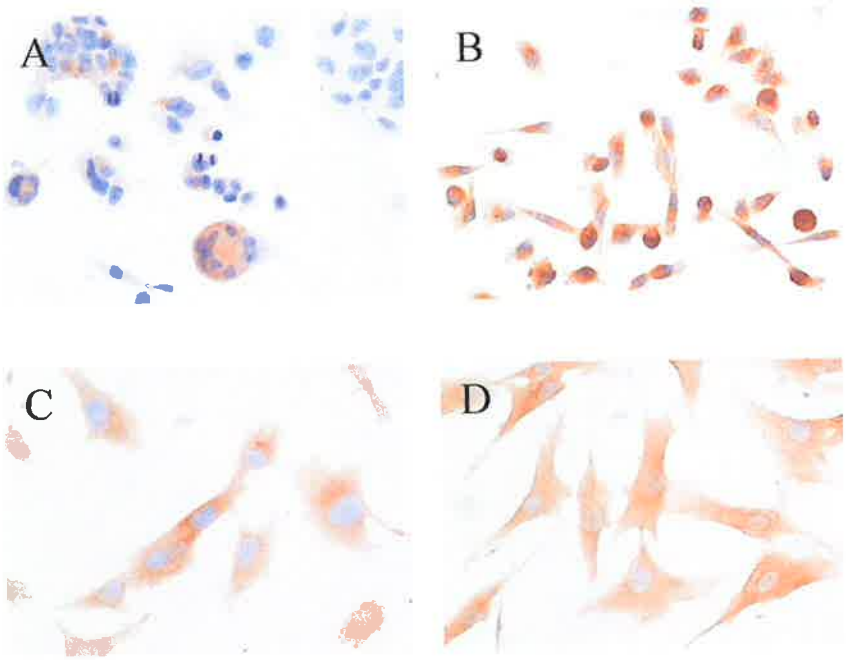

Figure 5.4. Expression of HA in breast cancer cell lines and mammary fibroblasts derived from breast cancer tissue. (A) Less than 10% of MCF-7 cells demonstrated positive staining for HA . Greater than 80% of MDA-MB-231cells (B), Hs578T cells (C), and mammary fibroblasts (D) were stained for HA . Magnification: x 200.

positive staining for HA (more than 80% positive cells) (Figure 5.4B-D), whereas MCF-7 showed weak HA staining (less than 10% positive cells) (Figure 5.4A). Specificity of staining for HA was controlled for by hyaluronidase digestion (not shown). Expression of CD44 was present in all of the breast cancer cell lines and the mammary fibroblasts (Figure 5.5). CD44 immunostaining was localized to the cell membrane. Stronger expression of CD44 was observed in MDA-MB-231 (Figure 5.5B), Hs578T (Figure 5.5C), and mammary fibroblasts (Figure 5.5D) than in MCF-7 (Figure 5.5A). The expression of HA and CD44 in these breast cancer cell lines and mammary fibroblasts is summarized in Table 5.1.

5.3.5 Pericellular matrix formation by breast cancer cell lines

MCF-7 cells (Figure 5.6A) and MDA-MB-231 cells (Figure 5.6B) did not assemble a pericellular sheath in control medium, whereas Hs578T cells were able to assemble sheaths (Figure 5.6C). After incubation with fibroblast CM, sheath was formed by MDA-MB-231 cells (Figure 5.6 E), but not by MCF-7 cells (Figure 5.6D). MDA-MB-231 cells demonstrated the sheath in about 10% of the cell population (coat: cell ratio 2.97 ± 0.88). Furthermore, addition of exogenous HA (15 μg/ml) and purified versican (fraction 7+8) from mammary fibroblast CM (17 μ g/ml) increased assembly of sheath by MDA-MB-231 cells in up to 37% of the cells (coat: cell ratio 3.04 ± 0.87). Hs578T cells showed an increase in sheath formation from 10% of the cell population (coat: cell ratio 2.80 ±1.00) in control medium to 25% of the cells (coat: cell ratio 2.82 ± 1.05) in the presence of fibroblast CM (Figure 5.6F). Pericellular sheaths were detected around mammary fibroblasts in about 80% of cells (coat: cell ratio 4.58 ± 1.15). The sheath assembled by MDA-MB-231, Hs578T, and mammary fibroblasts was degraded by treatment with *Streptomyces* hyaluronidase (5 unit/ml) at 37°C for 30 min as shown in Figure 5.7A-F. The

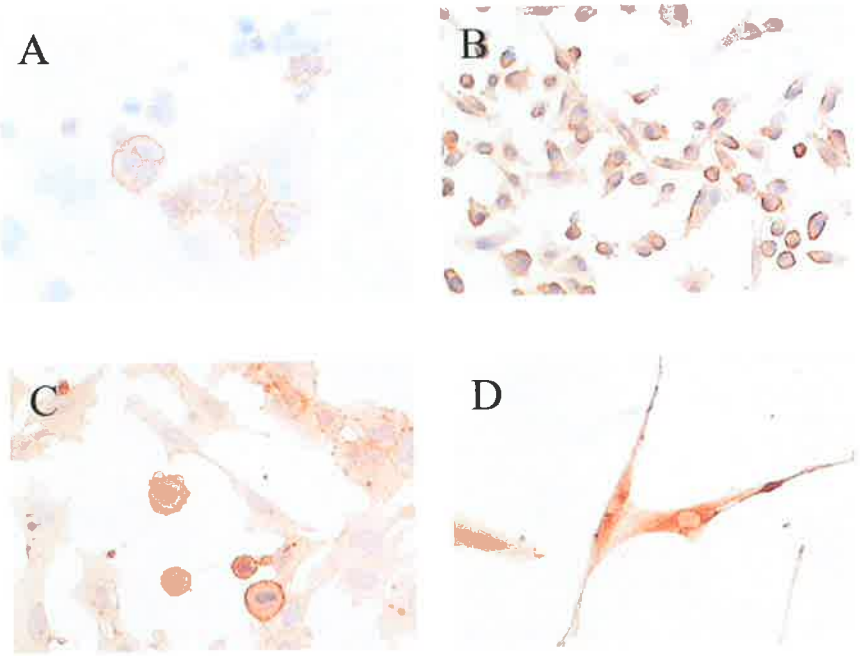

Figure 5.5. CD44 expression in breast cancer cell lines and mammary fibroblasts derived from breast cancer tissue. Immunoreactivity of CD44s was detected in cellular cytoplasm and membrane: (A) weak staining was observed for MCF-7, strong staining was observed for MDA-MB-231 (B), Hs578T (C), and mammary fibroblasts (D). Magnification: x 200.

Figure 5.6. Assembly of pericellular sheath by breast cancer cell lines. No sheath was assembled in control medium by MCF-7 (A) or MDA-MB-231 cells (B), but assembly of sheath was observed in Hs578T cells (C). Following 24 h treatment with FB-CM, no sheath was formed by MCF-7 (D), whereas MDA-MB-231 (E) and Hs578T (F) cells exhibited a distinct sheath, which appeared as a clear zone surrounding the cells. Magnification: x200

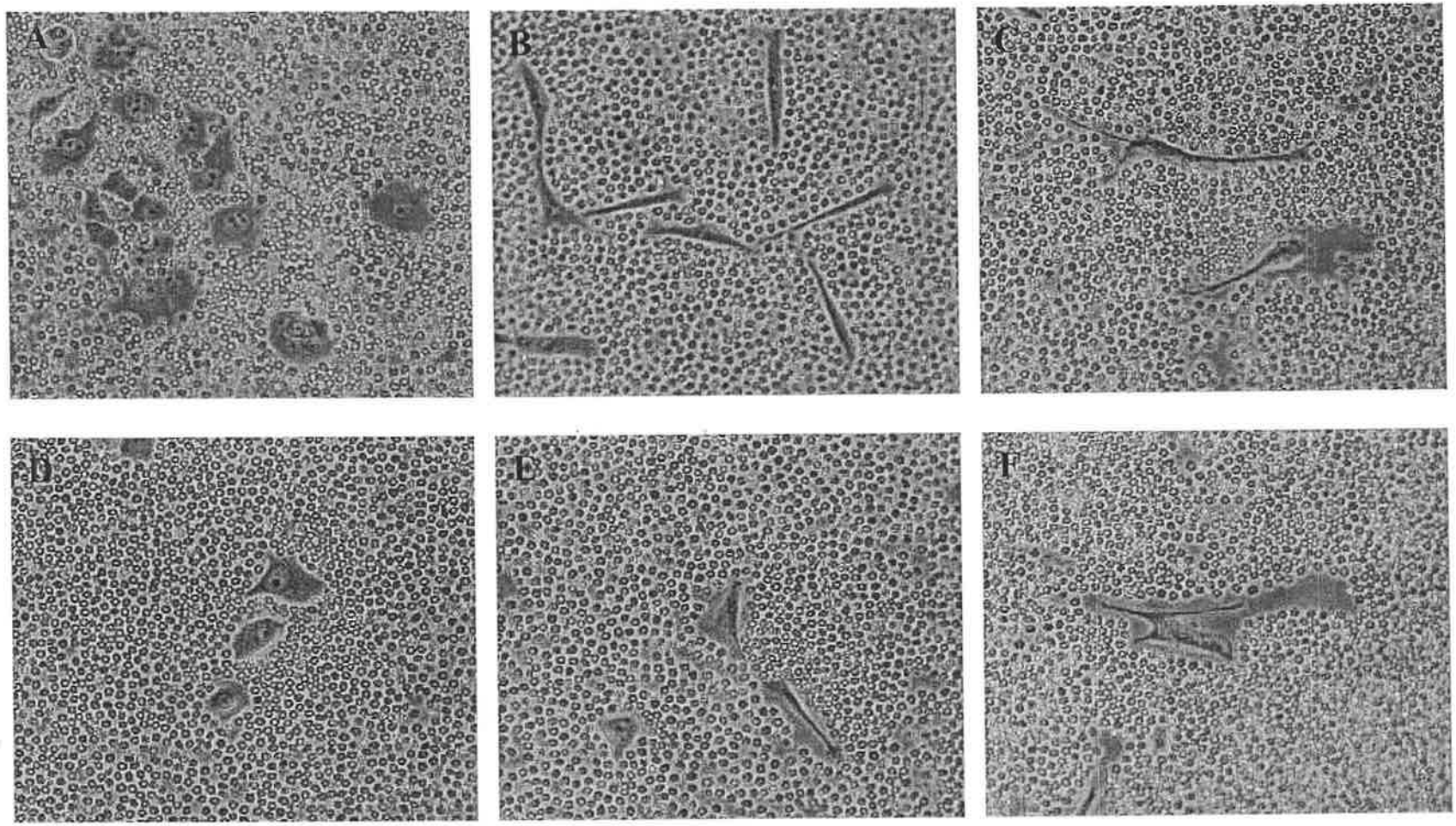
A
B
C
D
E
F

Figure 5.7. Dependence on HA for pericellular sheath formation by breast cancer cells and mammary fibroblasts. Sheath was detected in MDA-MB-231 (A), Hs578T (B), and mammary fibroblasts derived from breast cancer tissue (C). These sheaths were degraded following treatment with *Streptomyces* Hyaluronidase (5 unit/ml) for 30 min at 37°C (D,E,F). Magnification x 200.

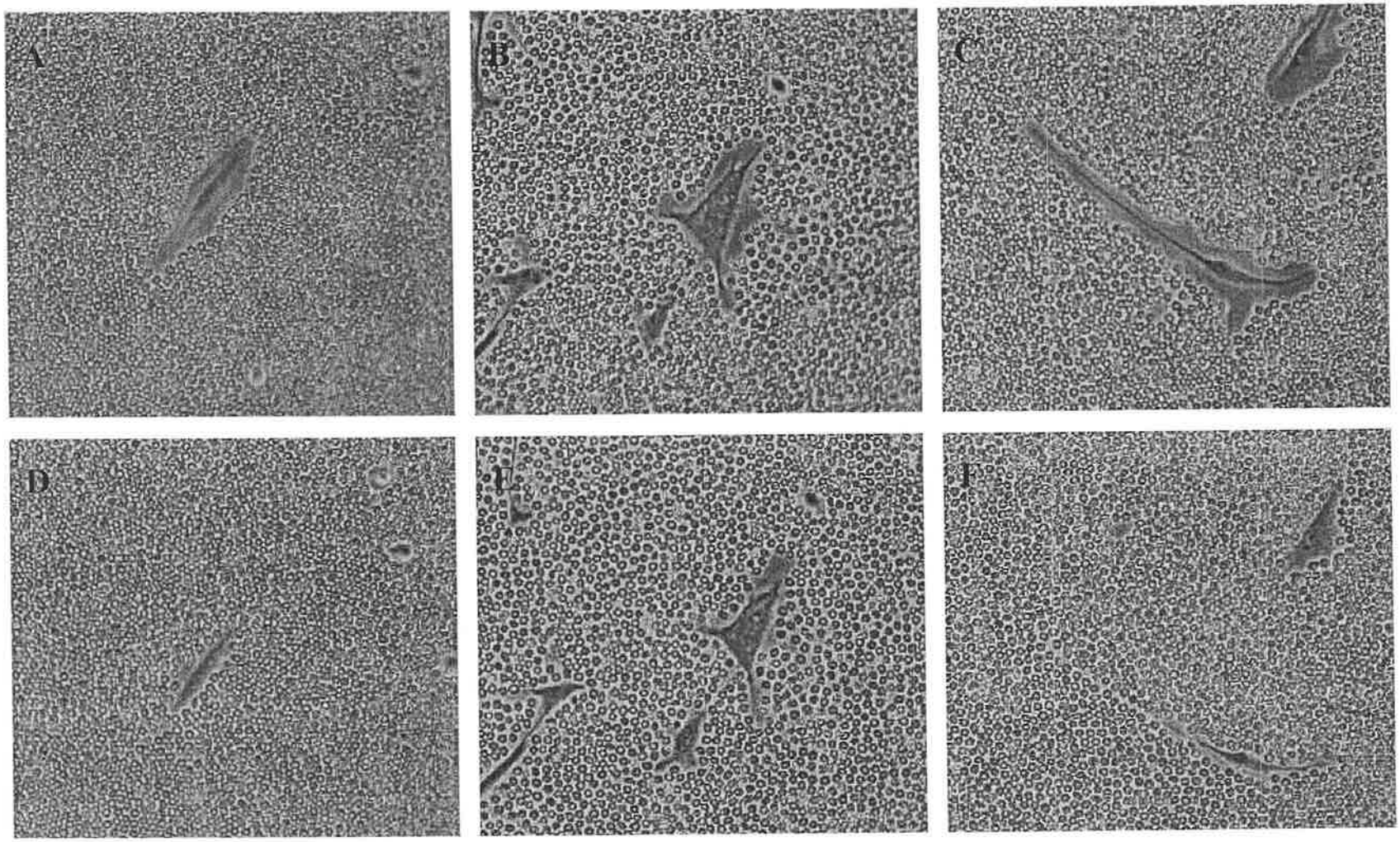
A
B
C
D
E
F

Table 5.1. Expression of CD44s and HA in breast cancer cell lines and mammary fibroblasts derived from breast cancer tissue.

Cell lines	CD44s intensity (percent of cells)	HA intensity (percent of cells)
MCF-7	weak (15-20%)	weak (10-15%)
MDA-MB-231	strong (80-90%)	strong (90-95%)
Hs578T	strong (75-80%)	strong (80-90%)
Mammary fibroblasts	strong (80-90%)	strong (90-95%)

Table 5.2. Morphometric analysis of pericellular matrices for breast cancer cell lines and mammary fibroblasts derived from breast cancer tissue.

Cell line	RPMI+ITS % cells (mean coat:cell ratio ±SD)	FB-CM % cells (mean coat:cell ratio ±SD)	HA+versican fractions 7+8 * % cells (mean coat:cell ratio ±SD)
MCF-7	ND	0	ND
MDA-MB-231	ND	10% (2.97 ± 0.88)	37% (3.04 ± 0.87)
Hs578T	10% (2.80 ± 1.00)	25% (2.82 ± 1.05)	ND
Mammary fibroblast	80% (4.58 ± 1.15)	ND	ND

* HA 15 µg/ml, purified versican (fractions 7+8, 17 µg/ml) from section 4.2.4.
ND = Not done

sizes of pericellular sheaths formed by each of the breast cancer cells and mammary fibroblasts are summarized in Table 5.2.

5.4 Discussion

This chapter determined that the necessary prerequisites for assembly of a pericellular sheath by mammary fibroblasts and breast cancer cells are the cellular expression of the CD44 HA receptor, HA, and the matrix hyaladherin versican. Mammary fibroblasts express high levels of CD44 and all three HA synthases (HAS 1, 2, 3). Accordingly, these cells bear high levels of HA on their outer membrane and secrete large amounts into the culture medium, along with versican. Conditioned medium from mammary fibroblasts provides a rich source of HA and versican, and as outlined in chapter 4, versican can be purified from fibroblast CM by conventional anion exchange and gel filtration chromatography.

The breast cancer cell lines examined in this chapter (MCF-7, MDA-MB-231, Hs578T) express CD44 and HAS synthase enzymes, but demonstrate differing abilities to assemble pericellular matrices. MCF-7 and MDA-MB-231 when cultured in normal medium secrete only small amounts of HA and do not display a sheath, whereas Hs578T cells secrete larger amounts of HA and do form a sheath. The major distinction between Hs578T and MCF-7 or MDA-MB-231 cells is the ability of the former cancer line to secrete versican. As adenocarcinoma cells in general do not secrete versican, the Hs578T line may have undergone an epithelial-mesenchymal transition (Lippman et al., 1988). Thus the only cell types in this study capable of assembling a sheath when cultured in normal medium (ie mammary fibroblasts, Hs578T cells) synthesize HA, its receptor (CD44), and an HA cross linking molecule (versican).

Under conditions when CM from mammary fibroblasts containing HA and versican is added to cell cultures of MCF-7 and MDA-MB-231, 10% of the cells of the latter cell line assemble a pericellular sheath. This proportion increases to 37% when HA and purified

versican are added to the MDA-MB-231 cell culture. This illustrates the dependence of sheath on the presence of versican, because all the cell lines secreted small amounts of HA into the culture medium. Furthermore, MDA-MB-231 cells retain large amounts of HA on the cell membrane, as indicated by the discrepancy between ELISA measurements on culture medium and immunocytochemical staining for these cells. Nonetheless, HA is also a necessary component as the sheath is rapidly dissolved by treatment with *Streptomyces* hyaluronase. Whether CD44 acts as the sole HA receptor for mammary fibroblasts and breast cancer cells, or whether HA synthase enzymes are responsible in whole or part for the linking of HA complexes to the cell membrane was not investigated in this study. However, the presence of sheath in this chapter was consistent with the cellular expression of both CD44 and the HA synthases.

With regard to MCF-7 cells, a previous report demonstrated that this cell line displayed strong immunostaining for CD44 , and when co-cultured with a rat fibrosarcoma cell line known to produce HA exhibited a pericellular sheath (Knudson, 1998). In this chapter MCF-7 cells were unable to assemble the sheath when incubated with fibroblast CM. There are several possibilities to account for this difference. It is possible that MCF-7 cells cultured in serum-free medium exhibited low level expression of CD44 that was insufficient to form pericellular sheath.

The data presented in this chapter is consistent with the requirements for formation of an HA- and versican-rich sheath by smooth muscle cells (Evanko et al., 1999). Expression of HA synthase enzymes is necessary for pericellular sheath as transfection of HAS1 into mutant mouse mammary carcinoma cells defective in HAS activity rescued HA production and permitted formation of pericellular matrix (Itano et al., 1999b). Up-regulation of HAS2 and consequent HA synthesis by PDGF in arterial smooth muscle cells also permitted

formation of pericellular matrix (Evanko et al., 2001). In addition, expression of HAS2 and HAS3 in metastatic prostate tumor cells correlated with the presence of pericellular matrix (Simpson et al., 2001). The necessity of CD44 HA receptor for retention of the matrix at the cell surface was demonstrated using CD44 blocking antibodies, which prevented the assembly of pericellular sheath by chondrocytes (Knudson et al., 1996). More recently, transfection of CD44H (haematopoietic isoform) into CD44-negative COS cells permitted sheath assembly in the presence of exogenous HA and proteoglycan, but COS cells transfected with a truncated mutant of CD44H, which lacked the cytoplasmic domain lacked sheath assembly (Jiang et al., 2002). Cross-linking of HA by hyaladherins eg. versican, aggrecan, and link protein is also necessary to maintain HA sheaths (Knudson and Knudson, 1993).

Pericellular sheaths are a prerequisite for proliferation and migration of vascular smooth muscle cells (Evanko et al., 1999). HA, by its property of hydrating and increasing osmotic pressure creates a loose matrix, which provides a favorable environment for mitotic cell rounding and cell movement. Immunocytochemical studies have shown that versican, HA, and CD44 were localized over the cell surface of cultured fibroblasts, but were specifically excluded from focal adhesion contacts with the substratum (Yamagata et al., 1993). The localization of these molecules away from points of contact of the cell with its micrenvironment suggests that they constitute a functional unit to destabilize cell adhesion.

In summary, elevated expression of versican, HA and CD44 have been correlated with disease progression in breast cancer, and all are necessary for the formation of pericellular matrix. The association of pericellular matrix with cellular movement suggests that this structure is important for breast cancer invasion and metastasis, and further study is required to determine the mechanism by which the sheath mediates cancer cell metastasis.

Chapter 6

General Discussion and Conclusion

The properties of the large proteoglycan versican are directly attributable to its structural composition. By virtue of its negatively charged chondroitin sulfate side chains, versican is a recognized modulator of cell-matrix attachment and motility for various mesenchymal cell types (viz fibroblasts, smooth muscle cells, nerve cells) and their malignant derivatives, eg astrocytoma. The core protein has a domain structure, the absence of one or other or both GAG-attachment domains leading to its characteristic 4 isoforms. Matrix aggregation is the principal function of the N-terminal HA-binding domain, permitting the assembly of pericellular sheaths around fibroblasts and smooth muscle cells. Versican has been shown to be a candidate prognostic marker for astrocytoma. Recent studies from this laboratory have indicated that although versican is a product of stromal cells, elevated expression of versican within peritumoral prostatic stroma predicted disease progression for men treated with surgery for early stage, organ-confined, prostate cancer (Ricciardelli et al., 1998).

At the conception of this research project, little was known about versican expression in breast cancer tissues, other than its presence at the invasive edge of breast cancers (Nara et al., 1997). However, the fact that versican was a candidate prognostic marker for prostate cancer suggested that elevated expression of versican in peritumoral stroma may also be prognostic for other types of adenocarcinoma, such as breast cancer. This thesis presents novel observations regarding the expression, regulation and function of versican in breast cancer.

The strongest predictor of relapse for women with breast cancer is the presence of cancer-involved lymph nodes. A diagnosis of node-negative primary breast cancer segregates patients into a category of low risk of relapse and death, but uncertainty of outcome remains. Although surgery is curative for the majority of women in this category, approximately 30% of patients will relapse with progressive disease. Currently, there is no reliable means to predict those patients who are likely to relapse, and would potentially benefit from more aggressive treatment at diagnosis. Based on the recent success of elevated versican in peritumoral stroma of the prostate in predicting relapse in men treated by surgery for early stage, organ-confined prostate cancer, Chapter 2 presented the first study to investigate whether versican might predict relapse in women treated with surgery for node-negative breast cancer. Moreover, because versican colocates in breast tissue with hyaluronan (HA) and TN-C, both of which have been implicated previously as predictors of outcome for women with breast cancer, the relative predictive power of these three matrix components for node-negative disease was investigated. The use of video image measurement of immunohistochemical staining for versican and tenascin, and histochemical staining for HA, analyzed by Cox regression and Kaplan-Meier life table plots provided a robust analysis of the relative predictive power. The results indicated that whereas tumor size was predictive of both relapse and overall survival in this cohort, versican was predictive of relapse only, TN-C was predictive of overall survival only, and HA was predictive of neither. Tumor grade, stage and steroid receptor status were also not predictive in this investigative cohort. These results were interpreted to suggest that whereas tumor burden (ie size) was directly related to relapse and death of the patient, the expression of versican played a paramount role only in disease relapse, ie local invasion and distant dissemination of cancer cells. Later chapters of this thesis throw light on why versican might be associated with breast cancer cell dissemination, but the reason why

versican is not related to patient death remains elusive. Interestingly, HA was not predictive for node-negative breast cancer in this cohort, nor in the node-negative sub-set of a cohort of breast cancer patients in which tumor expression of HA was predictive of disease progression (R Tammi, personal communication). The lack of predictive power for other breast cancer features might be due to the small size of this investigative cohort.

The elevated expression of versican in peritumoral stromal tissue in cancers which progress, suggests that the more aggressive tumors have the ability to modulate versican secretion by stromal fibroblasts. The second aim of this thesis was to determine whether soluble cancer cell mediators might regulate versican secretion in breast cancer. Chapter 3 investigated this premise by culturing mammary fibroblasts, derived from malignant and non-malignant breast tissue, in conditioned medium (CM) from several breast cancer cell lines. This study confirmed that versican was a product of mammary fibroblasts and not breast cancer cells. The largest two isoforms of versican, V0 and V1 were secreted by mammary fibroblasts, as determined by both RT-PCR and immunoblotting. This study is the first to indicate that soluble cancer cell mediators, capable of modulating versican secretion by mammary fibroblasts, are present in cancer cell conditioned medium. The use of recombinant growth factors and their respective specific neutralizing antibodies were used to identify PDGF and TGFβ1 as candidate mediators in cancer cell conditioned medium. Neutralising antibody to bFGF also inhibited increased production of versican by mammary fibroblasts cultured in cancer cell CM. Because of existing reports which indicate that the MCF-7, MDA-MB231 and ZR75-1 cell lines synthesize little or no bFGF, it is likely that the bFGF activity was endogenous to the mammary fibroblast population, ie the bFGF was an autocrine growth factor.

Versican acts as an anti-adhesive molecule for stromal cell (eg smooth muscle cells, astrocytoma, and melanoma cells) and for prostate cancer cell attachment to components of ECM. The aim of Chapter 4 was to investigate whether versican purified from the culture medium of mammary fibroblasts was able to modulate the attachment of breast cancer cells to the ECM components, fibronectin and laminin, using a standard cell attachment assay. The results indicated that versican V0 and V1 isoforms selectively inhibited attachment of breast cancer cells to fibronectin- but not laminin-coated substrates. This result is in agreement with previous reports that versican derived from fibroblasts bound directly to fibronectin, but not collagen type IV and laminin which are major components of basement membrane. This suggests that versican in stromal ECM surrounding breast cancer cells reduces cancer cell attachment, hence facilitating cell migration through the interstitial stroma rather than the glandular basement membrane. Our data also support that the anti-adhesive effect of versican is mediated in an RGD dependent manner. Both protein core and the presence of the CS side chains are required for the inhibitory activity of versican, because chondroitinase ABC digestion reduces but does not abolish this effect.

The evidence presented above on modulation of cell attachment by versican, together with similar published reports suggested that versican may effect the migration of breast cancer cells through interstitial matrix. The *in vitro* Boyden Chamber assay was modified to incorporate filters coated with fibronectin and collagen type I for studying cancer cell migration and invasion. The results presented in Chapter 4 confirmed that versican-containing fibroblast CM, when incorporated within the fibronectin-collagen type I coating of the filters, was able to promote breast cancer cell motility. However, the use of thick matrix coatings containing versican lead to decreased invasive capacity of the breast cancer cells. It was considered likely that the concentration of matrix binding sites within the

coating might have overwhelmed the inhibitory capacity of the versican-containing CM preparation.

Recent literature reports indicate that the motility of smooth muscle cells *in vitro* depends on the presence of a pericellular sheath of matrix consisting of HA cross-linked by an aggregating proteoglycan, viz versican or aggrecan. Chapter 5 investigates whether this is also true for breast cancer cells as unlike stromal cells, such as fibroblasts and smooth muscle cells, breast cancer cells synthesize minimal HA and no versican. Using a particle exclusion assay, this study indicated that mammary fibroblasts assembled a pericellular sheath from endogenously synthesized components comprising at least of HA receptor (CD44), HA, and matrix hyaladherin versican. Breast cancer cell lines although expressing CD44 do not assemble a pericellular sheath of matrix, but are capable of doing so if they are supplied with HA and versican from mammary fibroblasts. This result was supported from observations of pericellular sheath assembly by the breast cancer cell line Hs578T which is believed to have undergone epithelial-mesenchymal transition. Hs578T cells synthesize HA, CD44 and versican. The studies presented in Chapter 5 are consistent with previous reports that cells which express HA receptors eg human urinary bladder carcinoma, mouse melanoma and prostate cancer cell lines were able to form a pericellular sheath when incubated with HA and aggregating cartilage proteoglycan (aggrecan). This was also true for prostate cancer cell lines incubated in versican from prostate fibroblast culture medium (Ricciardelli, personal communication). Because expression of versican, HA, and CD44 have been associated with disease progression in breast cancer, the ability of breast cancer cells to integrate these components into a pericellular sheath suggests that the sheath may be important for breast invasion and metastasis.

In summary, this thesis presents new knowledge regarding the regulation and biological activity of versican, a candidate prognostic marker for node-negative breast cancer. This

study demonstrated for the first time that breast cancer cells can (i) induce mammary fibroblasts to up-regulate synthesis of versican, (ii) utilize versican to modulate cancer cell attachment to fibronectin, (iii) utilize HA and versican in the local microenvironment to assemble a pericellular sheath of matrix, (iv) utilize these materials to increase the rate of migration through a fibronectin-coated filter. As a consequence, we conclude that breast cancer cells are able to modulate expression of ECM components such as versican within their tumor microenviroment to facilitate an increased rate of cancer cell migration and hence potentially local invasion and metastasis.

References

Abetamann, V., Kern, H.F. and Elsasser, H.P., Differential expression of the hyaluronan receptors CD44 and RHAMM in human pancreatic cancer cells. *Clin Cancer Res*, **2,** 1607-18. (1996).

Adams, M., Jones, J.L., Walker, R.A., Pringle, J.H. and Bell, S.C., Changes in tenascin-C isoform expression in invasive and preinvasive breast disease. *Cancer Res*, **62,** 3289-97. (2002).

Albini, A., Iwamoto, Y., Kleinman, H.K., Martin, G.R., Aaronson, S.A., Kozlowski, J.M. and McEwan, R.N., A rapid in vitro assay for quantitating the invasive potential of tumor cells. *Cancer Res*, **47,** 3239-45. (1987).

Alini, M. and Losa, G.A., Partial characterization of proteoglycans isolated from neoplastic and nonneoplastic human breast tissues. *Cancer Res*, **51,** 1443-7. (1991).

Allred, D.C., Clark, G.M., Elledge, R., Fuqua, S.A., Brown, R.W., Chamness, G.C., Osborne, C.K. and McGuire, W.L., Association of p53 protein expression with tumor cell proliferation rate and clinical outcome in node-negative breast cancer. *J Natl Cancer Inst*, **85,** 200-6. (1993).

Andersen, T.I., Holm, R., Nesland, J.M., Heimdal, K.R., Ottestad, L. and Borresen, A.L., Prognostic significance of TP53 alterations in breast carcinoma. *Br J Cancer*, **68,** 540-8. (1993).

Andrulis, I.L., Bull, S.B., Blackstein, M.E., Sutherland, D., Mak, C., Sidlofsky, S., Pritzker, K.P., Hartwick, R.W., Hanna, W., Lickley, L., Wilkinson, R., Qizilbash, A., Ambus, U., Lipa, M., Weizel, H., Katz, A., Baida, M., Mariz, S., Stoik, G., Dacamara, P., Strongitharm, D., Geddie, W. and McCready, D., neu/erbB-2 amplification identifies a poor-prognosis group of women with node-negative breast cancer. Toronto Breast Cancer Study Group. *J Clin Oncol*, **16,** 1340-9. (1998).

Ang, L.C., Zhang, Y., Cao, L., Yang, B.L., Young, B., Kiani, C., Lee, V., Allan, K. and Yang, B.B., Versican enhances locomotion of astrocytoma cells and reduces cell adhesion through its G1 domain. *J Neuropathol Exp Neurol*, **58,** 597-605. (1999).

Ariad, S., Seymour, L. and Bezwoda, W.R., Platelet-derived growth factor (PDGF) in plasma of breast cancer patients: correlation with stage and rate of progression. *Breast Cancer Res Treat*, **20,** 11-7. (1991).

Asher, R.A., Morgenstern, D.A., Shearer, M.C., Adcock, K.H., Pesheva, P. and Fawcett, J.W., Versican is upregulated in CNS injury and is a product of oligodendrocyte lineage cells. *J Neurosci*, **22,** 2225-36. (2002).

Aspberg, A., Adam, S., Kostka, G., Timpl, R. and Heinegard, D., Fibulin-1 is a ligand for the C-type lectin domains of aggrecan and versican. *J Biol Chem*, **274,** 20444-9. (1999).

Aspberg, A., Binkert, C. and Ruoslahti, E., The versican C-type lectin domain recognizes the adhesion protein tenascin-R. *Proc Natl Acad Sci U S A*, **92,** 10590-4. (1995).

Aspberg, A., Miura, R., Bourdoulous, S., Shimonaka, M., Heinegard, D., Schachner, M., Ruoslahti, E. and Yamaguchi, Y., The C-type lectin domains of lecticans, a family of aggregating chondroitin sulfate proteoglycans, bind tenascin-R by protein-protein interactions independent of carbohydrate moiety. *Proc Natl Acad Sci U S A*, **94,** 10116-21. (1997).

Assmann, V., Marshall, J.F., Fieber, C., Hofmann, M. and Hart, I.R., The human hyaluronan receptor RHAMM is expressed as an intracellular protein in breast cancer cells. *J Cell Sci*, **111,** 1685-94. (1998).

Auvinen, P., Tammi, R., Parkkinen, J., Tammi, M., Agren, U., Johansson, R., Hirvikoski, P., Eskelinen, M. and Kosma, V.M., Hyaluronan in peritumoral stroma and malignant cells associates with breast cancer spreading and predicts survival. *Am J Pathol*, **156,** 529-36. (2000).

Balslev, I., Christensen, I.J., Rasmussen, B.B., Larsen, J.K., Lykkesfeldt, A.E., Thorpe, S.M., Rose, C., Briand, P. and Mouridsen, H.T., Flow cytometric DNA ploidy defines patients with poor prognosis in node-negative breast cancer. *Int J Cancer*, **56,** 16-25. (1994).

Bandtlow, C.E. and Zimmermann, D.R., Proteoglycans in the developing brain: new conceptual insights for old proteins. *Physiol Rev*, **80,** 1267-90. (2000).

Bankfalvi, A., Terpe, H.J., Breukelmann, D., Bier, B., Rempe, D., Pschadka, G., Krech, R. and Bocker, W., Gains and losses of CD44 expression during breast carcinogenesis and tumour progression. *Histopathology*, **33,** 107-16. (1998).

Bartsch, J.E., Staren, E.D. and Appert, H.E., Adhesion and migration of extracellular matrix-stimulated breast cancer. *J Surg Res*, **110,** 287-94. (2003).

Bergh, J., Norberg, T., Sjogren, S., Lindgren, A. and Holmberg, L., Complete sequencing of the p53 gene provides prognostic information in breast cancer patients, particularly in relation to adjuvant systemic therapy and radiotherapy. *Nat Med*, **1,** 1029-34. (1995).

Bertrand, P., Girard, N., Delpech, B., Duval, C., d'Anjou, J. and Dauce, J.P., Hyaluronan (hyaluronic acid) and hyaluronectin in the extracellular matrix of human breast carcinomas: comparison between invasive and non- invasive areas. *Int J Cancer*, **52,** 1-6. (1992).

Bland, K.I., Menck, H.R., Scott-Conner, C.E., Morrow, M., Winchester, D.J. and Winchester, D.P., The National Cancer Data Base 10-year survey of breast carcinoma treatment at hospitals in the United States. *Cancer*, **83,** 1262-73. (1998).

Blom, A., Pertoft, H. and Fries, E., Inter-alpha-inhibitor is required for the formation of the hyaluronan-containing coat on fibroblasts and mesothelial cells. *J Biol Chem*, **270,** 9698-701. (1995).

Bode-Lesniewska, B., Dours-Zimmermann, M.T., Odermatt, B.F., Briner, J., Heitz, P.U. and Zimmermann, D.R., Distribution of the large aggregating proteoglycan versican in adult human tissues. *J Histochem Cytochem*, **44,** 303-12. (1996).

Borsi, L., Carnemolla, B., Nicolo, G., Spina, B., Tanara, G. and Zardi, L., Expression of different tenascin isoforms in normal, hyperplastic and neoplastic human breast tissues. *Int J Cancer*, **52,** 688-92. (1992).

Bourguignon, L.Y., CD44-mediated oncogenic signaling and cytoskeleton activation during mammary tumor progression. *J Mammary Gland Biol Neoplasia*, **6,** 287-97. (2001).

Bourguignon, L.Y., Zhu, H., Chu, A., Iida, N., Zhang, L. and Hung, M.C., Interaction between the adhesion receptor, CD44, and the oncogene product, p185HER2, promotes human ovarian tumor cell activation. *J Biol Chem*, **272,** 27913-8. (1997).

Bourguignon, L.Y., Zhu, H., Shao, L. and Chen, Y.W., Ankyrin-Tiam1 interaction promotes Rac1 signaling and metastatic breast tumor cell invasion and migration. *J Cell Biol*, **150,** 177-91. (2000a).

Bourguignon, L.Y., Zhu, H., Shao, L. and Chen, Y.W., CD44 interaction with c-Src kinase promotes cortactin-mediated cytoskeleton function and hyaluronic acid-dependent ovarian tumor cell migration. *J Biol Chem*, **276,** 7327-36. (2001).

Bourguignon, L.Y., Zhu, H., Shao, L. and Chen, Y.W., CD44 interaction with tiam1 promotes Rac1 signaling and hyaluronic acid- mediated breast tumor cell migration. *J Biol Chem*, **275,** 1829-38. (2000b).

Bourguignon, L.Y.W., Zhu, D. and Zhu, H., CD44 isoform-cytoskeleton interaction in oncogenic signaling and tumor progression. *Front Biosci*, **3,** D637-49. (1998).

Bradbury, E.J., Moon, L.D., Popat, R.J., King, V.R., Bennett, G.S., Patel, P.N., Fawcett, J.W. and McMahon, S.B., Chondroitinase ABC promotes functional recovery after spinal cord injury. *Nature*, **416,** 636-40. (2002).

Braunewell, K.H., Pesheva, P., McCarthy, J.B., Furcht, L.T., Schmitz, B. and Schachner, M., Functional involvement of sciatic nerve-derived versican- and decorin-like molecules and other chondroitin sulphate proteoglycans in ECM-mediated cell adhesion and neurite outgrowth. *Eur J Neurosci*, **7,** 805-14. (1995).

Bronzert, D.A., Pantazis, P., Antoniades, H.N., Kasid, A., Davidson, N., Dickson, R.B. and Lippman, M.E., Synthesis and secretion of platelet-derived growth factor by human breast cancer cell lines. *Proc Natl Acad Sci U S A*, **84,** 5763-7. (1987).

Broome, M.A. and Hunter, T., Requirement for c-Src catalytic activity and the SH3 domain in platelet-derived growth factor BB and epidermal growth factor mitogenic signaling. *J Biol Chem*, **271,** 16798-806. (1996).

Brown, L.F., Guidi, A.J., Schnitt, S.J., Van De Water, L., Iruela-Arispe, M.L., Yeo, T.K., Tognazzi, K. and Dvorak, H.F., Vascular stroma formation in carcinoma in situ, invasive carcinoma, and metastatic carcinoma of the breast. *Clin Cancer Res*, **5,** 1041-56. (1999).

Brown, R.W., Allred, C.D., Clark, G.M., Osborne, C.K. and Hilsenbeck, S.G., Prognostic value of Ki-67 compared to S-phase fraction in axillary node-negative breast cancer. *Clin Cancer Res*, **2,** 585-92. (1996).

Bryant, J., Fisher, B., Gunduz, N., Costantino, J.P. and Emir, B., S-phase fraction combined with other patient and tumor characteristics for the prognosis of node-negative, estrogen-receptor-positive breast cancer. *Breast Cancer Res Treat*, **51,** 239-53. (1998).

Buell, P., Changing incidence of breast cancer in Japanese-American women. *J Natl Cancer Inst*, **51,** 1479-83. (1973).

Carter, C.L., Allen, C. and Henson, D.E., Relation of tumor size, lymph node status, and survival in 24,740 breast cancer cases. *Cancer*, **63,** 181-7. (1989).

Chiquet-Ehrismann, R., Tenascins, a growing family of extracellular matrix proteins. *Experientia*, **51,** 853-62. (1995).

Chiquet-Ehrismann, R., What distinguishes tenascin from fibronectin? *Faseb J*, **4,** 2598-604. (1990).

Chiquet-Ehrismann, R., Kalla, P. and Pearson, C.A., Participation of tenascin and transforming growth factor-beta in reciprocal epithelial-mesenchymal interactions of MCF7 cells and fibroblasts. *Cancer Res*, **49,** 4322-5. (1989).

Chiquet-Ehrismann, R., Kalla, P., Pearson, C.A., Beck, K. and Chiquet, M., Tenascin interferes with fibronectin action. *Cell*, **53,** 383-90. (1988).

Chiquet-Ehrismann, R., Mackie, E.J., Pearson, C.A. and Sakakura, T., Tenascin: an extracellular matrix protein involved in tissue interactions during fetal development and oncogenesis. *Cell*, **47,** 131-9. (1986).

Cichy, J., Bals, R., Potempa, J., Mani, A. and Pure, E., Proteinase-mediated release of epithelial cell-associated CD44. Extracellular CD44 complexes with components of cellular matrices. *J Biol Chem*, **277,** 44440-7. (2002).

Clark, G.M. and McGuire, W.L., Follow-up study of HER-2/neu amplification in primary breast cancer. *Cancer Res*, **51,** 944-8. (1991).

Clarris, B.J. and Fraser, J.R., On the pericellular zone of some mammalian cells in vitro. *Exp Cell Res*, **49,** 181-93. (1968).

Cobleigh, M.A., Vogel, C.L., Tripathy, D., Robert, N.J., Scholl, S., Fehrenbacher, L., Wolter, J.M., Paton, V., Shak, S., Lieberman, G. and Slamon, D.J., Multinational study of the efficacy and safety of humanized anti-HER2 monoclonal antibody in women who have HER2-overexpressing metastatic breast cancer that has progressed after chemotherapy for metastatic disease. *J Clin Oncol*, **17,** 2639-48. (1999).

Coussens, L., Yang-Feng, T.L., Liao, Y.C., Chen, E., Gray, A., McGrath, J., Seeburg, P.H., Libermann, T.A., Schlessinger, J., Francke, U. and et al., Tyrosine kinase receptor with extensive homology to EGF receptor shares chromosomal location with neu oncogene. *Science*, **230,** 1132-9. (1985).

Crossin, K.L., Tenascin: a multifunctional extracellular matrix protein with a restricted distribution in development and disease. *J Cell Biochem*, **61,** 592-8. (1996).

Cullen, K.J., Allison, A., Martire, I., Ellis, M. and Singer, C., Insulin-like growth factor expression in breast cancer epithelium and stroma. *Breast Cancer Res Treat*, **22,** 21-9. (1992).

Culty, M., Shizari, M., Thompson, E.W. and Underhill, C.B., Binding and degradation of hyaluronan by human breast cancer cell lines expressing different forms of CD44: correlation with invasive potential. *J Cell Physiol*, **160,** 275-86. (1994).

Current Protocols in Cell Biology. Chapter 9: Cell Adhesion. 2000. John Wiley & Sons, Inc. (Ref Type : Data File)

Dalal, B.I., Keown, P.A. and Greenberg, A.H., Immunocytochemical localization of secreted transforming growth factor-beta 1 to the advancing edges of primary tumors and to lymph node metastases of human mammary carcinoma. *Am J Pathol*, **143,** 381-9. (1993).

Davidoff, A.M., Kerns, B.J., Pence, J.C., Marks, J.R. and Iglehart, J.D., p53 alterations in all stages of breast cancer. *J Surg Oncol*, **48,** 260-7. (1991).

Dawson, P.J., Wolman, S.R., Tait, L., Heppner, G.H. and Miller, F.R., MCF10AT: a model for the evolution of cancer from proliferative breast disease. *Am J Pathol*, **148,** 313-9. (1996).

Day, A.J. and Prestwich, G.D., Hyaluronan-binding proteins: tying up the giant. *J Biol Chem*, **277,** 4585-8. (2002).

de Jong, J.S., van Diest, P.J., van der Valk, P. and Baak, J.P., Expression of growth factors, growth-inhibiting factors, and their receptors in invasive breast cancer. II: Correlations with proliferation and angiogenesis. *J Pathol*, **184,** 53-7. (1998).

Doerr, M.E. and Jones, J.I., The roles of integrins and extracellular matrix proteins in the insulin-like growth factor I-stimulated chemotaxis of human breast cancer cells. *J Biol Chem*, **271,** 2443-7. (1996).

Dupont, W.D., Parl, F.F., Hartmann, W.H., Brinton, L.A., Winfield, A.C., Worrell, J.A., Schuyler, P.A. and Plummer, W.D., Breast cancer risk associated with proliferative breast disease and atypical hyperplasia. *Cancer*, **71,** 1258-65. (1993).

Easton, D.F., Ford, D. and Bishop, D.T., Breast and ovarian cancer incidence in BRCA1-mutation carriers. Breast Cancer Linkage Consortium. *Am J Hum Genet*, **56,** 265-71. (1995).

Ehnis, T., Dieterich, W., Bauer, M., Lampe, B. and Schuppan, D., A chondroitin/dermatan sulfate form of CD44 is a receptor for collagen XIV (undulin). *Exp Cell Res*, **229,** 388-97. (1996).

Ellis, M.J., Singer, C., Hornby, A., Rasmussen, A. and Cullen, K.J., Insulin-like growth factor mediated stromal-epithelial interactions in human breast cancer. *Breast Cancer Res Treat*, **31,** 249-61. (1994).

Entwistle, J., Zhang, S., Yang, B., Wong, C., Li, Q., Hall, C.L., A, J., Mowat, M., Greenberg, A.H. and Turley, E.A., Characterization of the murine gene encoding the hyaluronan receptor RHAMM. *Gene*, **163,** 233-8. (1995).

Epidemiology of Cancer in South Australia, South Australia Cancer Registry. Department of Human Services vol 23, 2001.

Erickson, H.P. and Bourdon, M.A., Tenascin: an extracellular matrix protein prominent in specialized embryonic tissues and tumors. *Annu Rev Cell Biol*, **5,** 71-92. (1989).

Evanko, S.P., Angello, J.C. and Wight, T.N., Formation of hyaluronan- and versican-rich pericellular matrix is required for proliferation and migration of vascular smooth muscle cells. *Arterioscler Thromb Vasc Biol*, **19,** 1004-13. (1999).

Evanko, S.P., Johnson, P.Y., Braun, K.R., Underhill, C.B., Dudhia, J. and Wight, T.N., Platelet-derived growth factor stimulates the formation of versican- hyaluronan aggregates and pericellular matrix expansion in arterial smooth muscle cells. *Arch Biochem Biophys*, **394,** 29-38. (2001).

Evanko, S.P., Raines, E.W., Ross, R., Gold, L.I. and Wight, T.N., Proteoglycan distribution in lesions of atherosclerosis depends on lesion severity, structural characteristics, and the proximity of platelet-derived growth factor and transforming growth factor-beta. *Am J Pathol*, **152,** 533-46. (1998).

Faham, S., Hileman, R.E., Fromm, J.R., Linhardt, R.J. and Rees, D.C., Heparin structure and interactions with basic fibroblast growth factor. *Science*, **271,** 1116-20. (1996).

Falette, N., Paperin, M.P., Treilleux, I., Gratadour, A.C., Peloux, N., Mignotte, H., Tooke, N., Lofman, E., Inganas, M., Bremond, A., Ozturk, M. and Puisieux, A., Prognostic value of P53 gene mutations in a large series of node-negative breast cancer patients. *Cancer Res*, **58,** 1451-5. (1998).

Fieber, C., Plug, R., Sleeman, J., Dall, P., Ponta, H. and Hofmann, M., Characterisation of the murine gene encoding the intracellular hyaluronan receptor IHABP (RHAMM). *Gene*, **226,** 41-50. (1999).

Fisher, B., Redmond, C., Fisher, E.R. and Caplan, R., Relative worth of estrogen or progesterone receptor and pathologic characteristics of differentiation as indicators of prognosis in node negative breast cancer patients: findings from National Surgical Adjuvant Breast and Bowel Project Protocol B-06. *J Clin Oncol*, **6,** 1076-87. (1988).

Fisher, E.R., Anderson, S., Redmond, C. and Fisher, B., Pathologic findings from the National Surgical Adjuvant Breast Project protocol B-06. 10-year pathologic and clinical prognostic discriminants. *Cancer*, **71,** 2507-14. (1993).

Fitzgibbons, P.L., Page, D.L., Weaver, D., Thor, A.D., Allred, D.C., Clark, G.M., Ruby, S.G., O'Malley, F., Simpson, J.F., Connolly, J.L., Hayes, D.F., Edge, S.B., Lichter, A. and Schnitt, S.J., Prognostic factors in breast cancer. College of American Pathologists Consensus Statement 1999. *Arch Pathol Lab Med*, **124,** 966-78. (2000).

Fosang, A.J., Hey, N.J., Carney, S.L. and Hardingham, T.E., An ELISA plate-based assay for hyaluronan using biotinylated proteoglycan G1 domain (HA-binding region). *Matrix*, **10,** 306-13. (1990).

Fries, H., Elsasser, H.P., Mahlbacher, V., Neumann, K. and Kern, H.F., Localisation of hyaluronate (HA) in primary tumors and nude mouse xenografts of human pancreatic carcinomas using a biotinylated HA-binding protein. *Virchows Arch*, **424,** 7-12. (1994).

Gerdes, J., Lemke, H., Baisch, H., Wacker, H.H., Schwab, U. and Stein, H., Cell cycle analysis of a cell proliferation-associated human nuclear antigen defined by the monoclonal antibody Ki-67. *J Immunol*, **133,** 1710-5. (1984).

Glebov, O.K., McKenzie, K.E., White, C.A. and Sukumar, S., Frequent p53 gene mutations and novel alleles in familial breast cancer. *Cancer Res*, **54,** 3703-9. (1994).

Goepel, C., Buchmann, J., Schultka, R. and Koelbl, H., Tenascin-A marker for the malignant potential of preinvasive breast cancers. *Gynecol Oncol*, **79,** 372-8. (2000).

Goodison, S., Urquidi, V. and Tarin, D., CD44 cell adhesion molecules. *Mol Pathol*, **52,** 189-96. (1999).

Gorsch, S.M., Memoli, V.A., Stukel, T.A., Gold, L.I. and Arrick, B.A., Immunohistochemical staining for transforming growth factor beta 1 associates with disease progression in human breast cancer. *Cancer Res*, **52,** 6949-52. (1992).

Gotz, W., Osmers, R. and Herken, R., Localisation of extracellular matrix components in the embryonic human notochord and axial mesenchyme. *J Anat*, **186,** 111-21. (1995).

Gould, V.E., Koukoulis, G.K. and Virtanen, I., Extracellular matrix proteins and their receptors in the normal, hyperplastic and neoplastic breast. *Cell Differ Dev*, **32,** 409-16. (1990).

Grumet, M., Milev, P., Sakurai, T., Karthikeyan, L., Bourdon, M., Margolis, R.K. and Margolis, R.U., Interactions with tenascin and differential effects on cell adhesion of neurocan and phosphacan, two major chondroitin sulfate proteoglycans of nervous tissue. *J Biol Chem*, **269,** 12142-6. (1994).

Gui, G.P., Puddefoot, J.R., Vinson, G.P., Wells, C.A. and Carpenter, R., In vitro regulation of human breast cancer cell adhesion and invasion via integrin receptors to the extracellular matrix. *Br J Surg*, **82,** 1192-6. (1995).

Gulcher, J.R., Nies, D.E., Marton, L.S. and Stefansson, K., An alternatively spliced region of the human hexabrachion contains a repeat of potential N-glycosylation sites. *Proc Natl Acad Sci U S A*, **86,** 1588-92. (1989).

Gunthert, U., Hofmann, M., Rudy, W., Reber, S., Zoller, M., Haussmann, I., Matzku, S., Wenzel, A., Ponta, H. and Herrlich, P., A new variant of glycoprotein CD44 confers metastatic potential to rat carcinoma cells. *Cell*, **65,** 13-24. (1991).

Haase, H.R., Clarkson, R.W., Waters, M.J. and Bartold, P.M., Growth factor modulation of mitogenic responses and proteoglycan synthesis by human periodontal fibroblasts. *J Cell Physiol*, **174,** 353-61. (1998).

Hall, C.L., Wang, C., Lange, L.A. and Turley, E.A., Hyaluronan and the hyaluronan receptor RHAMM promote focal adhesion turnover and transient tyrosine kinase activity. *J Cell Biol*, **126,** 575-88. (1994).

Hall, C.L., Yang, B., Yang, X., Zhang, S., Turley, M., Samuel, S., Lange, L.A., Wang, C., Curpen, G.D., Savani, R.C. and et al., Overexpression of the hyaluronan receptor RHAMM is transforming and is also required for H-ras transformation. *Cell*, **82,** 19-26. (1995).

Hall, J.M., Lee, M.K., Newman, B., Morrow, J.E., Anderson, L.A., Huey, B. and King, M.C., Linkage of early-onset familial breast cancer to chromosome 17q21. *Science*, **250,** 1684-9. (1990).

Hardingham, T.E. and Fosang, A.J., Proteoglycans: many forms and many functions. *Faseb J*, **6,** 861-70. (1992).

Hardwick, C., Hoare, K., Owens, R., Hohn, H.P., Hook, M., Moore, D., Cripps, V., Austen, L., Nance, D.M. and Turley, E.A., Molecular cloning of a novel hyaluronan receptor that mediates tumor cell motility. *J Cell Biol*, **117,** 1343-50. (1992).

Harris, J.R., Lippman, M.E., Veronesi, U. and Willett, W., Breast cancer (3). *N Engl J Med*, **327,** 473-80. (1992).

Hawkins, D.S., Demers, G.W. and Galloway, D.A., Inactivation of p53 enhances sensitivity to multiple chemotherapeutic agents. *Cancer Res*, **56,** 892-8. (1996).

Hayen, W., Goebeler, M., Kumar, S., Riessen, R. and Nehls, V., Hyaluronan stimulates tumor cell migration by modulating the fibrin fiber architecture. *J Cell Sci*, **112,** 2241-51. (1999).

Heldin, P. and Pertoft, H., Synthesis and assembly of the hyaluronan-containing coats around normal human mesothelial cells. *Exp Cell Res*, **208,** 422-9. (1993).

Henderson, D.J., Ybot-Gonzalez, P. and Copp, A.J., Over-expression of the chondroitin sulphate proteoglycan versican is associated with defective neural crest migration in the Pax3 mutant mouse (splotch). *Mech Dev*, **69,** 39-51. (1997).

Herrera-Gayol, A. and Jothy, S., CD44 modulates Hs578T human breast cancer cell adhesion, migration, and invasiveness. *Exp Mol Pathol*, **66,** 99-108. (1999).

Heylen, N., Baurain, R., Remacle, C. and Trouet, A., Effect of MRC-5 fibroblast conditioned medium on breast cancer cell motility and invasion in vitro. *Clin Exp Metastasis*, **16,** 193-203. (1998).

Hindermann, W., Berndt, A., Borsi, L., Luo, X., Hyckel, P., Katenkamp, D. and Kosmehl, H., Synthesis and protein distribution of the unspliced large tenascin-C isoform in oral squamous cell carcinoma. *J Pathol*, **189,** 475-80. (1999).

Hofmann, M., Assmann, V., Fieber, C., Sleeman, J.P., Moll, J., Ponta, H., Hart, I.R. and Herrlich, P., Problems with RHAMM: a new link between surface adhesion and oncogenesis? *Cell*, **95,** 591-2; author reply 592-3. (1998a).

Hofmann, M., Fieber, C., Assmann, V., Gottlicher, M., Sleeman, J., Plug, R., Howells, N., von Stein, O., Ponta, H. and Herrlich, P., Identification of IHABP, a 95 kDa intracellular hyaluronate binding protein. *J Cell Sci*, **111,** 1673-84. (1998b).

Horsfall, D.J., Tilley, W.D., Orell, S.R., Marshall, V.R. and Cant, E.L., Relationship between ploidy and steroid hormone receptors in primary invasive breast cancer. *Br J Cancer*, **53,** 23-8. (1986).

Howeedy, A.A., Virtanen, I., Laitinen, L., Gould, N.S., Koukoulis, G.K. and Gould, V.E., Differential distribution of tenascin in the normal, hyperplastic, and neoplastic breast. *Lab Invest*, **63,** 798-806. (1990).

Huff, K.K., Kaufman, D., Gabbay, K.H., Spencer, E.M., Lippman, M.E. and Dickson, R.B., Secretion of an insulin-like growth factor-I-related protein by human breast cancer cells. *Cancer Res*, **46,** 4613-9. (1986).

Iida, N. and Bourguignon, L.Y., Coexpression of CD44 variant (v10/ex14) and CD44S in human mammary epithelial cells promotes tumorigenesis. *J Cell Physiol*, **171,** 152-60. (1997).

Ikeda, K., Yashiro, M., Sawada, T., Hato, F., Hasuma, T., Ishikawa, T. and Hirakawa, Y.K., M(R) 77 KDA factor derived from fibroblasts stimulates the invasion ability of breast-cancer cells. *Int J Cancer*, **92,** 181-6. (2001).

Ioachim, E., Charchanti, A., Briasoulis, E., Karavasilis, V., Tsanou, H., Arvanitis, D.L., Agnantis, N.J. and Pavlidis, N., Immunohistochemical expression of extracellular matrix components tenascin, fibronectin, collagen type IV and laminin in breast cancer: their prognostic value and role in tumour invasion and progression. *Eur J Cancer*, **38,** 2362-70. (2002).

Iozzo, R.V., Matrix proteoglycans: from molecular design to cellular function. *Annu Rev Biochem*, **67,** 609-52. (1998).

Iozzo, R.V., Naso, M.F., Cannizzaro, L.A., Wasmuth, J.J. and McPherson, J.D., Mapping of the versican proteoglycan gene (CSPG2) to the long arm of human chromosome 5 (5q12-5q14). *Genomics*, **14,** 845-51. (1992).

Ishihara, A., Yoshida, T., Tamaki, H. and Sakakura, T., Tenascin expression in cancer cells and stroma of human breast cancer and its prognostic significance. *Clin Cancer Res*, **1,** 1035-41. (1995).

Iskaros, B.F., Hu, X., Sparano, J.A. and Fineberg, S.A., Tenascin pattern of expression and established prognostic factors in invasive breast carcinoma. *J Surg Oncol*, **68,** 107-12. (1998).

Itano, N., Sawai, T., Miyaishi, O. and Kimata, K., Relationship between hyaluronan production and metastatic potential of mouse mammary carcinoma cells. *Cancer Res*, **59,** 2499-504. (1999a).

Itano, N., Sawai, T., Yoshida, M., Lenas, P., Yamada, Y., Imagawa, M., Shinomura, T., Hamaguchi, M., Yoshida, Y., Ohnuki, Y., Miyauchi, S., Spicer, A.P., McDonald, J.A. and Kimata, K., Three isoforms of mammalian hyaluronan synthases have distinct enzymatic properties. *J Biol Chem*, **274,** 25085-92. (1999b).

Jahkola, T., Toivonen, T., Nordling, S., von Smitten, K. and Virtanen, I., Expression of tenascin-C in intraductal carcinoma of human breast: relationship to invasion. *Eur J Cancer*, **34,** 1687-92. (1998a).

Jahkola, T., Toivonen, T., Virtanen, I., von Smitten, K., Nordling, S., von Boguslawski, K., Haglund, C., Nevanlinna, H. and Blomqvist, C., Tenascin-C expression in invasion border of early breast cancer: a predictor of local and distant recurrence. *Br J Cancer*, **78,** 1507-13. (1998b).

Jahkola, T., Toivonen, T., von Smitten, K., Blomqvist, C. and Virtanen, I., Expression of tenascin in invasion border of early breast cancer correlates with higher risk of distant metastasis. *Int J Cancer*, **69,** 445-7. (1996).

Jalkanen, S. and Jalkanen, M., Lymphocyte CD44 binds the COOH-terminal heparin-binding domain of fibronectin. *J Cell Biol*, **116,** 817-25. (1992).

Jiang, H., Peterson, R.S., Wang, W., Bartnik, E., Knudson, C.B. and Knudson, W., A requirement for the CD44 cytoplasmic domain for hyaluronan binding, pericellular matrix

assembly, and receptor-mediated endocytosis in COS- 7 cells. *J Biol Chem*, **277,** 10531-8. (2002).

Jones, F.S. and Jones, P.L., The tenascin family of ECM glycoproteins: structure, function, and regulation during embryonic development and tissue remodeling. *Dev Dyn*, **218,** 235-59. (2000a).

Jones, P.L. and Jones, F.S., Tenascin-C in development and disease: gene regulation and cell function. *Matrix Biol*, **19,** 581-96. (2000b).

Junqueira, L., Carneiro, J. and Kelley, R., The female reproductive system. In: Basic Histology, 8 th ed, pp. 443-446, Appleton & Lange, Norwalk (1995).

Kahari, V.M., Larjava, H. and Uitto, J., Differential regulation of extracellular matrix proteoglycan (PG) gene expression. Transforming growth factor-beta 1 up-regulates biglycan (PGI), and versican (large fibroblast PG) but down-regulates decorin (PGII) mRNA levels in human fibroblasts in culture. *J Biol Chem*, **266,** 10608-15. (1991).

Kaplan, K.B., Swedlow, J.R., Morgan, D.O. and Varmus, H.E., c-Src enhances the spreading of src-/- fibroblasts on fibronectin by a kinase-independent mechanism. *Genes Dev*, **9,** 1505-17. (1995).

Kaplony, A., Zimmermann, D.R., Fischer, R.W., Imhof, B.A., Odermatt, B.F., Winterhalter, K.H. and Vaughan, L., Tenascin Mr 220,000 isoform expression correlates with corneal cell migration. *Development*, **112,** 605-14. (1991).

Kawashima, H., Hirose, M., Hirose, J., Nagakubo, D., Plaas, A.H. and Miyasaka, M., Binding of a large chondroitin sulfate/dermatan sulfate proteoglycan, versican, to L-selectin, P-selectin, and CD44. *J Biol Chem*, **275,** 35448-56. (2000).

Kawashima, H., Li, Y.F., Watanabe, N., Hirose, J., Hirose, M. and Miyasaka, M., Identification and characterization of ligands for L-selectin in the kidney. I. Versican, a large chondroitin sulfate proteoglycan, is a ligand for L-selectin. *Int Immunol*, **11,** 393-405. (1999).

Kleihues, P., Schauble, B., zur Hausen, A., Esteve, J. and Ohgaki, H., Tumors associated with p53 germline mutations: a synopsis of 91 families. *Am J Pathol*, **150,** 1-13. (1997).

Knabbe, C., Lippman, M.E., Wakefield, L.M., Flanders, K.C., Kasid, A., Derynck, R. and Dickson, R.B., Evidence that transforming growth factor-beta is a hormonally regulated negative growth factor in human breast cancer cells. *Cell*, **48,** 417-28. (1987).

Knudson, C.B. and Knudson, W., Hyaluronan-binding proteins in development, tissue homeostasis, and disease. *Faseb J*, **7,** 1233-41. (1993).

Knudson, C.B., Munaim, S.I. and Toole, B.P., Ectodermal stimulation of the production of hyaluronan-dependent pericellular matrix by embryonic limb mesodermal cells. *Dev Dyn*, **204,** 186-91. (1995).

Knudson, C.B. and Toole, B.P., Changes in the pericellular matrix during differentiation of limb bud mesoderm. *Dev Biol*, **112,** 308-18. (1985).

Knudson, W., The role of CD44 as a cell surface hyaluronan receptor during tumor invasion of connective tissue. *Front Biosci*, **3,** D604-15. (1998).

Knudson, W., Tumor-associated hyaluronan. Providing an extracellular matrix that facilitates invasion. *Am J Pathol*, **148,** 1721-6. (1996).

Knudson, W., Aguiar, D.J., Hua, Q. and Knudson, C.B., CD44-anchored hyaluronan-rich pericellular matrices: an ultrastructural and biochemical analysis. *Exp Cell Res*, **228,** 216-28. (1996).

Knudson, W., Bartnik, E. and Knudson, C.B., Assembly of pericellular matrices by COS-7 cells transfected with CD44 lymphocyte-homing receptor genes. *Proc Natl Acad Sci U S A*, **90,** 4003-7. (1993).

Knudson, W., Biswas, C. and Toole, B.P., Interactions between human tumor cells and fibroblasts stimulate hyaluronate synthesis. *Proc Natl Acad Sci U S A*, **81,** 6767-71. (1984).

Knudson, W. and Knudson, C.B., Assembly of a chondrocyte-like pericellular matrix on non-chondrogenic cells. Role of the cell surface hyaluronan receptors in the assembly of a pericellular matrix. *J Cell Sci*, **99,** 227-35. (1991).

Kohda, D., Morton, C.J., Parkar, A.A., Hatanaka, H., Inagaki, F.M., Campbell, I.D. and Day, A.J., Solution structure of the link module: a hyaluronan-binding domain involved in extracellular matrix stability and cell migration. *Cell*, **86,** 767-75. (1996).

Kollias, J., Elston, C.W., Ellis, I.O., Robertson, J.F. and Blamey, R.W., Early-onset breast cancer--histopathological and prognostic considerations. *Br J Cancer*, **75,** 1318-23. (1997).

Konttinen, Y.T., Li, T.F., Mandelin, J., Ainola, M., Lassus, J., Virtanen, I., Santavirta, S., Tammi, M. and Tammi, R., Hyaluronan synthases, hyaluronan, and its CD44 receptor in tissue around loosened total hip prostheses. *J Pathol*, **194,** 384-90. (2001).

Koukoulis, G.K., Gould, V.E., Bhattacharyya, A., Gould, J.E., Howeedy, A.A. and Virtanen, I., Tenascin in normal, reactive, hyperplastic, and neoplastic tissues: biologic and pathologic implications. *Hum Pathol*, **22,** 636-43. (1991).

Krishnamurthy, S. and Sneige, N., Molecular and biologic markers of premalignant lesions of human breast. *Adv Anat Pathol*, **9,** 185-97. (2002).

Kumar, V., Cotran, R. and Robbins, S., Female genital system and breast. In: Basic Pathology, 6 th ed, pp. 623-635, WB Saunders Co, Philadelphia (1997).

Landolt, R.M., Vaughan, L., Winterhalter, K.H. and Zimmermann, D.R., Versican is selectively expressed in embryonic tissues that act as barriers to neural crest cell migration and axon outgrowth. *Development*, **121,** 2303-12. (1995).

Larson, C.M., Kelley, S.S., Blackwood, A.D., Banes, A.J. and Lee, G.M., Retention of the native chondrocyte pericellular matrix results in significantly improved matrix production. *Matrix Biol*, **21,** 349-59. (2002).

Laurent, T.C. and Fraser, J.R., Hyaluronan. *Faseb J*, **6,** 2397-404. (1992).

Lebaron, R.G., Versican. *Perspect Dev Neurobiol*, **3,** 261-71 (1996).

LeBaron, R.G., Zimmermann, D.R. and Ruoslahti, E., Hyaluronate binding properties of versican. *J Biol Chem*, **267,** 10003-10. (1992).

Lei, X., Bandyopadhyay, A., Le, T. and Sun, L., Autocrine TGFbeta supports growth and survival of human breast cancer MDA-MB-231 cells. *Oncogene*, **21,** 7514-23. (2002).

Leong, A. and Lee, A., Biological indices in the assessment of breast cancer. *J Clin Pathol*, **48,** M221-M238 (1995).

Lesley, J., Hyman, R. and Kincade, P.W., CD44 and its interaction with extracellular matrix. *Adv Immunol*, **54,** 271-335. (1993).

Levine, A.J., p53, the cellular gatekeeper for growth and division. *Cell*, **88,** 323-31. (1997).

Liotta, L.A. and Kohn, E., Cancer invasion and metastases. *Jama*, **263,** 1123-6. (1990).

Lippman, M.E., Dickson, R.B., Gelmann, E.P., Rosen, N., Knabbe, C., Bates, S., Bronzert, D., Huff, K. and Kasid, A., Growth regulatory peptide production by human breast carcinoma cells. *J Steroid Biochem*, **30,** 53-61. (1988).

Lochter, A. and Bissell, M.J., Involvement of extracellular matrix constituents in breast cancer. *Semin Cancer Biol*, **6,** 165-73. (1995).

Lokeshwar, V.B., Fregien, N. and Bourguignon, L.Y., Ankyrin-binding domain of CD44(GP85) is required for the expression of hyaluronic acid-mediated adhesion function. *J Cell Biol*, **126,** 1099-109. (1994).

Lokeshwar, V.B., Iida, N. and Bourguignon, L.Y., The cell adhesion molecule, GP116, is a new CD44 variant (ex14/v10) involved in hyaluronic acid binding and endothelial cell proliferation. *J Biol Chem*, **271,** 23853-64. (1996).

London, S.J., Connolly, J.L., Schnitt, S.J. and Colditz, G.A., A prospective study of benign breast disease and the risk of breast cancer. *Jama*, **267,** 941-4. (1992).

Luke, H.J. and Prehm, P., Synthesis and shedding of hyaluronan from plasma membranes of human fibroblasts and metastatic and non-metastatic melanoma cells. *Biochem J*, **343,** 71-5. (1999).

Luqmani, Y.A., Graham, M. and Coombes, R.C., Expression of basic fibroblast growth factor, FGFR1 and FGFR2 in normal and malignant human breast, and comparison with other normal tissues. *Br J Cancer*, **66,** 273-80. (1992).

Lynn, B.D., Turley, E.A. and Nagy, J.I., Subcellular distribution, calmodulin interaction, and mitochondrial association of the hyaluronan-binding protein RHAMM in rat brain. *J Neurosci Res*, **65,** 6-16. (2001).

Malkin, D., Li, F.P., Strong, L.C., Fraumeni, J.F., Jr., Nelson, C.E., Kim, D.H., Kassel, J., Gryka, M.A., Bischoff, F.Z., Tainsky, M.A. and et al., Germ line p53 mutations in a familial syndrome of breast cancer, sarcomas, and other neoplasms. *Science*, **250,** 1233-8. (1990).

Masellis-Smith, A., Belch, A.R., Mant, M.J., Turley, E.A. and Pilarski, L.M., Hyaluronan-dependent motility of B cells and leukemic plasma cells in blood, but not of bone marrow plasma cells, in multiple myeloma: alternate use of receptor for hyaluronan-mediated motility (RHAMM) and CD44. *Blood*, **87,** 1891-9. (1996).

McBride, W.H. and Bard, J.B., Hyaluronidase-sensitive halos around adherent cells. Their role in blocking lymphocyte-mediated cytolysis. *J Exp Med*, **149,** 507-15. (1979).

Mighell, A.J., Thompson, J., Hume, W.J., Markham, A.F. and Robinson, P.A., Human tenascin-C: identification of a novel type III repeat in oral cancer and of novel splice variants in normal, malignant and reactive oral mucosae. *Int J Cancer*, **72,** 236-40. (1997).

Miosge, N., Sasaki, T., Chu, M.L., Herken, R. and Timpl, R., Ultrastructural localization of microfibrillar fibulin-1 and fibulin-2 during heart development indicates a switch in molecular associations. *Cell Mol Life Sci*, **54,** 606-13. (1998).

Mirza, A.N., Mirza, N.Q., Vlastos, G. and Singletary, S.E., Prognostic factors in node-negative breast cancer: a review of studies with sample size more than 200 and follow-up more than 5 years. *Ann Surg*, **235,** 10-26. (2002).

Mjaatvedt, C.H., Yamamura, H., Capehart, A.A., Turner, D. and Markwald, R.R., The Cspg2 gene, disrupted in the hdf mutant, is required for right cardiac chamber and endocardial cushion formation. *Dev Biol*, **202,** 56-66. (1998).

Mobus, V.J., Moll, R., Gerharz, C.D., Kieback, D.G., Merk, O., Runnebaum, I.B., Linner, S., Dreher, L., Grill, H.J. and Kreienberg, R., Differential characteristics of two new tumorigenic cell lines of human breast carcinoma origin. *Int J Cancer*, **77,** 415-23. (1998).

Moch, H., Torhorst, J., Durmuller, U., Feichter, G.E., Sauter, G. and Gudat, F., Comparative analysis of the expression of tenascin and established prognostic factors in human breast cancer. *Pathol Res Pract*, **189,** 510-4. (1993).

Molino, A., Micciolo, R., Turazza, M., Bonetti, F., Piubello, Q., Bonetti, A., Nortilli, R., Pelosi, G. and Cetto, G.L., Ki-67 immunostaining in 322 primary breast cancers: associations with clinical and pathological variables and prognosis. *Int J Cancer*, **74,** 433-7. (1997).

Morris-Wiman, J. and Brinkley, L., An extracellular matrix infrastructure provides support for murine secondary palatal shelf remodelling. *Anat Rec*, **234,** 575-86. (1992).

Muss, H.B., Thor, A.D., Berry, D.A., Kute, T., Liu, E.T., Koerner, F., Cirrincione, C.T., Budman, D.R., Wood, W.C., Barcos, M. and et al., c-erbB-2 expression and response to adjuvant therapy in women with node-positive early breast cancer. *N Engl J Med*, **330,** 1260-6. (1994).

Nakamura, T., Matsumoto, K., Kiritoshi, A. and Tano, Y., Induction of hepatocyte growth factor in fibroblasts by tumor-derived factors affects invasive growth of tumor cells: in vitro analysis of tumor-stromal interactions. *Cancer Res*, **57,** 3305-13. (1997).

Nara, Y., Kato, Y., Torii, Y., Tsuji, Y., Nakagaki, S., Goto, S., Isobe, H., Nakashima, N. and Takeuchi, J., Immunohistochemical localization of extracellular matrix components in human breast tumours with special reference to PG-M/versican. *Histochem J*, **29,** 21-30. (1997).

Naso, M.F., Zimmermann, D.R. and Iozzo, R.V., Characterization of the complete genomic structure of the human versican gene and functional analysis of its promoter. *J Biol Chem*, **269,** 32999-3008. (1994).

Natali, P.G. and Zardi, L., Tenascin: a hexameric adhesive glycoprotein. *Int J Cancer Suppl*, **4,** 66-8. (1989).

Nobes, C.D. and Hall, A., Rho, rac and cdc42 GTPases: regulators of actin structures, cell adhesion and motility. *Biochem Soc Trans*, **23,** 456-9. (1995).

Noble, P.W., Hyaluronan and its catabolic products in tissue injury and repair. *Matrix Biol*, **21,** 25-9. (2002).

Norenberg, U., Wille, H., Wolff, J.M., Frank, R. and Rathjen, F.G., The chicken neural extracellular matrix molecule restrictin: similarity with EGF-, fibronectin type III-, and fibrinogen-like motifs. *Neuron*, **8,** 849-63. (1992).

Olin, A.I., Morgelin, M., Sasaki, T., Timpl, R., Heinegard, D. and Aspberg, A., The proteoglycans aggrecan and Versican form networks with fibulin-2 through their lectin domain binding. *J Biol Chem*, **276,** 1253-61. (2001).

Page, D.L., Dupont, W.D., Rogers, L.W. and Rados, M.S., Atypical hyperplastic lesions of the female breast. A long-term follow-up study. *Cancer*, **55,** 2698-708. (1985).

Paik, S., Bryant, J., Park, C., Fisher, B., Tan-Chiu, E., Hyams, D., Fisher, E.R., Lippman, M.E., Wickerham, D.L. and Wolmark, N., erbB-2 and response to doxorubicin in patients with axillary lymph node-positive, hormone receptor-negative breast cancer. *J Natl Cancer Inst*, **90,** 1361-70. (1998).

Patterson, R.L., Peterson, D.A., Deinhardt, F. and Howard, F., Rubella and rheumatoid arthritis: hyaluronic acid and susceptibility of cultured rheumatoid synovial cells to viruses. *Proc Soc Exp Biol Med*, **149,** 594-8. (1975).

Paulus, W., Baur, I., Dours-Zimmermann, M.T. and Zimmermann, D.R., Differential expression of versican isoforms in brain tumors. *J Neuropathol Exp Neurol*, **55,** 528-33. (1996).

Penc, S.F., Pomahac, B., Winkler, T., Dorschner, R.A., Eriksson, E., Herndon, M. and Gallo, R.L., Dermatan sulfate released after injury is a potent promoter of fibroblast growth factor-2 function. *J Biol Chem*, **273,** 28116-21. (1998).

Peres, R., Betsholtz, C., Westermark, B. and Heldin, C.H., Frequent expression of growth factors for mesenchymal cells in human mammary carcinoma cell lines. *Cancer Res*, **47,** 3425-9. (1987).

Perides, G., Erickson, H.P., Rahemtulla, F. and Bignami, A., Colocalization of tenascin with versican, a hyaluronate-binding chondroitin sulfate proteoglycan. *Anat Embryol (Berl)*, **188,** 467-79. (1993).

Pichon, M.F., Broet, P., Magdelenat, H., Delarue, J.C., Spyratos, F., Basuyau, J.P., Saez, S., Rallet, A., Courriere, P., Millon, R. and Asselain, B., Prognostic value of steroid receptors after long-term follow-up of 2257 operable breast cancers. *Br J Cancer*, **73,** 1545-51. (1996).

Polyak, K., On the birth of breast cancer. *Biochim Biophys Acta*, **1552,** 1-13. (2001).

Ponting, J., Howell, A., Pye, D. and Kumar, S., Prognostic relevance of serum hyaluronan levels in patients with breast cancer. *Int J Cancer*, **52,** 873-6. (1992).

Ponting, J., Kumar, S. and Pye, D., Co-localisation of hyaluronan and hyaluronectin in normal and neoplastic breast tissues. *Int J Oncol*, **2,** 889-893 (1993).

Recklies, A.D., White, C., Melching, L. and Roughley, P.J., Differential regulation and expression of hyaluronan synthases in human articular chondrocytes, synovial cells and osteosarcoma cells. *Biochem J*, **354,** 17-24. (2001).

Reed, W., Hannisdal, E., Boehler, P.J., Gundersen, S., Host, H. and Marthin, J., The prognostic value of p53 and c-erb B-2 immunostaining is overrated for patients with lymph node negative breast carcinoma: a multivariate analysis of prognostic factors in 613 patients with a follow-up of 14-30 years. *Cancer*, **88,** 804-13. (2000).

Relf, M., LeJeune, S., Scott, P.A., Fox, S., Smith, K., Leek, R., Moghaddam, A., Whitehouse, R., Bicknell, R. and Harris, A.L., Expression of the angiogenic factors vascular endothelial cell growth factor, acidic and basic fibroblast growth factor, tumor growth factor beta-1, platelet-derived endothelial cell growth factor, placenta growth factor, and pleiotrophin in human primary breast cancer and its relation to angiogenesis. *Cancer Res*, **57,** 963-9. (1997).

Ricciardelli, C., Brooks, J.H., Suwiwat, S., Sakko, A.J., Mayne, K., Raymond, W.A., Seshadri, R., LeBaron, R.G. and Horsfall, D.J., Regulation of stromal versican expression by breast cancer cells and importance to relapse-free survival in patients with node-negative primary breast cancer. *Clin Cancer Res*, **8,** 1054-60. (2002).

Ricciardelli, C., Mayne, K., Sykes, P.J., Raymond, W.A., McCaul, K., Marshall, V.R. and Horsfall, D.J., Elevated levels of versican but not decorin predict disease progression in early-stage prostate cancer. *Clin Cancer Res*, **4,** 963-71. (1998).

Ropponen, K., Tammi, M., Parkkinen, J., Eskelinen, M., Tammi, R., Lipponen, P., Agren, U., Alhava, E. and Kosma, V.M., Tumor cell-associated hyaluronan as an unfavorable prognostic factor in colorectal cancer. *Cancer Res*, **58,** 342-7. (1998).

Rosen, P.P., Groshen, S., Kinne, D.W. and Norton, L., Factors influencing prognosis in node-negative breast carcinoma: analysis of 767 T1N0M0/T2N0M0 patients with long-term follow-up. *J Clin Oncol*, **11,** 2090-100. (1993).

Rudzki, Z. and Jothy, S., CD44 and the adhesion of neoplastic cells. *Mol Pathol*, **50,** 57-71. (1997).

Russell, D.L., Ochsner, S.A., Hsieh, M., Mulders, S. and Richards, J.S., Hormone-regulated expression and localization of versican in the rodent ovary. *Endocrinology*, **144,** 1020-31. (2003).

Sahin, A.A., Ro, J.Y., el-Naggar, A.K., Wilson, P.L., Teague, K., Blick, M. and Ayala, A.G., Tumor proliferative fraction in solid malignant neoplasms. A comparative study of Ki-67 immunostaining and flow cytometric determinations. *Am J Clin Pathol*, **96,** 512-9. (1991).

Saimura, M., Fukutomi, T., Tsuda, H., Sato, H., Miyamoto, K., Akashi-Tanaka, S. and Nanasawa, T., Prognosis of a series of 763 consecutive node-negative invasive breast cancer patients without adjuvant therapy: analysis of clinicopathological prognostic factor. *J Surg Oncol*, **71,** 101-5. (1999).

Sakko, A.J., Ricciardelli, C., Mayne, K., Suwiwat, S., LeBaron, R.G., Marshall, V.R., Tilley, W.D. and Horsfall, D.J., Modulation of prostate cancer cell attachment to matrix by versican. *Cancer Res*, **63,** 4786-91. (2003).

Sakko, A.J., Ricciardelli, C., Mayne, K., Tilley, W.D., Lebaron, R.G. and Horsfall, D.J., Versican accumulation in human prostatic fibroblast cultures is enhanced by prostate cancer cell-derived transforming growth factor beta1. *Cancer Res*, **61,** 926-30. (2001).

Samuel, S.K., Hurta, R.A., Spearman, M.A., Wright, J.A., Turley, E.A. and Greenberg, A.H., TGF-beta 1 stimulation of cell locomotion utilizes the hyaluronan receptor RHAMM and hyaluronan. *J Cell Biol*, **123,** 749-58. (1993).

Schlessinger, J., Lax, I. and Lemmon, M., Regulation of growth factor activation by proteoglycans: what is the role of the low affinity receptors? *Cell*, **83,** 357-60. (1995).

Schonherr, E., Jarvelainen, H.T., Sandell, L.J. and Wight, T.N., Effects of platelet-derived growth factor and transforming growth factor-beta 1 on the synthesis of a large versican-like chondroitin sulfate proteoglycan by arterial smooth muscle cells. *J Biol Chem*, **266,** 17640-7. (1991).

Seiter, S., Arch, R., Reber, S., Komitowski, D., Hofmann, M., Ponta, H., Herrlich, P., Matzku, S. and Zoller, M., Prevention of tumor metastasis formation by anti-variant CD44. *J Exp Med*, **177,** 443-55. (1993).

Seshadri, R., Leong, A.S., McCaul, K., Firgaira, F.A., Setlur, V. and Horsfall, D.J., Relationship between p53 gene abnormalities and other tumour characteristics in breast-cancer prognosis. *Int J Cancer*, **69,** 135-41. (1996).

Setala, L.P., Tammi, M.I., Tammi, R.H., Eskelinen, M.J., Lipponen, P.K., Agren, U.M., Parkkinen, J., Alhava, E.M. and Kosma, V.M., Hyaluronan expression in gastric cancer cells is associated with local and nodal spread and reduced survival rate. *Br J Cancer*, **79,** 1133-8. (1999).

Seymour, L. and Bezwoda, W.R., Positive immunostaining for platelet derived growth factor (PDGF) is an adverse prognostic factor in patients with advanced breast cancer. *Breast Cancer Res Treat*, **32,** 229-33. (1994).

Sherman, L., Sleeman, J., Herrlich, P. and Ponta, H., Hyaluronate receptors: key players in growth, differentiation, migration and tumor progression. *Curr Opin Cell Biol*, **6,** 726-33. (1994).

Shoji, T., Kamiya, T., Tsubura, A., Hamada, Y., Hatano, T., Hioki, K. and Morii, S., Tenascin staining positivity and the survival of patients with invasive breast carcinoma. *J Surg Res*, **55,** 295-7. (1993).

Shoji, T., Kamiya, T., Tsubura, A., Hatano, T., Sakakura, T., Yamamoto, M. and Morii, S., Immunohistochemical staining patterns of tenascin in invasive breast carcinomas. *Virchows Arch A Pathol Anat Histopathol*, **421,** 53-6. (1992).

Simpson, M.A., Reiland, J., Burger, S.R., Furcht, L.T., Spicer, A.P., Oegema, T.R., Jr. and McCarthy, J.B., Hyaluronan synthase elevation in metastatic prostate carcinoma cells correlates with hyaluronan surface retention, a prerequisite for rapid adhesion to bone marrow endothelial cells. *J Biol Chem*, **276,** 17949-57. (2001).

Siri, A., Carnemolla, B., Saginati, M., Leprini, A., Casari, G., Baralle, F. and Zardi, L., Human tenascin: primary structure, pre-mRNA splicing patterns and localization of the epitopes recognized by two monoclonal antibodies. *Nucleic Acids Res*, **19,** 525-31. (1991).

Siri, A., Knauper, V., Veirana, N., Caocci, F., Murphy, G. and Zardi, L., Different susceptibility of small and large human tenascin-C isoforms to degradation by matrix metalloproteinases. *J Biol Chem*, **270,** 8650-4. (1995).

Sobol, H., BRCA1-p53 relationship in hereditary. *Int J Oncol*, **10,** 349-353 (1997).

Spessotto, P., Rossi, F.M., Degan, M., Di Francia, R., Perris, R., Colombatti, A. and Gattei, V., Hyaluronan-CD44 interaction hampers migration of osteoclast-like cells by down-regulating MMP-9. *J Cell Biol*, **158,** 1133-44. (2002).

Spicer, A.P. and McDonald, J.A., Characterization and molecular evolution of a vertebrate hyaluronan synthase gene family. *J Biol Chem*, **273,** 1923-32. (1998).

Spicer, A.P., Roller, M.L., Camper, S.A., McPherson, J.D., Wasmuth, J.J., Hakim, S., Wang, C., Turley, E.A. and McDonald, J.A., The human and mouse receptors for hyaluronan-mediated motility, RHAMM, genes (HMMR) map to human chromosome 5q33.2-qter and mouse chromosome 11. *Genomics*, **30,** 115-7. (1995).

Spillmann, D., Witt, D. and Lindahl, U., Defining the interleukin-8-binding domain of heparan sulfate. *J Biol Chem*, **273,** 15487-93. (1998).

Spring, J., Beck, K. and Chiquet-Ehrismann, R., Two contrary functions of tenascin: dissection of the active sites by recombinant tenascin fragments. *Cell*, **59,** 325-34. (1989).

Sriramarao, P. and Bourdon, M.A., A novel tenascin type III repeat is part of a complex of tenascin mRNA alternative splices. *Nucleic Acids Res*, **21,** 163-8. (1993).

Takeuchi, J., Sobue, M., Sato, E., Shamoto, M. and Miura, K., Variation in glycosaminoglycan components of breast tumors. *Cancer Res*, **36,** 2133-9. (1976).

Tammi, R., Ronkko, S., Agren, U.M. and Tammi, M., Distribution of hyaluronan in bull reproductive organs. *J Histochem Cytochem*, **42,** 1479-86. (1994).

Tan, E.M., Hoffren, J., Rouda, S., Greenbaum, S., Fox, J.W.t., Moore, J.H., Jr. and Dodge, G.R., Decorin, versican, and biglycan gene expression by keloid and normal dermal fibroblasts: differential regulation by basic fibroblast growth factor. *Exp Cell Res*, **209,** 200-7. (1993).

Teder, P., Bergh, J. and Heldin, P., Functional hyaluronan receptors are expressed on a squamous cell lung carcinoma cell line but not on other lung carcinoma cell lines. *Cancer Res*, **55,** 3908-14. (1995).

Theocharis, A.D., Vynios, D.H., Papageorgakopoulou, N., Skandalis, S.S. and Theocharis, D.A., Altered content composition and structure of glycosaminoglycans and proteoglycans in gastric carcinoma. *Int J Biochem Cell Biol*, **35,** 376-90. (2003).

Thompson, E.W., Paik, S., Brunner, N., Sommers, C.L., Zugmaier, G., Clarke, R., Shima, T.B., Torri, J., Donahue, S., Lippman, M.E. and et al., Association of increased basement membrane invasiveness with absence of estrogen receptor and expression of vimentin in human breast cancer cell lines. *J Cell Physiol*, **150,** 534-44. (1992).

Thor, A.D., Moore, D.H., II, Edgerton, S.M., Kawasaki, E.S., Reihsaus, E., Lynch, H.T., Marcus, J.N., Schwartz, L., Chen, L.C., Mayall, B.H. and et al., Accumulation of p53 tumor suppressor gene protein: an independent marker of prognosis in breast cancers. *J Natl Cancer Inst*, **84,** 845-55. (1992).

Tiedemann, K., Malmstrom, A. and Westergren-Thorsson, G., Cytokine regulation of proteoglycan production in fibroblasts: separate and synergistic effects. *Matrix Biol*, **15,** 469-78. (1997).

Tokes, A.M., Hortovanyi, E., Csordas, G., Kulka, J., Mozes, G., Hatalyak, A. and Kadar, A., Immunohistochemical localisation of tenascin in invasive ductal carcinoma of the breast. *Anticancer Res*, **19,** 175-9. (1999).

Touab, M., Villena, J., Barranco, C., Arumi-Uria, M. and Bassols, A., Versican is differentially expressed in human melanoma and may play a role in tumor development. *Am J Pathol*, **160,** 549-57. (2002).

Tsukita, S., Oishi, K., Sato, N., Sagara, J. and Kawai, A., ERM family members as molecular linkers between the cell surface glycoprotein CD44 and actin-based cytoskeletons. *J Cell Biol*, **126,** 391-401. (1994).

Tucker, R.P., Hagios, C. and Chiquet-Ehrismann, R., Tenascin-Y in the developing and adult avian nervous system. *Dev Neurosci*, **21,** 126-33. (1999).

Turley, E.A., Hyaluronan and cell locomotion. *Cancer Metastasis Rev*, **11,** 21-30. (1992).

Turley, E.A., Austen, L., Vandeligt, K. and Clary, C., Hyaluronan and a cell-associated hyaluronan binding protein regulate the locomotion of ras-transformed cells. *J Cell Biol*, **112,** 1041-7. (1991).

Turley, E.A., Belch, A.J., Poppema, S. and Pilarski, L.M., Expression and function of a receptor for hyaluronan-mediated motility on normal and malignant B lymphocytes. *Blood*, **81,** 446-53. (1993).

Turley, E.A., Moore, D. and Hayden, L.J., Characterization of hyaluronate binding proteins isolated from 3T3 and murine sarcoma virus transformed 3T3 cells. *Biochemistry*, **26,** 2997-3005. (1987).

Turley, E.A., Noble, P.W. and Bourguignon, L.Y., Signaling properties of hyaluronan receptors. *J Biol Chem*, **277,** 4589-92. (2002).

Underhill, C., CD44: the hyaluronan receptor. *J Cell Sci*, **103,** 293-8. (1992).

Valenti, M.T., Azzarello, G., Balducci, E., Sartore, S., Sandri, M., Manconi, R., Sicari, U., Bari, M. and Vinante, O., Conditioned medium from MCF-7 cell line induces myofibroblast differentiation, decreased cell proliferation, and increased apoptosis in cultured normal fibroblasts but not in fibroblasts from malignant breast tissue. *Histochem J*, **33,** 499-509. (2001).

van Leeuwen, F.N., van der Kammen, R.A., Habets, G.G. and Collard, J.G., Oncogenic activity of Tiam1 and Rac1 in NIH3T3 cells. *Oncogene*, **11,** 2215-21. (1995).

Veronese, S.M. and Gambacorta, M., Detection of Ki-67 proliferation rate in breast cancer. Correlation with clinical and pathologic features. *Am J Clin Pathol*, **95,** 30-4. (1991).

Voutilainen, K., Anttila, M., Sillanpaa, S., Tammi, R., Tammi, M., Saarikoski, S. and Kosma, V.M., Versican in epithelial ovarian cancer: relation to hyaluronan, clinicopathologic factors and prognosis. *Int J Cancer*, **107,** 359-64. (2003).

Walker, R.A. and Dearing, S.J., Transforming growth factor beta 1 in ductal carcinoma in situ and invasive carcinomas of the breast. *Eur J Cancer*, **28,** 641-4. (1992).

Walker, R.A., Dearing, S.J. and Gallacher, B., Relationship of transforming growth factor beta 1 to extracellular matrix and stromal infiltrates in invasive breast carcinoma. *Br J Cancer*, **69,** 1160-5. (1994).

Wang, C., Entwistle, J., Hou, G., Li, Q. and Turley, E.A., The characterization of a human RHAMM cDNA: conservation of the hyaluronan-binding domains. *Gene*, **174,** 299-306. (1996).

Wang, C., Thor, A.D., Moore, D.H., 2nd, Zhao, Y., Kerschmann, R., Stern, R., Watson, P.H. and Turley, E.A., The overexpression of RHAMM, a hyaluronan-binding protein that regulates ras signaling, correlates with overexpression of mitogen- activated protein kinase and is a significant parameter in breast cancer progression. *Clin Cancer Res*, **4,** 567-76. (1998).

Watanabe, H. and Yamada, Y., Mice lacking link protein develop dwarfism and craniofacial abnormalities. *Nat Genet*, **21,** 225-9. (1999).

Weber, P., Montag, D., Schachner, M. and Bernhardt, R.R., Zebrafish tenascin-W, a new member of the tenascin family. *J Neurobiol*, **35,** 1-16. (1998).

Wielenga, V.J., Heider, K.H., Offerhaus, G.J., Adolf, G.R., van den Berg, F.M., Ponta, H., Herrlich, P. and Pals, S.T., Expression of CD44 variant proteins in human colorectal cancer is related to tumor progression. *Cancer Res*, **53,** 4754-6. (1993).

Wolff, E.A., Greenfield, B., Taub, D.D., Murphy, W.J., Bennett, K.L. and Aruffo, A., Generation of artificial proteoglycans containing glycosaminoglycan-modified CD44. Demonstration of the interaction between rantes and chondroitin sulfate. *J Biol Chem*, **274,** 2518-24. (1999).

Wooster, R., Neuhausen, S.L., Mangion, J., Quirk, Y., Ford, D., Collins, N., Nguyen, K., Seal, S., Tran, T., Averill, D. and et al., Localization of a breast cancer susceptibility gene, BRCA2, to chromosome 13q12-13. *Science*, **265,** 2088-90. (1994).

Wu, Y., Chen, L., Zheng, P.S. and Yang, B.B., beta 1-Integrin-mediated glioma cell adhesion and free radical-induced apoptosis are regulated by binding to a C-terminal domain of PG- M/versican. *J Biol Chem*, **277,** 12294-301. (2002).

Yamagata, M. and Kimata, K., Repression of a malignant cell-substratum adhesion phenotype by inhibiting the production of the anti-adhesive proteoglycan, PG-M/versican. *J Cell Sci*, **107,** 2581-90. (1994).

Yamagata, M., Saga, S., Kato, M., Bernfield, M. and Kimata, K., Selective distributions of proteoglycans and their ligands in pericellular matrix of cultured fibroblasts. Implications for their roles in cell-substratum adhesion. *J Cell Sci*, **106,** 55-65. (1993).

Yamagata, M., Suzuki, S., Akiyama, S.K., Yamada, K.M. and Kimata, K., Regulation of cell-substrate adhesion by proteoglycans immobilized on extracellular substrates. *J Biol Chem*, **264,** 8012-8. (1989).

Yamagata, M., Yamada, K.M., Yoneda, M., Suzuki, S. and Kimata, K., Chondroitin sulfate proteoglycan (PG-M-like proteoglycan) is involved in the binding of hyaluronic acid to cellular fibronectin. *J Biol Chem*, **261,** 13526-35. (1986).

Yamashita, J., Ogawa, M., Yamashita, S., Nomura, K., Kuramoto, M., Saishoji, T. and Shin, S., Immunoreactive hepatocyte growth factor is a strong and independent predictor of recurrence and survival in human breast cancer. *Cancer Res*, **54,** 1630-3. (1994).

Yang, B., Yang, B.L., Savani, R.C. and Turley, E.A., Identification of a common hyaluronan binding motif in the hyaluronan binding proteins RHAMM, CD44 and link protein. *Embo J*, **13,** 286-96. (1994).

Yang, B., Zhang, L. and Turley, E.A., Identification of two hyaluronan-binding domains in the hyaluronan receptor RHAMM. *J Biol Chem*, **268,** 8617-23. (1993).

Yang, B.L., Zhang, Y., Cao, L. and Yang, B.B., Cell adhesion and proliferation mediated through the G1 domain of versican. *J Cell Biochem*, **72,** 210-20. (1999).

Yao, L.Y., Moody, C., Schonherr, E., Wight, T.N. and Sandell, L.J., Identification of the proteoglycan versican in aorta and smooth muscle cells by DNA sequence analysis, in situ hybridization and immunohistochemistry. *Matrix Biol*, **14,** 213-25. (1994).

Yong, B. and Heath, J., *Female reproductive system. In: Wheater functional histology : a text and color atlas*, 4 th ed , pp. 368-367, Harcourt Publishers, Grafos, SA (2000).

Zako, M., Shinomura, T., Ujita, M., Ito, K. and Kimata, K., Expression of PG-M(V3), an alternatively spliced form of PG-M without a chondroitin sulfate attachment in region in mouse and human tissues. *J Biol Chem*, **270,** 3914-8. (1995).

Zhang, S., Chang, M.C., Zylka, D., Turley, S., Harrison, R. and Turley, E.A., The hyaluronan receptor RHAMM regulates extracellular-regulated kinase. *J Biol Chem*, **273,** 11342-8. (1998a).

Zhang, Y., Cao, L., Yang, B.L. and Yang, B.B., The G3 domain of versican enhances cell proliferation via epidermial growth factor-like motifs. *J Biol Chem*, **273,** 21342-51. (1998b).

Zhu, D. and Bourguignon, L.Y., Interaction between CD44 and the repeat domain of ankyrin promotes hyaluronic acid-mediated ovarian tumor cell migration. *J Cell Physiol*, **183,** 182-95. (2000).

Zimmermann, D.R., Dours-Zimmermann, M.T., Schubert, M. and Bruckner-Tuderman, L., Versican is expressed in the proliferating zone in the epidermis and in association with the elastic network of the dermis. *J Cell Biol*, **124,** 817-25. (1994).

Zimmermann, D.R. and Ruoslahti, E., Multiple domains of the large fibroblast proteoglycan, versican. *Embo J*, **8,** 2975-81. (1989).